THE ROLE OF HOXD10 IN THE DEVELOPMENT OF MOTONEURONS IN THE POSTERIOR SPINAL CORD

by

Veeral Shailesh Shah

B.S., University of Pittsburgh, 2000

Submitted to the Graduate Faculty of

University of Pittsburgh School of Medicine

Department of Neurobiology in partial fulfillment

of the requirements for the degree of

Doctor of Philosophy

University of Pittsburgh

2006

UNIVERSITY OF PITTSBURGH

SCHOOL OF MEDICINE DEPARTMENT OF NEUROBIOLOGY

This thesis was presented

by

Veeral Shailesh Shah

It was defended on

January 17, 2006

and approved by

Paula Monaghan-Nichols, Ph. D, CNUP, Neurobiology

Debbie Chapman, Ph. D, Biological Sciences

Willi Halfter, Ph. D, CNUP, Neurobiology

Carl Lagenaur, Ph. D, CNUP, Neurobiology

Cynthia Forehand, Ph. D, University of Vermont, Anatomy and Neurobiology

Dissertation Advisor: Cynthia Lance-Jones, Ph. D, CNUP, Neurobiology

THE ROLE OF HOXD10 IN THE DEVELOPMENT OF MOTONEURONS IN THE POSTERIOR SPINAL CORD

Veeral Shah

University of Pittsburgh, 2007

Hox genes encode anterior-posterior identity during central nervous system development. Few studies have examined Hox gene function at lumbosacral (LS) levels of the spinal cord, where there is extensive information on normal development. Hoxd10 is expressed at high levels in the embryonic LS spinal cord, but not the thoracic (T) spinal cord. To test the hypothesis that restricted expression of Hoxd10 contributes to the attainment of an LS identity, and specifically an LS motoneuron identity, Hoxd10 was ectopically expressed in T segments in chick embryos via *in ovo* electroporation. Electroporations were carried out at early neural tube stages (stages 13-15) and at the onset of motoneuron differentiation (stages 17-18). Regional motoneuron identity was assessed after the normal period of motor column formation (stages 28-29). Subsets of motoneurons in transfected T segments developed a molecular profile normally shown by anterior LS LMCl motoneurons, including Lim 1 and RALDH2 expression. In addition, motoneurons in posterior T segments showed novel axon projections to two muscles in the anterodorsal limb, the sartorius and anterior iliotibialis muscles. These changes are accompanied by a significant reduction in the number of T motoneurons at stage 29. Analyses of Hoxd10 electroporated embryos at the onset of motor column formation (stage 18) suggest that early and high levels of Hoxd10 expression led to the death of some early differentiating motoneuron. Despite these adverse effects, our data indicate that Hoxd10 expression is sufficient to induce LS motoneuron identity and axon trajectories characteristic of motoneurons in the LS anterior spinal cord. Equivalent changes in motoneuron identity were not found with the ectopic expression of Hoxd9, a gene normally expressed in T as well as LS segments. In an additional series of experiments, Hoxd10 was overexpressed in LS segments via *in ovo* electroporation at early neural tube stages. Analyses at stage 29 indicated proportionate increases in LMCl (Lim 1+, RALDH2+) motoneurons, and proportionate decreases in LMCm and MMC motoneurons (Isl 1+) motoneurons. These findings suggest that Hoxd10 specifically promotes the development and/or survival of LMCl motoneurons.

TABLE OF CONTENTS

LIST OF TABLES

LIST OF FIGURES

PREFACE

In the past four years, I have had the fortune of working and interacting with amazing people, who have supported me during my graduate education.

First and foremost I like to thank my mentor, my advisor, my colleague, and my good friend Cynthia Lance-Jones. She is truly passionate about teaching and fostering the education of her students. Without her guidance I would not have gained the knowledge and experience to have completed by thesis. Even during times when "I can't see the forest before the trees", she has been a constant source of encouragement, motivation, and direction. It has been an honor to work with such a world-class researcher and person. My time in her lab and her friendship is priceless. I will truly miss working with her. Thank you for everything.

This brings me to the Lance-Jones lab. I am forever grateful to Emily Sours for her technical assistance, advice, and friendship. I would like to thank Mala for our daily discussions and making lab an enjoyable experience. Thank you both.

I would to thank Paula Monaghan-Nichols. If it wasn't for Paula's encouragement during my medical school education, I probably would not have entered graduate school. Looking back, how fortunate I have been to cross paths with her. Thank you.

I would like to thank the members of my committee Paula Monaghan-Nichols, Debbie Chapman, Carl Lagenaur, and Willi Halfter for providing me with much guidance during my graduate education. All your advice and support has had an significant influence on all my graduate school endeavors (p-value =.00000001; n=1). I am honored to have each one of you on my committee. Thank you.

I would especially like to thank my family, who are the source of my being. My mom and dad are my heart and soul. Without my father Shailesh, mother Neelam, and my brother

Veeshal Shah I could not accomplish anything and would truly be lost. Love you always. Thank you.

I would also like to thank all the administrators and secretaries in Department of Neurobiology for all their help over the years. A special thanks to Patti for making sure I was still a graduate student, in the program, every year.

Lastly, I would like to thank Dr. Cynthia Forehand for taking the time to read my thesis, and coming in all the way from Vermont to take part in my defense. I am touched and honored to have your involvement in the completion of my thesis. I hope you enjoyed reading the thesis. Thank you.

1.0 GENERAL INTRODUCTION

THESIS RATIONALE: Pattern formation is a critical event in embryonic development. In the nervous system, cells acquire unique identities in accord with their early embryonic position along the anterior-posterior (A-P) or rostral-caudal axis. What governs this process? The vertebrate spinal cord and its motoneurons serve as an excellent model for examining the development of A-P differences since there are striking differences in the segmental organization of motoneurons at limb levels (brachial and lumbosacral regions) and nonlimb levels (thoracic). There is a stereotyped relationship between the position of motoneurons in the spinal cord and targets in the periphery. Motoneurons extend axons along well delineated pathways at precise times in development to innervate skeletal muscles in a precise fashion. Hox genes encode homeodomain-containing proteins that are expressed in overlapping A-P domains in numerous tissues in the developing embryo including the neural tube. Prior studies have shown that the Hox family of transcription factors is actively involved in A-P patterning of the hindbrain and anterior spinal cord (Carpenter et al., 1993; Goddard et al., 1996; Gavalas et al., 1998; Dasen et al., 2003). However, little is known about the role of Hox genes in the specification of motoneurons in the posterior spinal cord.

Many early studies used a knockout strategy to disrupt the function of single or multiple Hox genes throughout development. Since Hox genes are expressed in neural tissues and in the periphery that motor axons traverse to reach their respective targets, it is difficult to interpret data from global perturbation experiments. It is unclear whether resulting nervous system defects reflect a direct effect of Hox disruption in the neural tube or an indirect effect of Hox disruption in other tissues.

To investigate the role of Hox genes in the posterior spinal cord, I chose to focus on the role of Hoxd10. This gene was selected because it is highly expressed in the LS spinal cord but not expressed in the T spinal cord (Lance-Jones et al., 2001). In addition, analyses of Hoxd10

mutant mice suggest that Hoxd10 has a prominent role in the development of LS segmental identity and nerve patterns in the hindlimb (Carpenter et al., 1997; Wahba et al., 2001). To test my hypothesis that Hoxd10 imparts an LS character to the segmental organization of motoneurons and their specific axonal trajectories, I have used the technique of *in ovo* electroporation to ectopically express Hoxd10 in T spinal segments. *In ovo* electroporation is a powerful gene-delivery approach that can be used to investigate the function of a gene at a specific time and place during development. Electroporations have been successfully applied to the transfection of embryonic chick tissue *in vivo* (Muramatsu et al., 1997). Since motoneuron development and axon pathfinding have been particularly well-studied in the avian embryo, I have used the avian embryo as a model system to determine if the ectopic expression of Hoxd10 in the neural tube alone imparts A-P identity to the molecular profile of developing motoneurons (Chapter 3). Few, if any, investigators have assessed the specificity of peripheral projections after the ectopic expression of a Hox gene. In this thesis, I have also analyzed axonal projections along the A-P axis following the misexpression of Hoxd10 (Chapter 4). Further, I have assessed motoneuron development in T segments after electroporations at stages when regional characteristics are normally programmed (Chapter 3 and 4) as well as shortly thereafter (Chapter 5).

Our *in ovo* electroporation experiments led not only to the expression of Hoxd10 at a foreign (T) axial level but also to the development of abnormally high expression of Hoxd10. To determine if increasing Hox levels in a normal domain changes the molecular profile of motoneurons. I have assessed the effects of Hoxd10 transfections on motoneurons in anterior LS segments that normally express Hoxd10 (Chapter 7). I have also examined the molecular profile of T motoneurons transfected with Hoxd9. As Hoxd9 is normally expressed in posterior T and LS spinal segments (Chapter 6), these experiments address the question of whether high expression of a non-LS restricted Hox gene is capable of inducing changes in motoneuron identity.

1.1 SIGNIFICANCE

In this thesis, I will examine the role of a single 5' Hox gene in patterning the spinal cord. Molecules involved in patterning body structures have direct clinical relevance to tissue engineering and stem cell research. Understanding transcriptional mechanisms that underlie the distinct specification of cell fates will be important in terms of directing the differentiation of progenitor cells. Since many 5' Hox genes are expressed early in the development of posterior organs like the uterus, kidney, and other urogenital structures, studying the role of Hox proteins in patterning the nervous system will also elucidate mechanisms that pattern other body structures (reviewed Kobayashi and Behringer, 2003).

The abnormal regulation of Hox molecules can also be associated with pathological development and human deformities. Mutations in 5'Hox gene expression result in an array of human diseases, including Charcot-Marie-Tooth disease (CMT), congenital vertical talus (CVT), synpolydactyly, hand-foot genital syndrome, and other urogenital abnormalities (Shrimpton et al., 2004). Mutations in Hox genes also result in abnormal proliferation of hematopoietic cells and leukemias (Bjornsson et al., 2001). Therefore, investigating molecules involved in normal and pathological development of motoneurons will increase our understanding of diseases at the molecular level and potentially elucidate new molecular targets for diagnosis and therapeutic intervention.

1.2 BACKGROUND

During gastrulation, three distinct layers are formed, the ectoderm (superficial layer), mesoderm (middle), and endoderm (innermost layer). Along with the complex cell rearrangements of gastrulation, the embryo must establish body axes in order to form a standard vertebrate body plan. Cells must recognize their positional status along the body axes and properly interpret this information to give rise to appropriate body structures. For example, the ectoderm mainly gives rise to skin epidermis; however, the dorsal ectoderm exclusively gives rise to the future neural tube. Later in development, the presence of these body axes becomes apparent with polarity and regionalization of body structures. The vertebrate nervous system is a

clear example of regional specialization. Early in development, signals from axial structures like the notochord and Hensen's node appear to establish specific patterns of transcription factors that, in turn, encode regional identity and cell fate on the dorsoventral and anteroposterior axes of the neural tube (Liem et al., 2000; Bel-Vialar et al., 2002; Lance-Jones et al., 2001). Normally, transcription factors function in hierarchical manner, in which early-expressed transcription factors drive the expression of downstream transcription factors during the process of cell differentiation.

A number of different types of embryos have been studied for understanding vertebrate development, including chick, mouse, and zebrafish. While, the mouse and zebrafish embryo are powerful genetic systems, the chick embryo is an excellent model for cut-and-paste embryology studies. Although there are major differences in the development of each of these embryos, molecular analysis has revealed clear similarities in establishing a body plan. In this thesis, I have chosen to study the avian embryo as model system because of its accessibility and the extensive available background on its normal development.

1.2.1 Early regulation of spinal neurogenesis and the specification of generic motoneuron identity.

In contrast to other regions of the central nervous system, the spinal cord develops in a progressive rostral-caudal manner over a long period of time. This gradual division between spatial and temporal events during neurogenesis makes the spinal cord an ideal model to study factors that regulate neural differentiation and patterning. In the developing spinal cord, neural progenitors acquire positional identity along the D-V and A-P axis by extrinsic signaling pathways (Lumsden and Krumlauf, 1996; Tanabe and Jessell 1995). Recent studies indicate that Sonic hedgehog (Shh), fibroblast growth factors (FGFs) and retinoids affect the identity and differentiation of spinal progenitors at early neural tube stages of development (Diez del Corral and Storey, 2004).

Shh. The specification of progenitor cells in the ventral spinal cord is initiated by signaling activities of a secreted glycoprotein, Shh (Briscoe et al., 2001). Shh is secreted from the notochord and floor plate around the time the neural tube is patterned along the D-V axis. Cell explant experiments showed that Shh induces the generation of motoneurons and specific

classes of ventral interneurons in a graded manner (Ericson et al., 1996; Tanabe and Jessell 1995). Shh signaling establishes ventral progenitor identities by regulating the spatial expression of homdeodomain transcription factors, which include: Nkx, Pax, Dbx , Irx and Olig (Briscoe et al., 1999; Ericson et al., 1997). These ventral patterning transcription factors can be subdivided into class I proteins and class II proteins. Class I proteins are repressed by Shh signaling, while the Class II proteins are induced in the presence of Shh. In response to Shh, the combinatorial expression of Class I and Class II proteins establish 5 progenitor domains in the ventral spinal cord. Each progenitor domain gives rise to distinct post-mitotic cells. For example, the motoneuron progenitor domain (pMN) is identified by the expression of Pax6, Nkx 6.1 and Olig2 (Briscoe et al., 1999; Ericson et al., 1997). Furthermore, these homeodomain transcription factors have several roles in the development of motoneurons including 1) the repression of developmental programs for other cell fates, 2) the initiation of neurogenesis, and 3) the promotion of downstream transcription factors involved in motoneuron specification (Briscoe et al., 1999; Muhr et al., 2001; Mizugchi et al., 2001; Novitch et al., 2001; Pfaff et al., 1996).

FGFs. Members of the FGF family are polypeptides that activate specific tyrosine kinase receptors. In the vertebrate embryo, FGFs are secreted from surrounding paraxial mesoderm and the Henson's Node (Niswander and Martin, 1992; Crossley and Martin, 1995). Early in the formation of the neural tube, FGFs play an important role in repressing neurogenic and ventral patterning genes. The removal of paraxial mesoderm results in the precocious expression of ventral patterning genes (Bertrand et al., 2000). Furthermore, when FGF signaling is disrupted by a pharmacological blockade or by the expression of a dominant negative FGF receptor, there is a subsequent upregulation of ventral patterning genes in the neural tube (Diez del Corral et al., 2003). These findings support the hypothesis that FGF signaling has a repressive effect on primary neural induction and maintains cells in an undifferentiated state. Recent studies have proposed that while FGF signaling primarily blocks differentiation in the spinal cord, it secondarily allows progenitor cells to respond to different posterior signals (Liu et al., 2001).

Retinoids. Retinoic acid (RA), a derivative of dietary vitamin A, is required for a number of developmental processes in the vertebrate embryo. Early studies recognized the critical role of retinoids in neural development, when developing embryo exposed to exogenous RA had severe disruptions in the longitudinal patterning of the nervous system (Durston et al., 1989; Maden et al., 1991). Unlike FGFs, which maintain cells in an undifferentiated state, retinoids are essential

for the differentiation of cells. The application of RA to embryonic stem cells results in the differentiation of these cells into oligodendrocytes and neurons, suggesting that RA-mediated signaling is important for the acquisition of a neural cell fate (Wohl and Weiss, 1998). The RA signaling pathway is mediated by the retinoic acid receptor (RAR) and retinoid X receptor (RXR). Both the RAR and RXR receptors have three subtypes: α, β, and γ. RA binds to a heterodimer of RAR/RXR receptors, which is then recruited to a retinoic acid response element (RARE). RAREs are found in the regulatory region of downstream target genes.

In early chick embryogenesis, FGFs and retinoids activate antagonistic pathways during the differentiation of CNS progenitor cells. Upon the formation of the neural plate, FGFs are highly expressed in the node and surrounding mesoderm (Niswander and Martin 1992; Crossley and Martin 1995). However, later during neural tube formation there is a decline in FGF levels, which is complemented by the upregulation of RALDH2 in the paraxial mesoderm (Novitch et al., 2003). RALDH2 is a synthetic enzyme that is important in the production of retinoic acid (Niederreither et al., 1999). The presence of RALDH2 expression is directly correlated with increased retinoid signaling in neural cells (Mendelson et al., 1991). The temporal switch from high FGF expression to RALDH2 expression directly coincides with the expression of ventral patterning genes in the neural tube. Neural tube explants cultured in RA selectively induce ventral patterning transcription factors (Pierni et al., 1999). Evidence also suggests that the joint exposure of FGF and RA is essential for the induction of ventral patterning genes that give rise to motoneuron progenitor cells (Novitch et al., 2003). *In vitro* and *in vivo* experiments have demonstrated that retinoid signaling is required to induce the expression of Olig2, a transcription factor that is a critical determinant for motoneuron differentiation. Explants cultured in either FGF or RA alone do not induce Olig2; however, explants cultured in both FGF and RA robustly expressed Olig2. Thus, retinoid and FGF signaling from mesodermal sources are required for motoneuron differentiation in early neural tube development.

1.2.2 Motoneuron organization and early morphological development.

Between stages 17-21 in limb innervating regions of the avian embryo, ventral progenitor cells exit the cell cycle and form immature post-mitotic motoneurons (Hollyday and Hamburger, 1977). When motoneurons leave the ventricular zone they migrate and segregate to specific

positions in the ventral spinal cord, and simultaneously develop axons that exit the neural tube ventrally. Motoneurons project axons to their targets in a very precise and stereotyped fashion. This pattern and sequence of events has been especially well delineated in the avian hindlimb. Between stages 18-21, motor axons grow to the base of the limb and stall at the plexus region for 24 hours. Subsequently, axons begin to segregate and sort themselves prior to entering individual limb muscle regions. Between stage 23 and 28, motoneurons form the dorsal and ventral nerve trunks, and project to specific muscles on the A-P axis (Lance-Jones and Landmesser, 1980; Tosney and Landmesser, 1984; see Figure 1).

In the spinal cord, motoneuron cell populations exhibit distinct A-P differences. The total number of motoneurons generated at the limb level is substantially greater than at the nonlimb level (Oppenheim et al., 1989). Additionally, motoneurons with common target projections are organized into columns that occupy distinct and discontinuous domains on the A-P axis. Along the A-P axis of the spinal cord, motoneuron subtypes can be distinguished molecularly, by their position in the transverse plane, and by their axonal projections to targets in the periphery (Figure 2). Thoracic (T) spinal segments contain Columns of Terni (CT) and Medial Motor Columns (MMC). The CT consists of motoneurons projecting to postganglionic sympathetic neurons (Levi-Montalcini, 1950; Prasad and Hollyday, 1991). In the T spinal cord, the MMC is subdivided into two subcolumns. Motoneurons innervating axial and body wall muscles are located in the medial MMC (MMCm) and lateral MMC (MMCl), respectively (Gutman et al., 1993). MMCm motoneurons are located at all segmental levels of the spinal cord but MMCl motoneurons are found only in the T spinal cord. Motoneurons innervating limb muscles are found in the Lateral Motor Columns (LMC), and are selectively generated at limb levels. Brachial and lumbosacral (LS) spinal segments, therefore, contain both LMC and MMCm motor columns. The LMC is further subdivided into subcolumns. The medial LMC (LMCm) and lateral LMC (LMCl) contain motoneurons that innervate ventral and dorsal limb muscles, respectively (Landmesser, 1978; reviewed by Jessell, 2000; see Figure 1).

Motoneurons that innervate specific individual muscles are functionally grouped together in discrete clusters termed motor pools. Retrograde labeling of motoneurons that innervate each limb muscle has demonstrated that motoneurons are arranged in stereotyped A-P and D-V positions within the MMC and LMC (Landmesser, 1979; Smith and Hollyday, 1983; Gutman et al., 1993).

During motoneuron development, the segregation of LMC motoneurons occurs by an "inside-out" migration. Early-born LMC motoneurons emerge out of the ventricular zone (VZ) and give rise to the LMCm. Subsequently, late – born LMC neurons leave the VZ and migrate past the LMCm motoneurons to arrive at their final destination as the LMCl (Hollyday and Hamburger, 1977).

1.2.3 Evidence of early specification of morphological features and projections

Morphological differences between limb (B and LS) and non-limb regions (T) of the spinal cord appears to be specified at early neural tube stages, prior to motoneurons birthdates (stage 17-21). When 3-4 segments of the LS neural tube are rotated along the A-P axis of stage 15 chick embryos, motoneurons develop reversed nerve projections that innervate targets associated with their former position (Lance-Jones and Landmesser, 1980). At later stages, motoneurons with altered A-P position continue to project to their original muscle targets. This finding demonstrates that at stage 15, the chick neural tube was irreversibly specified along the A-P axis. In contrast, A-P reversals performed earlier on stage 13 chick embryos lead to projections that correspond to the new position of motoneurons along the A-P axis, suggesting that at stage 13 the newly-closed neural tube can be respecified by the surrounding environment (Matise and Lance-Jones, 1996). Studies involving the displacement of T neural tube segments also provide evidence that regional programming occurs at or near the time of neural tube closure. When the T spinal cord is transplanted to the lumbar region at the time of neural tube closure, motoneurons in the transplanted T cord survive and initially differentiate in the same manner as it would in the normal T cord (O'Brien and Oppenheim, 1990). Taken together, these studies indicate that A-P identity of the neural tube is acquired early, prior to motoneuron birthdates, and that these graded positional values are linked to distinctive nerve patterns of somatic as well as visceral motoneurons (Laskowski and Sanes, 1987; Forehand et al., 1994; see Figure 2). A large body of literature indicates that Hox genes are important in establishing this early A-P identity.

1.2.4 Hox gene structure and expression.

Hox genes are vertebrate homologs of the Drosophila homeotic genes, and encode homeodomain –containing transcription factors. Homeotic genes were first isolated in *Drosophila* mutants that demonstrated defects in segmental identity (Akam, 1989). Here, mutations in homeotic genes like Antennapedia resulted in the conversion of the *Drosophila* antenna into a leg. Eight homeotic selector genes were identified in a single cluster in the *Drosophila* genome, and were found to be linearly arranged in a chromosome, in the exact order that these genes are expressed along the A-P axis. All Hox genes contain a highly conserved sequence of 183 nucleotides called the homeobox (Gehring et al., 1993). The homeobox encodes a 61 amino acid protein domain that folds into a helix-turn-helix motif, which in turn allows the Hox transcription factor to bind DNA and regulate the activity of other genes. Hox genes are highly conserved and have been identified in almost all major classes of animals. In higher vertebrates, Hox genes are arranged in 4 gene clusters or linkage groups (HoxA, HoxB, HoxC, and HoxD) found on different chromosomes (Mcginnis and Krumlauf, 1992, Krumlauf 1994). Within each cluster there are as many as 13 individual Hox genes, which are linearly arranged in a 3' to 5' order on the chromosome. Hox genes demonstrate both spatial and temporal colinearity (Duboule and Dolle, 1989; Izpisua-Belmonte et al., 1991). 3' Hox genes are expressed earlier and their anterior boundary of expression are found in more rostral areas. 5' Hox genes are expressed later in development and their anterior boundary of expression are found in more caudal regions of the embryo (Figure 3). Individual Hox genes that occupy the same linear position on the chromosome are referred to as paralogues (Hoxa10, b10, c10, and d10) (Krumlauf, 1994). Paralogues have a greater degree of homology with each other than with other Hox genes found in their linkage groups (Gaunt et al., 1989). For instance, Hoxa10 has a higher degree of sequence similarity to Hoxd10, than to Hoxa11. Although, paralogues are found on different chromosomes they have similar overlapping expression patterns (Carpenter, 2002).

1.2.5 Analyses of Hox gene function in the hindbrain

In vertebrates, Hox genes are expressed in overlapping A-P domains throughout the developing hindbrain and spinal cord. Much of what is known about the function of Hox genes

in neural tissue has been delineated by studies of hindbrain development. During development, the vertebrate hindbrain undergoes a segmentation process in which 8 rhombomeres(r) or hindbrain segments are formed along the A-P axis (Krumlauf., 1994). Each rhombomere has a distinctive character which is clearly evident in the development of motoneurons. The vertebrate hindbrain provides innervation to the muscles of the head and neck through a set of cranial nerves, which contain motor axons from motor nuclei within the hindbrain. Different classes of motoneurons match up with different rhombomeres, providing each rhombomere with a specific segmental identity. Motor nuclei in r1, r2, and r3 develop motor axons that converge to form the trigeminal nerve, which innervates 1st branchial arch muscles. Axons from motoneurons in r4 and r5 collect to form the facial nerve which innervates 2nd branchial arch muscles.

Individual anterior or 3'Hox gene expression patterns often coincide with rhombomere borders, raising the possibility that Hox genes establish rhombomere identity along the A-P axis. Targeted inactivation of 3' Hox genes results in altered or deleted rhombomere identities, and changes in motoneuron populations (Carpenter et al., 1993; Struder et al., 1996). Substantial data has been collected from loss-of- function studies of Hoxa1 and Hoxb1 in the hindbrain**.** Normally, both Hoxa1 and Hoxb1 have an anterior limit of expression at the r3-r4 boundary. The inactivation of Hoxa1 results in a partial loss of r4 and the deletion of r5. Hoxa1 mutants are largely missing facial motoneurons and the axons of the remaining facial motoneurons fail to converge to a single exit point at r4 (Carpenter et al., 1993). Hoxb1 mutants have a distinct and subtle defect (Goddard et al., 1996; Struder et al., 1996). In normal development, a subset of facial motoneurons generated in r4 migrates caudally to r5. In Hoxb1 mutants, facial motoneurons are generated normally but fail to migrate caudally to r5, and subsequently die. Finally, the Hoxa1-Hoxb1 double mutants exhibit more severe defects, with a loss of nearly all facial motoneurons (Struder et al., 1996; Gavalas et al., 1998; Gavalas et al., 2004).

The comparisons of the Hoxa1, Hoxb1, and double mutant phenotypes revealed several important traits about Hox genes. First, the phenotypes of each of the mutants demonstrate that Hox genes have multiple roles in the development of the hindbrain. Although both Hoxa1 and Hoxb1 are expressed very early in r4, the single inactivation of either of these genes does not entirely block the development of r4. Only double mutants of Hoxa1 and Hoxb1 fail to develop r4, suggesting that these genes act synergistically to promote r4 development (Struder et al., 1996; Gavalas et al., 1998; Gavalas et al., 2003). Also, while both Hoxa1 and Hoxb1 are

normally expressed from r4 to caudal regions, analyses of mutant mice demonstrated that patterning defects are found only within the anterior portions of their particular domains (Lufkin et al., 1991, Krumlauf, 1994). This observation suggests that Hox genes exert their primary influence within the anterior domain of their expression on the A-P axis.

3' Hox mutants exhibit a wide range of deficits including the loss of nerves, abnormal projections, fasciculation defects, and the departure of cranial nerves from erroneous exit points (Carpenter et. al., 1993; Goddard et al., 1996; Struder et al., 1998; Davenne et al., 1999). The complex nerve patterns observed in 3' Hox mutants are difficult to interpret as simple conversions in segmental identity. The complication may be due to fact that the majority of previous studies involved global manipulations of Hox genes. While Hox genes are expressed in motoneurons within the hindbrain, they are also expressed in peripheral tissue that motor axons encounter during projections to their targets. Evidence has suggested that Hox genes are involved in patterning peripheral tissue (Burke et al., 1995; Nowicki et al., 2000). Therefore, the abnormal development of motor projections after the global manipulations of Hox genes may be due to a loss of central Hox expression in motoneurons and/or a loss of peripheral Hox expression from surrounding tissue. One way to dissect the functional role of central vs peripheral Hox gene expression is to misexpress a single Hox gene in a tissue-specific manner. In a more direct test to examine the function of 3' Hox genes recent studies have ectopically expressed Hox genes in regions anterior to their normal domain. These studies demonstrated that the ectopic expression of a single Hox gene is able to induce ectopic motoneuron subtypes (Jungbluth et., al 1999; Bell et al., 1999; Guidato et al., 2003). The misexpression of either Hoxa2 or Hoxb1 induced *de novo* trigeminal or facial branchiomotor neurons, respectively. In addition, the results of rhombomere-restricted misexpression of Hox genes have more clearly linked segmental identity changes with altered nerve patterns. As mentioned above, Hoxb1 is normally expressed in r4 to more caudal regions, and r4 gives rise to facial motoneurons that innervate the second branchial arch. The misexpression of Hoxb1 in r2 induces ectopic facial motoneurons that project to the second branchial arch. Therefore, the ectopic expression of a posterior Hox gene can impart a posterior identity in dominating fashion over overlapping anterior Hox genes (Gonzalez-Reyes et al., 1990). In this thesis, I have used a similar restricted misexpression approach to gain an understanding of the function of Hoxd10 in the posterior spinal cord.

1.2.6 Analyses of Hox gene function in spinal cord

Recently, several studies have focused on the role of Hox in programming spinal cord identity. Normally, Hoxc8 is highly expressed in brachial motoneurons which innervate distal forelimb muscles. Targeted disruption of Hoxc8 results in mutant mice with severe deficits in forelimb locomotion and motoneuron development (Tiret et al., 1998). Hoxc8 mutant mice develop disorganized motor pools and an increased amount of apoptosis in brachial motoneuron populations. In addition, Hoxc8 mutant mice have a subset of cervical(C) C5-C6 motoneurons with misrouted projections. These motoneurons do not normally express Hoxc8, but their axons project through mesodermal regions that express Hoxc8. This raises the possibility that the misrouting of these motoneurons is not due to identity changes, but rather to altered axon pathfinding in the periphery due to a lack of Hoxc8 expression in the mesoderm (Tiret et al., 1998). There are other lines of evidence suggesting that Hox genes are important in establishing regional guidance cues for motoneuron pathfinding in peripheral tissue. For example, in the spinal cord, the ectopic expression of Hoxc6 in anterior lateral mesoderm results in the truncation of adjacent cervical spinal nerves suggesting that the peripheral expression of Hox genes in mesodermal cells may establish boundaries for axon outgrowth (Burke and Tabin 1996).

Studies that are most pertinent to the experiments described in this thesis are the loss-of-function studies involving the Hoxa10, Hoxd10 and double mutant animals. Mice carrying mutations in Hoxa10 display homeotic transformations of the vertebrae and spinal nerves. Hoxa10 mutants also develop an L1 vertebra with a T13 morphology (Rijli et al., 1995). Furthermore, these mutants have gross peripheral alterations in spinal nerves suggesting an anterior transformation of lumbar spinal nerves. Targeted inactivation of the paralogue, Hoxd10, also leads to homeotic transformations in skeletal and neural tissues (Carpenter et al., 1997). Hoxd10 mutants exhibit anterior transformation of the vertebrae at the sacral level. In the LS spinal cord, Hoxd10 mutant mice have a repositioned LMC, a reduced number of projecting motoneurons, and a possible anterior transformation of the L3 spinal segment. The Hoxd10/Hoxa10 double mutants have a greater level of motoneuron loss and peripheral nerve alterations (Lin and Carpenter, 2003). These observations suggest that Hox-10 paralogues work both synergistically and independently to pattern the LS spinal cord. This suggestion is further supported by analyses of nerve patterns from Hoxa10 and Hoxd10 mutant mice. Analyses of

Hoxa10 mutant mice revealed that mice developed a shortened tibial nerve with a lack of terminal branching. These findings indicate that Hoxa10 has a distinctive role in the lengthening and arborization of the tibial nerve (Wahba et al., 2001). In contrast, peripheral nerve patterns of Hoxd10 mutant mice exhibited specific defects which include: a severely reduced or absent deep peroneal nerve (which is part of the dorsal nerve trunk in the hindlimb), a thickened tibial nerve (which is part of the ventral nerve trunk in the hindlimb), axon fasciculation defects, and a loss of axons in peripheral nerves. These findings suggest that Hoxd10, rather than Hoxa10, has a prominent role in the development of peripheral nerve patterns (Wahba et al., 2001, Carpenter et al., 1997). However, no analyses of molecular identity or specific axon patterns have been made in Hoxd10 knockout mice, nor has Hoxd10 expression been specifically altered in the neural tube alone

In 1994, Tsuchida et al added a new dimension to studying the development of motoneurons by identifying LIM genes. These investigators showed that anatomically defined motoneuron subtypes can be molecularly distinguished by the combinatorial expression of LIM genes. Transplant experiments in chick embryos where either the neural tube or paraxial mesoderm was displaced between T and B levels demonstrated a transformation in molecular identity (LIM profiles) that matched changes in morphology and projection described earlier (see section 3, Ensini et al., 1998). Similarly in zebrafish, grafting individual primary motoneurons to different A-P levels results in a change in their identity as defined by LIM gene expression and respecified axon projections (Appel et al., 1994). Both these studies indicate that LIM profiles provide a reliable method for defining motoneuron identity. In this thesis, I have examined motoneuron columnar identity, after misexpressing a single posterior Hox gene, by looking for changes in LIM expression patterns. For this purpose, I have described LIM gene expression patterns and function in detail in the next section.

1.2.7 LIM transcription factors and the development of motoneuron subtypes

Studies in both invertebrates and vertebrates have shown that members of the LIM-HD family of transcription factors are expressed in distinct subsets of post-mitotic motoneurons (Thor and Thomas, 1997; Thor et al., 1991; Tokumoto et al., 1995). LIM-HD proteins have a DNA-binding domain and a protein motif that consists of N-terminus tandem repeats of two

cystine-rich metal-binding domains, known as LIM domains. The hallmark of the LIM domain is a modified Zn finger domain that can mediate protein-protein interaction (Dawid et al., 1998). There is evidence that LIM-HD proteins bind other nuclear factors and assemble into large complexes. The combinatorial expression of different LIM-HD proteins in post-mitotic motoneurons is thought to lead to the construction of homomeric and heteromeric complexes that activate unique differentiation programs (Thaler et al., 2002; Lee and Pfaff, 2003). Studies have identified four members of the LIM-HD family of transcription factors that have overlapping expression patterns in the embryonic chick spinal cord (Tsuchida et al., 1994): Islet 1 (Isl), Islet 2, Lim 1/2, and Lim3.

Islet 1. Isl 1 was first identified as a protein that binds to the enhancer region of the insulin I gene in rats (Karlsson et al., 1990). Immunocytochemical analysis of Isl1 expression in adult rats, demonstrated that the Isl 1 protein is expressed in motoneurons in the spinal cord and brainstem (Thor et al., 1991). In the embryonic chick spinal cord, Isl 1 is expressed in all motoneurons soon after their final cell division and before these cells display motoneuron properties (Ericson et al., 1992). This observation suggests that the early expression of the Isl 1 in developing motoneurons may contribute to the establishment of a motoneuron cell fate. Early-born MMCm, MMCl, and CT motoneurons begin expressing Isl 1 as early as stage 17 and continue to express Isl 1 past stage 35. In contrast, later born LMCm and LMCl motoneurons begin expressing Isl 1 at stage 18 and stage 20, respectively. LMCm motoneurons continue to express Isl 1 beyond stage 35, however, LMCl motoneurons extinguish Isl 1 expression by stage 24 (Tsuchida et al., 1994). Studies in both mice and chick suggest that Isl 1 is necessary for the generation of motoneurons. Isl 1 knockout mice exhibit a complete absence of motoneurons and the presence of apoptotic bodies at stages when Isl 1 is initially expressed. However, the misexpression of Isl 1 in the spinal cord does not lead to ectopic motoneuron generation, indicating that Isl 1 is necessary but not sufficient for motoneuron generation (Pfaff et al., 1996).

Islet 2. Soon after the discovery of Isl 1, Isl 2, an ortholog that showed 68% structural similarity to Isl 1 with roughly identical homeodomain regions, was isolated**.** Analysis of expression patterns indicate that Isl 2 is also transiently expressed in all motoneurons. All MMC and LMC motoneurons, except CT motoneurons, continue to express Isl 2 beyond stage 35 (Tsuchida et al., 1994). CT (visceral) motoneurons downregulate Isl 2, but maintain the expression of Isl 1. Loss of function experiments have demonstrated that the loss of Isl 2 does

not affect the generation of motoneurons. Isl 2 knockout mice showed normal early motoneuron differentiation; however, in later stages of motoneuron differentiation, Isl 2 mutant mice exhibited inappropriate migration and axonal projections of thoracic motoneurons (Thaler et al., 2004). Similarly, in zebrafish, the functional repression of Isl 2 in motoneurons resulted in abnormal soma positioning, loss of ventral projecting axons, and errors in neurotransmitter expression (Segawa et al., 2001). These observations suggest that *Isl 2* plays an important role in the terminal differentiation of motoneurons.

Lim 3. In the search for other LIM–HD proteins, Lim3 (also known as Lhx3) was found to be expressed in motoneurons and a dorsal subset of interneurons in the embryonic chick spinal cord. Like Isl 1 and Isl 2, Lim 3 is transiently expressed in all motoneurons that exit the cell cycle. However, all motoneurons, except MMCm subtype motoneurons, extinguish the expression of Lim 3 shortly thereafter between stages 17-20. MMCm motoneurons continue to express Lim 3 past stage 35 (Tsuchida et al., 1994). The forced maintenance of Lim3 in MMCl, LMC, and visceral motoneurons causes these cells to attain an MMCm identity and alters projections to axial muscles (Sharma et al., 1998). The early dynamic expression of Lim 3 is observed among only ventrally- projecting motoneurons and not dorsally-projecting motoneurons. In the mouse spinal cord, spinal accessory motoneurons project dorsally and innervate the neck and shoulder muscles. Lim 3 mutant mice have normal motoneuron differentiation; however, motoneurons that normally project ventrally altered their projections to exit the spinal cord dorsally. In chick embryos, the ectopic expression of Lim 3 in dorsally-projecting motoneurons causes these cells to alter projections to exit the spinal cord ventrally (Sharma et al., 1998). These findings indicate that the transient expression of Lim3 is a critical determinant of ventrally-projecting motoneurons, and the sustained expression of Lim3 is important in encoding MMCm identity in motoneurons.

Lim 1. Unlike the other LIM-HD proteins discussed, Lim1 is first expressed in only post-mitotic LMCl motoneurons. LMCl motoneurons are born between stages 19-22, and initially express Isl 1 (Whitelaw and Hollyday, 1983). Shortly after birth, LMCl motoneurons downregulate Isl 1 and begin to express Lim1 (stage 21- stage 35) (Tsuchida et al., 1994). Mice with targeted disruption of Lim 1 develop normal LMCl motoneurons with respect to motoneuron migration, soma patterns, and molecular profile. However, LMCl motoneurons of

Lim 1 mutant mice exhibit altered axonal projections, indicating that Lim 1 regulates axon pathfinding decisions of LMCl motoneurons in the periphery (Kania et al., 2000).

1.2.8 Establishing links between Hox genes and the establishment of motoneuron subtypes

Recent investigations of A-P patterning in the developing hindbrain have provided evidence that links Hox and development of specific motoneuron subtypes. For example, the ectopic expression of Hoxa3 in the anterior hindbrain induces somatic abducens motoneurons with a specific LIM profile (Guidato et al., 2003). Similarly, the ectopic expression of Hoxa2 and Hoxb1 induces branchiomotor neurons with a characteristic LIM profile (Jungbluth et al., 1999). Misexpression studies in the anterior spinal cord also suggest Hox genes affect LIM gene patterns and the columnar identity of motoneurons (Dasen et al., 2003). Hoxc6 is normally expressed in brachial spinal cord and Hoxc9 is restricted to the thoracic spinal cord. The ectopic expression of Hoxc6 into the thoracic spinal cord induced Lim1+ and RALDH2+ motoneurons, a molecular profile characteristic of motoneurons found within the brachial region. In contrast, the ectopic expression of Hoxc9 into the brachial spinal cord results in the loss of brachial LIM gene patterns and the development of thoracic –like LIM patterns. These results suggest that members of Hox-c gene family direct the expression of LIM genes, which in turn define motoneuron subtypes. These conclusions raise two important questions. How are Hox genes set-up and how are motoneuron molecular profiles translated into specific patterns of axon projections.

1.2.9 Secreted signaling molecules that set-up Hox and LIM genes.

FGF signaling and Hox genes in neural tissue. Recent studies have connected FGF signaling with the regulation of Hox genes in the spinal cord. FGFs are expressed by cells in developing tailbud or Henson's node. *In vitro* studies in which early stage chick embryos (HH7-9) were cultured in FGF showed an anterior shift in the expression of caudal HoxB genes (Hoxb6-Hoxb9) in the neural tube (Bel-Vialar et al., 2002). When these embryos were electroporated with an FGF dominant negative receptor and then cultured in FGF, the anterior

shift in caudal HoxB genes was blocked. This finding suggests that FGF signaling can mediate the activation of caudal HoxB genes in the neural tube. Similarly, the application of exogenous FGFs to spinal cord explants induces the expression of Hoxc6-Hoxc10 genes, and increasing the concentration of FGFs in culture progressively induces more posterior or 5' HoxC genes (i.e.Hoxc10) (Liu et al., 2001). More recent investigations have provided *in vivo* evidence that FGF signals regulate Hox gene expression. The ectopic expression of FGF8 in the brachial spinal cord of chick embryos results in an anterior shift of 5' Hox genes. These findings support a hypothesis in which nodal-derived (tailbud) FGFs produce graded signals that regulate the expression of 5' Hox genes in spinal motoneurons.

RA signaling and Hox genes in neural tissue. RA appears to regulate Hox expression at both hindbrain and spinal levels. During early gastrulation RA is produced by mesodermal cells adjacent to the node and primitive streak. Later during somitogenesis, RA synthesis becomes restricted to the surrounding mesoderm. Levels of RA peak in the paraxial mesoderm at the spinal cord/hindbrain boundary, with gradually decreasing levels in posterior direction (Niederreither et al., 1997, Swindell et al 1999; Berggren et al., 1999). In the hindbrain, excess RA causes a homeotic transformation of r2/3 to r4/5. This posterior transformation is accompanied by an anterior shift in 5' or posterior Hox genes (Marshall et al., 1992; Simeone et al., 1991; Conlon and Rossant, 1992; Kessel and Gruss, 1991). Conversely, experiments that have blocked RA- signaling result in the anteriorization of rhombomeres in the hindbrain. Furthermore, genetic studies have identified retinoic acid response elements (RARE) in the regulatory regions of Hox genes indicating that RA directly influences the expression of Hox genes (Marshall et al., 1994; Struder et al., 1998).

Growing evidence indicates that the role of RA in the caudal neural tube may be different than RA at anterior levels. During stages when AP identity is acquired, the presence of RA and RALDH2 is high in the anterior paraxial mesoderm but low in posterior paraxial mesoderm (Berggren et al., 1999; Swindell et al., 1999; Maden et al., 1998). Prior studies have shown that early RA signaling has a posteriorizing effect on neural tissue and appears to define a generic spinal cord identity in the developing CNS (Muhr et al., 1999). A more recent study demonstrated that RA also has a later role in establishing segmental identity within the spinal cord. The exposure of spinal cord explants to increasing levels of RA induced 3' Hox genes and repressed 5' Hox genes (Liu et al., 2001). This finding suggests that RA regulates Hox gene

expression to impose an anterior spinal identity rather than a posterior spinal identity within the developing spinal cord.

There is strong evidence that RA regulates Hox gene expression during early stages of motoneuron development, however, the effects of RA and Hox genes on developing axon projections is not well understood. Prior studies have demonstrated that manipulation of retinoid signaling by either excess RA or an RA synthesis blocker (citral) in the paraxial mesoderm, leads to alterations in the segment-specific nerve patterns of preganglionic sympathetic neurons (Forehand et al., 1998). The altered projections of preganglionic sympathetic neurons suggest that retinoids can induce changes in the intrinsic identity of these neurons at different spinal segments along the AP axis. Forehand et al. (1998) have suggested that Hox genes are a possible molecular link between the RA and the altered nerve patterns of preganglionic sympathetic neurons. Very little is known on how RA and Hox genes affect the motor axon projections into the limb.

RA signaling and LIM genes in neural tissue. Recent studies have demonstrated that RA is also expressed by motoneurons, and that RA signaling is involved in motoneuron specification by setting up LIM-HD expression patterns. Transgenic studies using RA reporters to label RA activity demonstrated that retinoid signaling occurs in paraxial mesoderm during periods of early neuronal differentiation and later in the ventral spinal cord at limb levels (Rossant et al., 1991). To define the contribution of retinoid signaling during periods of motoneuron differentiation, expression studies examined the spatiotemporal patterns of RALDH2. RALDH2 expression is first initiated during the early phase of motoneuron generation at limb levels of the chick spinal cord. Expression studies showed that RALDH2 expression is restricted to the ventral motor column, and precedes the presence of Isl2 (+), Lim 1(+) LMCl motoneuron (Sockanathan and Jessell, 1998). As cells withdraw from the cell cycle, all post-mitotic somatic motoneurons express Isl 1 and Isl 2. Later-born motoneurons destined to become lateral LMC motoneurons extinguish Isl 1 expression and begin to express Lim 1. The switch in LIM genes expression appears to be dependent on retinoid signaling by early born LMC motoneurons. *In vitro* and *in vivo* experiments demonstrated that the exposure of motoneurons to retinoids inhibits the expression of Isl 1 and promotes the upregulation of Lim 1. Ectopic *in vivo* expression of RALDH2 by retroviruses in thoracic spinal cord results in LMCl motoneuron induction; however, the RALDH2(+) cells did not overlap with Isl 2 (+) Lim 1 (+)

LMCl neurons. This finding suggests that RA can induce LMCl neurons in a non-cell-autonomous manner (Sockanathan and Jessell, 1998). Analysis of the RALDH2 mutant embryos also revealed a loss of Lim 1(+) brachial motoneurons and severe alterations in the settling patterns of Isl 1(+) cells (Vermot et al., 2005).

1.2.10 The growth cone and general mechanisms of axon pathfinding

In the developing embryo, growing axons must navigate through an increasingly complex environment and reach their appropriate targets without any errors. The tip of the growing axon has a specialized structure called the growth cone. The growth cone is a highly dynamic structure consisting of actin-bundled filapodia that make spoke-like protrusions into the periphery (Sanes et al., 2000). Growth cones of motoneurons have the ability to sense their environment and respond to cues by growth-cone steering and axonal extension. Guidance molecules can be classified as short-range or long-range cues that have either positive or negative effects on the growth cone. Short-range guidance cues act locally within close proximity to the growth cone to elicit an effect; conversely, long-range guidance cues are diffusible molecules that act over some distance (Tessier-Lavigne and Goodman, 1996). A large amount of data concerning the behavior of growth cones and their interaction with guidance molecules has been measured and manipulated in cell culture experiments (Gundersen and Barrett, 1979). A positive or chemoattractive guidance cue will promote the extension of an axon towards the source of the attractant. In cell culture, when growth cones are exposed to a gradient of a diffusible chemoattractant, they are able to grow or orient themselves towards the source. These findings indicate that growth cones can detect differences in concentrations of the chemoattractive guidance cue which they can translate into axon extension and directional information. In contrast, negative or chemorepulsive cues will inhibit or repel the extension of an axon. When growth cones contact certain chemorepulsive cues, they retract their filapodia and temporarily become paralyzed, or collapsed (Kapfhammer and Raper, 1987). Alternatively, growth cones can respond to chemorepulsive cues by repelling the growth cone in the opposite direction without collapsing it (Fan and Raper, 1995). While, tissue experiments have been useful in identifying guidance cues that influence that rate and direction of axonal growth, understanding how these diverse cues are integrated *in vivo* to guide developing axons to their targets remains unclear.

1.2.11 Evidence of specific and general guidance cues within the limb.

Many of the cellular and tissue interactions that affect motor axon pathfinding have been extensively analyzed in the avian embryo. In vertebrates, coordinated movement is dependent on the ability of hundreds of motoneurons to selectively send axons to appropriate target muscles. Early studies that manipulated motoneuron position and limb targets in chick embryos revealed the existence of both specific and general guidance cues within the limb. In a set of experiments where small portions of the lumbosacral (LS) neural tube at stage 15 were rotated along the anterior-posterior (A-P) axis, dislocated motoneurons were able to make novel trajectories and project to their appropriate targets (Lance-Jones and Landmesser, 1981). Similarly, studies where the limb buds were rotated along the dorsoventral (D-V) axis also revealed that motoneuron axons innervated their appropriate muscle targets (Ferguson, 1983). Both of these observations suggest that axons are able to compensate and project to their appropriate targets because their growth cones dynamically respond to target-specific guidance cues within the limb.

Although A-P rotations of small number of LS segments suggest the presence of target-specific guidance cues, A-P rotation experiments with the entire LS segment suggest otherwise. In AP rotations with large displacements of LS segments, some displaced motoneurons sent projections to their appropriate targets (Lance-Jones and Landmesser, 1981). However, other displaced motoneurons were restricted to the anatomical pathways appropriate for that foreign limb region, and thus sent projections to foreign limb targets. Several studies have also shown that distal limb bud rotations along the D-V axis cause motoneurons to send projections to foreign targets. These findings suggest that growth cones of motoneurons were constrained to a defined anatomical pathway that normally develops in that region of the limb (Summerbell and Stirling, 1981; Whitelaw and Hollyday, 1983). In summary, manipulation of motoneuron positioning and limb targets has revealed that there are permissive signals in the periphery that establish anatomical limits by which motor axons passively travel along defined nerve pathways. There are also instructive signals that guide migrating axons to their appropriate targets.

1.2.12 Factors affecting exit from the spinal cord and spinal nerve formation.

As post-mitotic motoneurons leave the ventricular zone and terminally settle in the ventral spinal cord, they simultaneously undergo axogenesis. Soon after axogenesis, motor axons are required to make pathfinding decisions along the AP and DV axes (Schneider and Granato, 2003). Newly developed axons move away from the floor plate and pierce through the neuroepithelium at specific exit points to enter the periphery. Collagen co-culture experiments, where ventral spinal cord explants are grown adjacent to floor plate cells demonstrated that motor axons grow away from the floor plate (Guthrie and Pini, 1995). Recent studies identified several diffusible guidance cues from the floor plate, including semaphorins and slits that have a repellant effect on developing motor axons. Cell aggregates that express either SEMA2A or Slit2 can repel spinal motor axons from long distances (Varela-Echavarria et al., 1997; Brose et al., 1999). These observations suggest that the floor plate is the primary source for the chemorepellant effect that causes newly developed motor axons to move laterally towards the exit point.

During spinal cord development, all spinal motor axons within a segment leave the spinal cord through a single ventral root. Thus, motor axons are organized to exit the spinal cord at specific points, along the AP axis, through a series of segmental nerves (Keynes and Stern, 1984). The segmental nerve pattern of the spinal cord suggests that motor axons recognize the appropriate AP level to properly exit the spinal cord. Evidence from prior studies indicated that the somatic mesoderm is involved in establishing guidance cues that are responsible for the segmental nerve pattern. Researchers observed that motor axons only passed through the rostral sclerotome within each somatic hemisegment. Anterior-posterior rotations of somatic mesoderm demonstrated that motor axons altered their trajectories and traveled only through the posterior (originally the rostral sclerotome) half of the somite (Keynes and Stern, 1984). These observations suggest that motor axons preferentially migrate through the rostral half of the somatic mesoderm and avoid entering the caudal half of each somite. In experiments where the somatic mesoderm is ablated, motor axons lose their segmental nerve pattern and exit at all rostrocaudal levels, suggesting that somitic guidance cues are chemorepulsive in nature (Oakley and Tosney, 1993; Tannahill et al., 1997). There is now considerable evidence that the segmental nerve pattern of motor axons is accomplished by the chemorepulsive activity derived from the

caudal sclerotome. Molecular candidates for the chemorepulsive effect of the caudal sclerotome include contact-mediated repulsive cues, extracellular matrix molecules (ECM), and cell adhesion molecules.

Several studies have shown that the tyrosine kinase receptors of Eph family and their membrane-bound ligands participate in short-range contact-dependent axonal guidance. There are two subclasses of receptors, EphA and EphB. EphA receptors preferentially bind Ephrin A ligands which are tethered to the membrane. In contrast, EphB receptors preferentially bind Ephrin B ligands which are transmembrane proteins. In chick embryos, Ephrin-B1 and Ephrin-B4 ligands are expressed in the caudal sclerotome, and motor axons express the corresponding EphB2 and EphB3 receptors (Wang and Anderson, 1997; Kilpatrick et al., 1996; Ohta et al., 1996). Semaphorins are another large family of molecules that are found in both membrane-bound and secreted forms. Semaphorins bind to the neuropilin receptor to transduce either chemoattraction or chemorepulsion (He et al., 1997). *In vitro* experiments showed that both ephrins and semaphorins can cause motoneuron growth cones to collapse (Koblar et al., 2000; Vermeren et al., 2000; Varela-Echavarria et al., 1997) However, the removal of ephrins and semaphorins does not alter the segmental pattern of motor axon outgrowth suggesting that there are multiple redundant mechanisms that mediate the barrier repellant effect of the caudal sclerotome**.**

Many studies have identified ECM and cell adhesion molecules that are distinctively expressed in the caudal sclerotome. The following ECM molecules have restricted expression in the caudal sclerotome: Peanut agglutinin (PNA)-binding glycoproteins, Chondroitin sulfate proteoglycans, Collagen IX, Tenascin-C, and F-spondin. In cell culture experiments, each of these molecules has the ability to inhibit motor axon outgrowth (Oakley and Tosney, 1991; Debby-Brafman et al., 1999, Yip and Yip, 1995; Martini and Schachner, 1991). Similarly, T-cadherin is a cell adhesion molecule expressed in the caudal sclerotome. Soluble T-cadherins can inhibit motor axon outgrowth *in vitro*, and function-blocking antibody to T-cadherin can block this inhibition (Fredette et al., 1996). While there is evidence that these ECM and cell adhesion molecules in the caudal sclerotome contribute to the inhibition of growing motor axons *in vitro*, how these molecules are responsible for segmental patterning of motor axons *in vivo* remains unclear.

1.2.13 Factors affecting axon growth into the limb.

Prior studies have also shown that limb mesoderm secretes molecules that can attract developing spinal motoneurons. Hepatocyte Growth factor/scattering factor (HGF/SF) is multifunctional growth factor that is expressed in the developing wing and hindlimb of chick embryos. RT-PCR studies demonstrated that HGF/SF is highly expressed in chick limb muscles during axon outgrowth (Ebens et al., 1996, Novak et al., 2000). Motor axons express the HGF/SF receptor, c-Met, as they invade the limb mesenchyme (Sonnenberg et al., 1993; Novak et al., 2000). Several lines of evidence indicate that HGF/SF is an axonal chemoattractant and neurotrophic factor for lumbar spinal motoneurons. In spinal cord explants co-cultured with cells that express HGF/SF, there is excessive motoneuron outgrowth and chemoattraction of axons towards HGF/SF secreting cells (Ebens et al., 1996). In spinal cord slices, limb derived chemoattraction was found to be mediated by HGF/SF, and can be inhibited by antibodies to HGF/SF (Ebens et al., 1996). Additionally, LS motoneurons, but not brachial or thoracic, displayed a dose-dependent increase in motoneuron survival *in vitro* (Yamamato et al., 1997; Novak et al., 2000).

1.2.14 Factors affecting axon pathfinding at choice points.

As mentioned previously, migrating motor axons exit the spinal cord as segmental spinal nerves. The proximal segments of the spinal nerve consist of motor axons from different motor pools that are spatially intermixed and travel fasciculated together along a common path. However, further along their common pathway, migrating motor axons reach certain “decision” or “choice points”, where individual motor axons can respond to specific guidance cues in these regions. Chick hindlimb segmental spinal nerves, which contain a medley of LMCm and LMCl axons, converge at the base of the limb to form two lumbosacral plexi, the crural and sciatic plexi. Studies have shown that when migrating axons reach the plexus region, they defasciculate, distinctively re-sort themselves into muscle-specific fascicles, and depart the plexus as dorsal and ventral nerve trunks. (Landmesser, 1978; Lance-Jones and Landmesser, 1981; Tosney, 1991). Soon afterwards, motor axons in the nerve trunks encounter other choice points and send

out intramuscular nerves to innervate specific muscle fibers in a stereotyped manner. The observed motoneuron nerve pattern suggests that motoneurons have acquired motor-pool specific identities by the time of their initial outgrowth, such that their axons can differentially respond to specific guidance molecules.

When migrating motor axons reach the plexus mesenchyme, they appear larger, lamellipodial, and convoluted in trajectory. This observation suggests that when migrating axons enter the plexus region their axons defasciculate and undergo a process of dynamic rearrangement. During this process, axons begin to sort into groups destined for different targets. Even when distal tissues are ablated, motor axons can sort out in the plexus region, indicating that these guidance cues are found locally (Tosney and Landmesser, 1984, 1985). Studies have identified molecules that maybe involved in the sorting of motor axons at the plexus region. There is evidence that NCAM, a cell surface recognition molecule, is involved in the selective re-assortment of the motor axons within the plexus. Instead of changing the expression levels of NCAM, proper axon fasciculation is achieved by the modifying the polysialic acid (PSA) residues found on NCAM. PSA modification diminishes homophilic interactions of NCAM. Within the plexus, migrating axons that project dorsally have higher levels of PSA expression than ventrally projecting axons. The enzymatic removal of PSA *in ovo*, leads to increased fasciculation of axons in the plexus, which interferes with the ability of growing axons to respond to directional guidance cues (Tang et al., 1994). Also, studies have shown that semaphorin signaling appears to mediate axonal adhesion to some extent within the plexus. Mice with targeted disruption of either semaphorin or neuropilin exhibit a high degree of defasciculation and erroneous projections at the plexus (Taniguchi et al., 1997; Kitsukawa et al., 1997; Giger et al., 2000).

At the plexus, the decision of axons to choose a dorsal or ventral trajectory is to a certain extent dependent on Ephrin/Eph signaling. Expression studies have shown that Eph A subfamily receptors and their ephrin ligands have dynamic expression patterns in subsets of motoneurons and muscle targets (Ohta et al., 1997). The EphA4 receptor kinase is strongly expressed by LMCl motoneurons and their axons that project into the dorsal limb. At stage 21 (E3), all axon projections to the base of the hindlimb express EphA4. By stage 23, EphA4 is selectively expressed in axons projecting into the dorsal nerve trunk of the crural plexus (Eberhart et al., 2002). The ventral limb mesenchyme expresses two EphA4 ligands, Ephrin-A2 and Ephrin-A5

(Ohta et al., 1997). The interaction of EphA4+ motor axons with Ephrin-A2 and Ephrin-A5, leads to the chemorepulsion of EphA4+ axons into the dorsal trajectory (Eberhart et al., 2004). EphA4 mutant mice have LMCl motoneurons that misproject into the ventral nerve trunk, suggesting that the lack of inhibitory signaling results in aberrant projections into the ventral limb (Helmbacher et al., 2000). The ectopic expression of EphA4 in LMCm motoneurons, which normally project in the ventral nerve trunk, alters their projections towards a dorsal trajectory into the limb (Eberhart et al., 2002).

1.2.15 Establishing links between Hox genes and axon guidance.

Hox mutants exhibit very complex anatomical nerve patterns, including abnormal fasciculation, truncated or missing nerves, and altered nerve trajectories (Carpenter et al., 1993; Goddard et al., 1996; Gavalas et al., 1998). How Hox genes affect the development of motor projections is not well understood. Until recently, only one study has ectopically expressed Hox genes in developing neural tissue and showed specific changes in trajectory that correspond to new molecular identity (Bell et al., 2001). There are several possibilities on how Hox genes can influence axon pathfinding.

Hox-mediated changes to LIM gene expression could lead to changes in EphA/Ephrin patterns. Recent studies have linked LIM-HD transcription factors to axonal pathfinding. The misexpression of Lim1 in the LS spinal cord is able to induce high levels of EphA4 expression in LMC motoneurons (Kania and Jessell, 2003). These findings demonstrate that transcription factors involved in motoneuron specification are also functionally linked to guidance cues involved in axon pathfinding. In addition, studies of the Hoxa1 and Hoxb1 mutants have also shown that Hox genes regulate the expression EphA receptor in the hindbrain, suggesting that Eph/ Ephrin interactions are a possible target of Hox encoded information (Struder et al., 1998).

There is emerging evidence that has linked Hox genes with the expression of Slit/Robo and HGF/c-met signaling. Studies in the development of Drosophila embryonic sense organs have provided evidence that Hox genes regulate Slit-Robo expression and the segment-specific migration of sensory neurons (Kraut and Zinn, 2004). Investigations into the development of the mammary gland suggest that Hox genes affect HGF/c-met signaling which promotes branching of the epithelial ductal system in the mammary mesenchyme (Chen and

Capecchi, 1999). A central aim of this study was to detail molecular profiles and axon projections in a well characterized system and we specifically chose to examine the role Hoxd10 in the posterior spinal cord

1.2.16 Hoxd10 in the Posterior Spinal Cord

In the avian embryo, *Hoxd10* is expressed at high levels is the LS region, from the early stages of motor column formation to the late stages of motor neuron outgrowth. Experiments involving the transposition of LS and T segments show that *Hoxd10* expression is programmed within the LS region, at or around the time of neural tube closure and at stages when motoneuron projection patterns are also known to be programmed (Lance-Jones et al., 2001; Omelchenko and Lance-Jones, 2003; Matise and Lance-Jones, 1996). Data suggests that the tail bud provides inductive signals that program Hoxd10 in early neural tube stages (Omelchenko and Lance-Jones, 2003). Hoxd10 is initially expressed at low and diffuse levels in the newly closed lumbosacral spinal cord. Subsequently, high levels of Hoxd10 expression are observed in the ventral motor column, during stages of motoneuron birthdates and the initiation of motor axon outgrowth. As the LS motor column expands and motoneurons extend axons into the limb, all LS segments, adjacent paraxial mesoderm, and hindlimb mesoderm show high *Hoxd10* expression, while T segments show no Hoxd10 expression (Lance-Jones et al., 2001).

The above observations raise the possibility that Hoxd10 plays a role in the encoding of an LS motoneuron identity. Few studies have examined Hox gene function at caudal spinal levels, and furthermore, no analyses of motor projections or molecular profiles have been made after the ectopic expression of a Hox gene in the posterior neural tube. To test the hypothesize that Hoxd10 imparts an LS character to the segmental organization of motoneurons and their specific axonal trajectories, I have ectopically expressed Hoxd10 in the T spinal cord and analyzed changes in molecular profiles and axon projections of spinal motoneurons.

2.0 METHODS AND MATERIALS

2.1 EMBRYOS

Fertilized White Leghorn chick eggs (SPAFAS or CBT farms) were incubated at 38 ˚ C in a forced-draft incubator for 2-2.5 days. Eggs were candled, to mark the position of the embryo, and windowed. The vitelline membrane was removed and a dorsal application of 0.5 % neutral red stain was used to visualize embryos. Embryos were staged by number of somites and the Hamilton and Hamburger (H&H) stage series. Embryos ranging from stage 12 (15-18 somites) to stage 18 (tailbud morphology) were selected for electroporations. Presumptive thoracic and lumbosacral segmental levels were identified with respect to adjacent somites or somite-equivalent length of paraxial mesoderm.

2.2 HOXD9/EGFP, HOXD10/EGFP, AND EGFP EXPRESSION CONSTRUCTS

The PMES vector (5.5 kb), a construct that leads to the expression of enhanced green fluorescent protein (EGFP) alone was kindly provided by C. Krull. This construct was made by placing an IRES-EGFP sequence from pIRES2-EGFP (Clonetech) into a pCAX vector. The pCAX vector drives the expression of EGFP under the control of the ß-actin promoter/ CMV-IE enhancer. This construct was used as an EGFP control in our experiments. Experimental constructs Hoxd9/EGFP and Hoxd10/EGFP was made by placing a full length chick Hoxd9 (1.26 kb) and Hoxd10 (1.7 kb), respectively, into the PMES construct. The Hoxd9 and Hoxd10 cDNA was provided by C. Tabin (Appendix D).

Eluting DNA. In a sterile eppendorf, DNA was eluted from filter paper in 100 ul of TE (pH 8.0), vortexed and incubated at 4˚C overnight. **Transformation.** 100 µL of competent cells

(bacterial vector has Amp resistance) were thawed and placed on ice for 15 minutes. DNA was spun and brought to the bottom of the tube. 5 µL of DNA was taken off the top of solution, and added to 100 µL of cell in chilled tubes. Cells and DNA were incubated in ice for 30-45 minutes. This mixture was heat-shocked at 42˚C for 90 seconds, and placed on ice for 2 minutes. 800 uL of 1x L- broth was added to the mixture, and then test tubes were shaken at 37˚C for 45 minutes. 100-200 uL of the mixture was plated on LB-Amp plates and incubated overnight at 37˚C. Colonies were obtained and a Filter Maxiprep (Qiagen) was performed to isolate the DNA of interest. PMES, Hoxd9, and Hoxd10 were all isolated. **Linearization.** Hoxd9, Hoxd10 and PMES were all linearized with an EcoR1 restriction enzyme. DEPC water, restriction enzyme buffer, BSA and PMES plasmid were warmed to room temperature. Individual mixtures were digested in EcoR1 at 37 ˚C for 1 hour. Diagnostic gels were performed and DNA of interest was identified. Next, the DNA of interest was excised from the gel and a Qiagen extraction protocol was performed. Extraction procedure allowed for the isolation of linearized DNA. **Ligation.** To ligate the insert (Hoxd9 or Hoxd10) into the vector (PMES), varying concentration of the insert, vector, Ligase (T4), and buffer were placed into several test tubes, including controls (either insert or vector alone). A diagnostic gel was run to identify sense and antisense ligation products**.** To distinguish the sense and antisense products of the Hoxd10-PMES ligation, a diagnostic digest was performed using 2 uL of the mini-prepped DNA (eluted to 50 uL). Hoxd10/PMES was cut by the Sal I and Bgl II restriction enzymes, and products of the ligation were run on a gel. To distinguish the sense and antisense of the Hoxd9/PMES ligation, a diagnostic digest was performed using 2 uL of the mini-prepped DNA. The Hoxd9/ PMES construct was cut by the SmaI restriction enzyme and products of this ligation were run on a gel.

2.3 *IN OVO* ELECTROPORATION AND EMBRYO SACRIFICE

For our electroporations, either EGFP DNA (0.625 -2.5µg/µL)**,** Hoxd10/EGFP DNA (0.625 -2.5 µg/µL), or Hoxd9/EGFP DNA (1.25 -2.5 µg/µL) was injected into the newly closed neural tube at posterior axial levels of stage 12-18 (embryonic day 2-3) chick embryos. Once injected, saline solution was quickly administered. Either gold or platinum electrodes (0.5mm) were placed on either side of neural tube and a square-pulse electroporator (BTX) was used to

deliver current (3 pulses of 50 ms duration, 15-17 charging voltage). Embryos were sacrificed at stage 16-29, placed in a cold saline and quickly decapitated. Posterior embryonic regions were immediately examined under a compound or inverted microscope for evidence of EGFP expression. Only embryos showing high EGFP expression were used for analyses.

Embryos were fixed in 4% paraformaldehyde/PBS for 2-8 hours at 4˚C. Subsequently, embryos were washed in 1X PBS (3 times for 10 min), followed by a 1 hour wash in 1xPBS at 4˚C. Embryos were transferred to 30% sucrose in PBS for 4- 6 hours or overnight, and then mounted in 50:50 OCT/30% sucrose. Embedded blocks mounted with OCT/30% sucrose were stored at -80˚C until sectioning. All blocks were sectioned at approximately -28˚C using a Leica cryostat. 14 μm sections were placed on slides, and slides were stored at -80˚C.

2.4 IMMUNOHISTOCHEMISTRY

Slides containing sectioned spinal tissue were placed in blocking buffer and incubated for 1 hour at room temperature. Blocking buffer was removed and sections were covered with 1° antibodies, diluted in blocking buffer and incubated overnight at 4°C. Antibodies used included rabbit anti-GFP 1:1500 (Molecular Probes), mouse anti-LIM 1:10, mouse anti-Islet 1/2 1:25 (Developmental Hybridoma), rabbit anti-RALDH-2 1:2500 (from P. McCaffery, Berggren et all 1999), rabbit anti-Lim1 1:10000 (from T. Jessell lab), anti mouse-Lim3 , anti-rabbit Lim1 (Chemicon) (1: 500), and anti-rabbit activated caspase-3 (Promega). Next, slides were washed 3X10 min in 1X PBT (0.02%Triton). Slides were covered with 2° Ab diluted in blocking buffer and incubated at room temperature for 2 hours.(Cy2 anti-rabbit 1:1000, Cy3 anti-mouse 1:1500, Cy2 anti-mouse 1:1000, Cy3 anti-rabbit 1:1500). Slides were then washed 3 X 5 min in 1X PBS. Sections used for cell counts were incubated in DAPI for 1 minute and then washed 3X5 min in 1X PBS. Slides were mounted with Fluoromount G and stored at 4°C in the dark. Tissue processed for DAB staining are described below.

2.5 *IN SITU* HYBRIDIZATION

A standard DIG label *in situ* hybridization protocol (Jonathan Lin /T. Jessell lab), modified from by Schaeren-Wiemers and Gerfin-Moser (1993) was used for tissue sections. Steps were taken to assure that all solutions were made in RNase free water through hybridization steps of the procedure. Glassware was rinsed and made RNase- free by DEPC treatment.

Tissue preparation. Before processing, slides were dried for 1- 3 hours at room temperature. Slides were then fixed in 4% paraformaldehyde/PBS for 10 minutes at room temperature, followed by washes with PBS 3X3 min. Slides were digested in proteinase K (1 μg/ml in 50 mM Tris 7.5, 5mM EDTA) for 3-4 min at RT, and then fixed in 4% paraformaldehyde/PBS for 5 min at RT. Next, slides were washed with PBS 3X3 min and then acetylated (295 ml H2O, 4ml triethanolamine (Fluka 90279), 0.525 ml HCL, 0.75 ml acetic anhydride) for 10 min at room temperature. Slides were washed with PBS 3X5 min.

Hybridization. Slides were placed individually in a humidity chamber and covered with hybridization buffer (50% formamide, 5X SSC, 5X Denhardt's reagent, 250μg/ml Baker's yeast RNA, 500μg/ml Herring sperm DNA). Slides were incubated at room temperature for 2 hours in the humidified chamber, horizontally. The pre-hyb buffer was removed, and replaced with at least 80μl per slide of hybridization buffer containing probe at 200-400 ng/ml DIG RNA, and coverslipped (1:100 for *Islet ,* 1:100 *Hoxd10,* 1:75 *c-met,* 1:75 *Hoxd9*). Diluted probe was initially heated to 80˚C for 5 min on the block heater and then iced before use. Coverslipped slides were placed in humidified chamber overnight at 72˚C, saturated with 5xSSC/50% formamide.

Immunological staining. Slides were submerged in 150 ml beaker of 72˚C 5X SSC for 5 minutes and coverslips were removed. The slides were transferred to 0.2 X SSC at 72˚C for 1-3 hours and then washed with 0.2X SSC at room temperature for 5 min. Slides were next placed in B1 buffer (0.1M Tris-HCl pH 7.5, 0.15M NaCl) for 5 min at RT, and then covered in 10% heat inactivated sheep serum in B1 and incubated at room temperature for 1 hour. After the incubation, anti-DIG Ab (1:5000 dilution in B1 + 1% sheep serum) was placed on each slide, and slides were placed in humidified chamber at 4˚C overnight.

Next, slides were washed with B1 3X 5 min, and then equilibrated with B3 (0.1M Tris-HCl pH 9.5, 0.1M NaCl, 50mM $MgCl_2$) for 5 minutes. 80 µl of B4 (100 mg/ml NBT, 50 mg/ml BCIP, 0.24 mg Levamisole) was placed onto parafilm in plastic tray and on each slide was inverted carefully into the B4 solution. Slides were placed in humidified chamber and incubated in a dark room at room temperature for 6 hours to 3 days. Reaction was stopped with 1x PBS and washed 3 X5 min. After a final rinse with water, slides were mounted with aqueous mounting medium.

Double Immunohistochemistry /In situ Hybridization Procedure. After *in situ* processing, slides were washed 3 X 5 minutes in 1X PBS followed by a wash in MilliQ water for 1 hour to overnight. These slides were then covered with blocking buffer (1% goat serum, 0.2% Triton X-100, 1% BSA in 1X PBS) for 1 hour at room temperature. Slides were incubated with primary antibodies overnight at 4˚C. Primary antibodies were removed and slides were washed 3 x 5 min by 1X PBS. A biotinylated secondary antibody, from a Vectastain kit (1 drop in 10 mL of blocking buffer), was added to the slides and incubated 1.5 hours at room temperature. The kit's ABC reagent (2 drops of reagent A, 2 drops of reagent B in 5 mL PB) was made, mixed well, and allowed to sit at least 30 minutes before using. Slides were washed 3 x 5 min with 1X PBS and then incubated in the ABC reagent for 1 hour at room temperature. Slides were washed 3 x 5 min 1X PBS, and then with PB (10mM sodium phosphate, 0.9% saline) for 5 minutes. A Vector DAB kit was used for further processing according to manufacturing instructions. DAB solution was made wearing gloves in hood and in the dark (DAB solution: 2 drops of buffer to 5 mL MilliQ water, 4 drops of DAB stock solution , 2 drops of hydrogen peroxide solution). Slides were incubated in a DAB solution until the desired intensity of stain was obtained. The DAB solutions were then removed and slides were washed five times with 1X PBS. Finally, slides were rinsed with MilliQ water for 3 minutes and coverslipped with Gel/mount.

Transcribing DIG-labeled RNA probe. Sterile water (up to 20µl), transcription buffer (10X 2µl), DIG RNA labeling mix (2µl, BM/Roche), and linear plasmid (1µg determined from gel) were placed in 0.5 ml eppendorf tubes at room temperature and mixed. Test tubes were incubated in 37°C water bath for 2 minutes. Then sequentially, Rnase inhibitor (0.5µl of 40U/µl, Promega) and Polymerase (2µl of 20U/µl) were added and mixed in the test tube. The test tube was incubated in 37°C water bath for 2 hours. Then 0.2 M EDTA (2µl at pH 8) was added to the test tube and vortexed. Next, 4 M LiCl (2.5µl) was added to the test tube and vortexed. Lastly,

100% ethanol (75µl at -20°C) was added to the test tube and vortexed. The test tube was next incubated for 1 hour at -20°C. The test tube mixture was spun for 10 minutes at 14,000 RPM at 4°C. The extraction solution was removed and pellet was washed with 100µl of 70% ethanol. Then, the test tube mixture was spun for 5 minutes at 14,000 RPM, and ethanol was removed from the pellet. Dried pellet was resuspended in 20µl of sterile water and stored at -20°C.

Blot analysis of RNA probes. Membrane (Immunobilon Ny+) was previously sunk in distilled water and washed with 10x SSC. Placed RNA (diluted at 1ng, 10ng, 100ng) on the membrane and completely air dried membrane. RNA was crosslinked and rinsed with distilled water. Membrane was washed with B1 two times for 15 minutes in a dish, then blocked with B1+ sheep serum, and incubated in Ab solution (10ml B1, 100µl sheep serum, 2 µl of anti-DIG Ab) for 30 minutes. Next, membrane was washed in B1 3X10 minutes, in B3 for 15 minutes, and then placed on parafilm with B4. The membrane was wrapped in saran wrap and observed for a signal.

2.6 WHOLEMOUNT NEUROFILAMENT STAINING:

Wholemount neurofilament protocol from Kury et al. 2000 was used. Dissected embryos were fixed in 4% paraformaldehyde for 4 hours at 4˚C and washed with PBS 3X 5 minutes. Embryos were than placed in Dent's bleach overnight shaking at 4 ˚C. The next day, embryos were rinsed with methanol 5X 5 minutes, and fixed with Dent's fixative for 24 hours at 4˚C. On the third day, embryos were rehydrated through a methanol series: MeOH for 10 minutes, 75% MeOH/PBS 2x 10 minutes, 50% MeOH/PBS 2x 10 minutes, 25% MeOH/PBS 2x 10 minutes, and PBS. Embryos were then washed in PBS 3 X 1 hour in PBS. After application of blocking buffer (10% sheep serum 0.1% Triton X in PBS) for 2 hours, embryos were incubated overnight in 1˚ primary antibody diluted in blocking buffer (3A10 1:100, T. Jessell). Incubations were done at 4˚C on a shaker. Embryos were then washed in blocking buffer 2 X 1 hours at 4˚C, followed by 3 X 1 hour washes at room temperature on a shaker. Embryos were incubated overnight in secondary antibody (peroxidase conjugated anti-mouse IgG, Jackson Immunoresearch, 1: 100 in blocking buffer) diluted in blocking buffer shaking at room temperature. Transferred embryos to

50 ml test tube, rinsed 3X 5 minutes in blocking buffer, then followed by 5 X 1 hour in blocking buffer at room temperature. In preparation for the DAB reaction, embryos were washed in PBT for 10 minutes and transferred into small plastic vials. In the hood, DAB was added (0.5 mg/ml in PBT) to the embryos for 1 hour. DAB was then removed, and hydrogen peroxide was added to the removed solution. Embryos were then incubated with the DAB solution/ hydrogen peroxide solution until desired staining intensity (10-20 minutes). Embryos were rinsed with 1X PBT five times, and dehydrated through a methanol series: 25 % MeOH/PBS 2x 10 minutes, 50% MeOH/PBS 2x 10 minutes, 75% MeOH/PBS 2x 10 minutes, and MeOH 2x 10 minutes. Embryos were stored embryos in BABB.

2.7 RETROGRADE LABELING:

Axon tracing was performed using a standard retrograde horseradish peroxidase (HRP) labeling protocol (methods of Landmesser 1978, Lance-Jones and Landmesser 1981). Stage 13-15 embryos were electroporated with a full length Hoxd10/EGFP and sacrificed at stage 28-29. A ventral laminectomy was performed on dissected embryos in an oxygenated Tyrodes bath. A 10% solution of horseradish peroxidase was pressure-injected into either the sartorius or anterior iliotibialis muscle on both the nontransfected and transfected sides of experimental embryos. HRP-injected embryos were incubated in a 32˚ C oxygenated Tyrodes solution for 4-6 hours. Following incubation, embryos were fixed in 4% paraformaldehdye, washed with 1X PBS, and embedded in 30% sucrose-OCT. Embryos were either horizontally or transversely cryostat sectioned. HRP labeled axons were identified using a fluorescent-conjugated antibody (HRP-conjugated Cy3, Jackson Laboratories). All sections were also labeled with an anti-EGFP antibody.

2.8 CONFOCAL IMAGING:

Optical images at 2 um intervals were collected from transverse sections (14 um) labeled with antibodies using an Olympus confocal microscope. Z-series stack was assembled from the sections using QImaging software**.** Images were processed using Adobe Photoshop 7.0.

2.9 MOTONEURON CELL COUNTS:

The majority of cell counts were made on photograph images of double labeled sections using IP lab software (Scanlytics, Fairfax, Virginia). This software was used to merge fluorescent images of a single section that were double labeled. In a minority of cases, counts were made directly on tissue stained with Isl 1/2 antibodies and processed with DAB.

To determine the transfection efficiency of the electroporations in stage 28-29 embryos, counts were made of DAPI+ and DAPI/EGFP+ cells in a sample region. The sample region consisted of a rectangular strip fixed at 50um width through the ventral spinal cord of stage experimental and control embryos at stage 28-29. The top of the strip was aligned with the dorsal-most cluster of Isl 1/2 + within the somatic motor column (See Chapter 3, Figure 12).

To quantify motoneuron numbers after electroporation, counts were made of the number Isl 1/2+ cell in somatic motor column (SM) and Column of Terni (CT) regions. Figure 11A shows a section depicting how the SM and CT regions were defined. First, a line was drawn from the top of the dorsal-most cluster of Isl 1/2 + cells within the somatic motor column, to the top Isl 1/2 + cluster in the CT. This line was then bisected with a line to the floor plate to form two distinct regions, a ventrolateral SM and a dorsolateral CT region. In each region, the number of Isl1/2+ and Isl1/2-EGFP+ cells were counted. Counts that compared the number of Isl 1/2+ cells on the transfected side and nontransfected were immunostained and processed for bright-field observation (DAB labeled). For each embryo, three sections corresponding to the anterior border, midpoint, and posterior border of the T6 segment were counted. To quantify motoneurons numbers in embryos sacrificed at stage 18, counts were made of all Isl1/2+ cell in the ventral spinal cord on the transfected and nontransfected sides.

2.10 STATISTICAL ANALYSIS:

Counts were subjected to statistical analysis using the Statview 5.01 software. Cell counts from Hoxd10/EGFP and EGFP electroporated embryo were compared using an unpaired t-test. Comparison of cell counts from the transfected and nontransfected sides were made using a paired t-test.

3.0 ECTOPIC EXPRESSION OF HOXD10 IN THORACIC SEGMENTS AT EARLY NEURAL TUBE STAGES INDUCES LS MOTONEURON SUBTYPES

3.1 INTRODUCTION

A central aim of this thesis is to assess the role of Hoxd10 in the development of the posterior spinal cord. In this chapter we describe motor columnar identity and organization in T segments after the ectopic expression of Hoxd10 at early neural tube stages.

We chose to analyze motoneuron organization because these patterns are particularly well characterized. Motoneurons show a remarkable diversity with respect to positional organization in the ventral CNS. Thus, they provide an attractive model system for defining the mechanisms that regulate cellular diversification. In the spinal cord, motoneuron subtypes are organized into motor columns. Somatic motor columns are positionally distinct from visceral motor columns. Further, motoneurons that project to limb regions occupy different columns than motoneurons that project to axial or body wall muscles. Finally, each spinal region on the A-P axis (i.e. T vs LS) contains a distinctive complement of columns.

Motoneurons can be distinguished not only by their position but also by the transcription factors that they express (Tsuchida et al., 1994). Four members of the LIM family of transcription factors: Islet (Isl) 1, Isl 2, Lim 1, and Lim3, are expressed by motoneurons in the embryonic chick spinal cord. Individually, these LIM genes do not distinguish specific motor columnar subtypes; however the combinatorial expression of these genes is able to define molecular profiles of motoneuron subtypes that occupy specific columns in the spinal cord (Fig. 1). For example, the LMCl motoneurons that project to dorsal limb musculature can be identified by the coexpression of Isl 2 and Lim 1. The unique patterns of LIM profiles in turn define different axial regions.

In limb innervating regions, retinoid signaling plays an important role in establishing LIM-HD patterns and the specification of motor columns. Different spinal regions and motoneuron subtypes can also be distinguished by patterns of RALDH2 expression. RALDH2 is a synthetic enzyme for retinotic acid and a molecular marker for RA- mediated activity. During early motor column formation, RALDH2 is expressed in subsets of motoneurons at limb levels but not at non-limb levels (Sockanathan and Jessell, 1998).

We chose to examine the role of Hox genes at early neural tube stages for two reasons. First, morphological and molecular differences between limb (B and LS) and non-limb regions (T) of the spinal cord are specified at early neural tube stages (stages 13-15) (O'Brien and Oppenheim 1990, Matise and Lance-Jones 1996, Ensini et al. 1998). Second, Hox genes are first expressed at high levels as motoneurons withdraw from the cell cycle. Motoneurons appear to attain motor columnar identity in accord with their position on the A-P axis (Liu et al, 2001, Bel-Vialar et al 2002). Studies of hindbrain and anterior spinal cord development suggest that Hox proteins are principal molecules that encode A-P identity (Carpenter et al. 1993, Dolle et al. 1993, Goddard et al. 1996, Dasen et al. 2003).

Hoxd10 was chosen because is highly expressed in the LS spinal cord but not the T spinal cord (see Figure 3 and 4C, Lance-Jones et al. 2001). In addition, mice with a loss-of-function of Hoxd10 show a shift in the position of the lateral motor column (LMC) and peripheral alterations in spinal nerves originating from the LS spinal cord (Carpenter et al. 1997). However, since Hoxd10 is expressed in non-neural as well as neural tissue, it is not known if the Hoxd10 knockout phenotype reflects indirect global deficits of Hoxd10 or a specific loss in neural tissue. Further, no analyses of molecular identity of motoneurons or specific axon projections were made in the Hoxd10 mutant. Based on the observed abnormalities from the Hoxd10 mutant mice and the normal expression of Hoxd10, we hypothesized that Hoxd10 imparts an LS character to the segmental organization of motoneurons. In this chapter, we ectopically express Hoxd10 in T segments and analyzed molecular profiles for possible changes in LIM and RALDH2 patterns.

3.2 RESULTS

3.2.1 Electroporation of Hoxd10 into the thoracic spinal cord

Two DNA constructs were used for the electroporations. A construct that leads to the expression of enhanced green fluorescent protein (EGFP) alone was kindly provided by C. Krull. This construct was made by placing an IRES-EGFP sequence into a pCAX vector where the expression of EGFP was under the control of the ß-actin promoter/ CMV-IE enhancer. This construct was used as a control. A second construct (Hoxd10/EGFP) was made by placing a full-length chick Hoxd10 into the EGFP construct. The Hoxd10 DNA was provided by C. Tabin. Either EGFP (0.625 -2.5µg/µL) or Hoxd10/EGFP DNA (0.625 -2.5 µg/µL) was injected into the newly closed neural tube at posterior axial levels of stages 12-15 chick embryos and electroporated at 15-17 V (Figure. 4 A, B).

Most embryos were sacrificed at stage 28-29, after the normal period of motor column formation and early axon outgrowth but before the peak period of normal motoneuron cell death. A few embryos were sacrificed at stage 24 in preliminary experiments to assess the effectiveness of the electroporation, and at stage 16-18 to examine features of early motor column formation. All embryos were immediately examined under a compound or inverted microscope for evidence of EGFP expression in T segments. Embryos that showed sparse or widely distributed and punctate EGFP+ cell clusters in T segments were not examined further. Preliminary embryos transfected with Hoxd10/EGFP were fixed and processed via *in situ* hybridization with a *Hoxd10* mRNA probe either on sections or as wholemounts. Expression was present unilaterally in the T spinal cord with occasional expression in anterior LS regions (Figure 4 E, F). High Hoxd10 expression was evident in T segments at levels comparable to those of normal LS segments (Figure 4C,D). The position of *Hoxd10* + cells corresponds to that of EGFP+ cells in adjacent antibody-stained sections (compare Figure 4F and G).

3.2.2 Hoxd10 transfected thoracic motoneurons develop lumbosacral-like LIM-profiles.

In normal stage 28-29 embryos, motoneurons in LS and T segments show well characterized and distinctive patterns of LIM protein or gene expression (Figure 5, Tsuchida et al., 1994). In order to identify motoneurons and their different subtypes, we used three different anti-LIM proteins antibodies and one mRNA probe (obtained from Developmental Hybridoma or kindly provided by T. Jessell). Their staining characterizations are shown in Table 1. Normal

patterns of LIM expression for stage 28-29 embryos are schematized in Figure 5. Representative antibody-stained and mRNA probed sections are shown in Figure 6. We used an Isl 1/2 antibody as a pan-motoneuron marker, as all motoneurons in T and LS segments express either Isl 1, Isl 2, or both. Staining with an Isl 1 probe, and Lim 1/2 and Lim3 antibodies were used to distinguish different subsets of motoneurons in T and LS segments.

To determine if Hoxd10 transfections changed the LIM identity of motoneurons in T segments, we examined the expression of different LIM genes in sections from 24 HOXD10/EGFP and 9 EGFP embryos. While the axial extent of the transfections were often great (Figure 4), we focused our analyses on posterior T segments. Lim 1 is normally expressed in LMCl motoneurons in LS segments (Figure 6 F, arrow). The antibody we used to recognize Lim 1 + cells was a Lim 1/2 antibody, but no cells in the spinal cord express Lim 2 (Tsuchida et al., 1994). On the transfected side of the Hoxd10/EGFP electroporated sections stained with the Lim 1/2 antibody, we noted that Lim 1/2 + cells extended ventrally into the motor column region (Fig. 7 E and F). This extension was evident in the lateral portion of the motor column region, similar to the position of LMCl in the LS spinal cord (Figure 6 F). No Lim1/2 + extension was observed on the nontransfected side or in T segments transfected with EGFP alone (Figure 7 F and A, B).

To determine if this Lim 1/2 + extension in Hoxd10/EGFP electroporated embryos consisted of motoneurons or misplaced interneurons, sections were double labeled with Isl1/2 and Lim 1/2 antibodies. As noted above, all motoneurons express Isl 2, and thus, the Isl 1/2 antibody is a pan-motoneuron marker. As shown in Figure 8B, the ventral extension of Lim1/2 + cells was also Isl1/2 + indicating that this cluster consisted of motoneurons. To assess the number of motoneurons that were Lim 1/2 + in the thoracic region, counts of Lim1/2 +, Isl1/2 + cells were made. The number of Lim1/2 +, Isl1/2 + cells in the posterior T segments (T4-T6) of

experimental embryos ranged from 4-26 with a mean of 12.8 cells per section (n=10). While the number of Lim1/2 +, Isl1/2 + cells in normal LS sections is much greater (mean = 67.1± ; n=3), it should be noted that only about ¼- ½ of the motoneurons in T segments appeared to be transfected at stage 28-29 (see also section on cell numbers) (Figure 8A). Isolated clusters of Hoxd10/EGFP transfected cells were also observed to be Lim1/2 +, suggesting that Hoxd10 induces Lim1 in a cell autonomous manner (Figure 8C). The expression of Lim 1 in somatic motoneurons is a unique feature of the LS spinal cord. The presence of Lim 1 in Hoxd10/EGFP-transfected somatic motoneurons is therefore compatible with the hypothesis that Hoxd10 expression alters the LIM profile of T motoneurons to that of LS motoneurons.

In a normal stage 28-29 embryo, LMCl motoneurons differ from MMC and LMCm, not only in their expression of Lim1 but also in their lack of Isl 1 expression (Figure 6G and H). In the LMCl, Isl 1 is downregulated at early stages coincident with the onset of Lim1 expression (Tsuchida et al., 1994). Prior studies also indicate cross-repressive interactions between Isl 1 and Lim 1 (Kania et al. 2000). In the experiments described above we used an Isl 1/2 antibody and therefore, could not determine if Isl 1 expression was specifically altered in Hoxd10/EGFP transfected T motoneurons.

As we were unable to get a reliable Isl 1 antibody we instead obtained material for a preparation of an Isl1 mRNA probe. Shown in Figure 7 are sections from a T segment transfected with Hoxd10/EGFP and a T segment transfected with EGFP alone. In each case adjacent sections were stained with either Isl 1/2 antibodies or probed for Isl 1 mRNA (Fig 7 C, D, G, and H). On the Hoxd10/EGFP electroporated side of sections, Isl 1 expression in the ventral spinal cord is reduced, particularly in regions corresponding to the position of Lim1/2 + cells (n= 11). Furthermore, the Isl 1 + cells appear to be a smaller subset of the overall Isl 1/2 + cells, suggesting the presence of Isl 1(-), Isl 2 + motoneurons (Figure 7 G and H). A number of Isl 1(-) ,Isl 2 + motoneurons were distinctively found in the dorsolateral region of the somatic motor region that coincided with the Hoxd10/EGFP expression.

To verify that the Lim 1 extension observed in Hoxd10/EGFP transfected T motoneurons is complemented with a loss in Isl 1 in the same cells, we performed double *in situ* hybridization/ immunohistochemistry on sections from Hoxd10/EGFP electroporated embryos using an *Isl 1* probe and a Lim 1/2 antibody. On the transfected side of Hoxd10/EGFP electroporated T segments (Figure 9 A,C), Lim 1/2 + cells that extend into the motor column do not overlap with

Isl 1 mRNA staining (n=6). Conversely, on the nontransfected side of these embryos there was no Lim 1 extension, and a clear boundary existed between Lim 1/2 + cells and Isl 1+ cells with little to no overlap (Fig 9 D).These findings suggest that a loss of Isl1 accompanies Lim 1 expression in transfected T motoneurons, and provides further support for the hypothesis that Hoxd10/EGFP transfected T motoneurons select an LMCl molecular profile.

While the ectopic expression of Hoxd10 in the T spinal cord results in Lim 1 + , Isl 1-, Isl 2+ motoneurons characteristic of an LMC molecular profile, it is possible that these motoneurons also retain characteristics of T somatic motoneurons (an MMC profile). To determine if Hoxd10/EGFP transfected T motoneurons show strictly an LMC molecular profile or a hybrid (MMC-LMC) identity, we examined the expression Lim 3. Lim 3 is first expressed in early motoneuron progenitors that are in their final cell division. Motoneurons that exit the cell cycle and project their axons ventrally from the spinal cord continue to express Lim 3. Later in development, Lim3 expression becomes restricted to motoneurons in the MMCm and V2 interneurons in the spinal cord (Sharma et al 1999). Adjacent Hoxd10/EGFP transfected T sections were either double labeled with antibodies Lim1 and Lim3, or Isl1/2 and EGFP.

At stage 29, the normal thoracic spinal cord consists of MMCm and MMCl. Both the MMCm and MMCl are Isl 1/2 +; however, neither motor columns express Lim 1 (Figure 10 A, B and C**).** The MMCm forms a crescent-shaped cluster that can be clearly distinguished from the MMCl by the expression of Lim 3 (Figure 10D). As previously observed, Hoxd10/EGFP transfections resulted in a ventrolateral extension of Lim 1+ motoneurons into the somatic motor columns. The Hoxd10/EGFP transfected Lim1+ cells in theT somatic motor region do not overlap with Lim3+ motoneurons (n=5) (Figure 10 G-J). These results provide evidence that Hoxd10/EGFP transfected T motoneurons show a distinct LMCl profile (Lim 1+, Isl 2+, Lim3 -) rather than a hybrid one.

3.2.3 Electroporations with Hoxd10/EGFP leads to a decrease in motoneuron numbers at stage 28-29.

On the transfected side of stage 28-29 Hoxd10/EGFP electroporated embryos, we frequently found a marked decrease in the number of Isl 1/2 + cells (motoneurons) when

compared to the nontransfected side (Figure 11C). We also noted that the spinal cord on the transfected side of experimental embryos appeared reduced in size suggesting a broad reduction in overall cell numbers. In contrast, transfected and non-transfected sides of EGFP electroporated embryos appeared similar in size. A series of cell counts were made to assess the effects of Hoxd10/EGFP and EGFP electroporations on cell numbers. All cell counts were made on sections from embryos electroporated at stage 13-15 and sacrificed at stage 28-29. All cell counts were made on three sections corresponding to the anterior border, midpoint, and posterior border of a single T segment (T6). We first asked if electroporations of EGFP led to changes in somatic motoneuron numbers. Counts were made of the number of Isl 1/2 + cells in the somatic motor column region (see Figure 11A, for definition of regions on transfected and nontransfected side). No significant difference in the numbers of somatic motoneurons on the transfected and nontransfected sides were found (mean number of somatic motoneuron on transfected side = 102.6 % of the transfected side; p-value = .5500, n=4, Appendix B3). This finding suggests that the process of electroporation did not affect cell numbers.

We next asked if there was a significant difference in the numbers of Isl 1/2 + cells in the somatic motor regions on the transfected sides of EGFP and HOXD10/EGFP electroporated embryos. The numbers of somatic motoneurons on the transfected side of Hoxd10/EGFP electroporated embryos (n=19) were 30.0% fewer than the numbers on the transfected side of EGFP electroporated embryos (n=10; p-value = .0003; Appendix B4) (Figure 11D). To determine if differences in motoneuron numbers were accompanied by differences in the number of transfected somatic motoneurons we also counted EGFP+/Isl 1/2+ cells in the somatic motor regions (Figure 11 F-H). There was no significant difference in the percentage of transfected motoneurons in the somatic motor regions of EGFP and Hoxd10/EGFP embryos (p-value = 0.71 unpaired t-test Appendix B5).

The CT (visceral motor column) is a unique feature of the T spinal cord located medially and dorsal to the somatic motor columns. Counts of Isl 1/2 + cells in the CT region (see Methods and schematic) indicated a 44 % reduction in Isl 1/2 + cells (p-value= 0.0007, Fig.11 G,H; Appendix B6). When we examined the percentage of transfected motoneurons (EGFP+ / Isl1/2 + cells) there was a significant reduction in the percentage of transfected motoneurons in the CT region of Hoxd10/ EGFP electroporated embryos when compared to EGFP electroporated embryos (p-value= 0.0043, Fig 11 G,H; Appendix B7). This pronounced reduction of CT

motoneurons suggests that Hoxd10 may specifically repress CT development or affect early CT motoneuron survival.

The counts described above were obtained from embryos with electroporations performed at stages 13-15, and electroporations that used DNA concentrations ranging from 0.625- 2.5 μg/μL. No correlations were found between stage of electroporation or DNA concentration and extent of survival (Appendix B8-B9, B10). For example, to determine if a reduction in DNA concentration would increase motoneuron survival, we have assessed motoneuron numbers after electroporation with 0.625 (n= 7) and 2.5 μg/μL (n=10) cDNA of Hoxd10/EGFP. Cell counts were made on EGFP/Isl 1/2 stained sections as described above. There was no significant difference in overall cell numbers when comparing experimental embryos that were electroporated with either 0.625 or 2.5 μg/μL DNA (p-value = .161; Appendix B10).

Finally, we asked if Hoxd10/EGFP electroporations caused a broad reduction in cell numbers on the transfected side of the spinal cord, or if the observed reductions were specific to the motoneuron cell population. To address this question, transverse sections from Hoxd10/EGFP (n=10) and EGFP (n=7) transfected embryos were stained for DAPI and EGFP. DAPI is a nuclear counterstain used in multicolor fluorescent studies. We counted cells that were DAPI+ and DAPI+/EGFP+ in a sample region shown in Figure 12. This sample region consisted of a rectangular strip through the ventral spinal cord which excluded the ventricular zone (Figure 12 B). While the transfection levels (DAPI+/EGFP+ expressed in percentage) of Hoxd10/EGFP (n=10, 44.3± 4.9%) and EGFP (n = 7, 50.4± 4.2) transfected embryos were similar, there was a significant reduction in the number of DAPI+ cells in the Hoxd10/EGFP transfected embryos when compared to EGFP transfected embryos. Hoxd10/EGFP embryos showed a mean reduction of 16.1 % (p= 0.0427, unpaired t-test, Appendix B11-12). This reduction is considerably less than that found for SM + CT motoneurons. This observation may be related to the fact that motoneurons are normally born early. Having gone through few divisions after electroporation, they may have retained more exogenous DNA.

3.2.4 Hoxd10 transfection has an early influence on cell survival.

Our cell counts indicate a significant decrease in motoneuron numbers in T spinal segments transfected with Hoxd10/EGFP. One possible explanation for this outcome is that the ectopic expression of Hoxd10 initiated a premature cell death of T motoneurons. In normal development, motoneurons undergo programmed cell death (PCD). While, the peak period of death extends from stage 30-35, cell death can begin as early as stage 27 (Hamburger, 1975; Oppenheim and Chu-Wang, 1983). Hoxd10 may have activated an early onset of the cell death period, for example at stage 26, which would lead to a abnormal reduction of motoneurons numbers at stage 28-29. An alternative possibility is that high levels of Hoxd10 expression may have had an adverse effect on motoneuron development from the onset of their differentiation (stage 18 +). A third possibility is that ectopic Hoxd10 expression caused the precocious withdrawal of motoneuron progenitors from the cell cycle, resulting in a depletion of the motoneuron progenitor pool and an eventual reduction in motoneuron numbers. If the observed motoneuron reduction in stage 29 embryos is due to precocious withdrawal of motoneuron progenitors then one might expect an increase in the size of the motor columns (number of post-mitotic Isl 1/2 + cells) at early embryonic stages.

To address these questions we first carried out electroporations at stages 13-15 and sacrificed embryos at stage 16, a time when the earliest motoneurons begin to exit the cell cycle (Hollyday and Hamburger 1977). Transverse sections were immunostained for EGFP and Isl 1/2. In experimental embryos (n=3), there were only a few Isl 1/2 + cells and no apparent differences between the transfected and nontransfected side of T segments (Figure 13 A, B). These data suggest that early Hoxd10 electroporations do not cause the precocious withdrawal of motoneuron progenitor cells. To determine if cell death was occurring at stage 16, adjacent sections of experimental embryos were immunostained for activated-caspase-3, a marker for the last step in cell apoptosis. In each case, experimental embryos (n=3) had only a few, if any, activated caspase-3 + cells, with no apparent differences between the transfected and nontransfected side of ventral regions of T segments (Figure 13 C). These observations suggest that at stage 16, Hoxd10 electroporations do not promote cell death.

We next asked if a reduction in motoneuron numbers were present at an early stage of motor column formation (stage 18). Autoradiographic studies have shown that motoneuron

birthdates begin as early as stage 15 (52.5 hrs) in T segments and stage 17 (58 hrs) in LS segments. Birthdates of motoneurons peak at stage 20 (71hrs) in both the T and LS segments (Prasad and Hollyday, 1991; Hollyday and Hamburger, 1977). During this 20 hour period motor neuroblasts undergo rapid mitotic division giving rise to 50% of the total motoneurons in T and LS segments (Hollyday and Hamburger, 1977). These findings suggested there would be variations in the number of post-mitotic motoneurons between individual stage 18 embryos. For this purpose, counts of motoneurons on the transfected and nontransfected sides of individual stage 18 T spinal segments were compared. Sections from experimental and control embryos were immunostained with EGFP and Islet 1/2 antibodies. In each experimental or control embryo, three sections from a single posterior T segment were chosen for cell counts (see Methods).

In EGFP electroporated embryos (n=3), the number of Isl 1/2 + cells on the nontransfected side ranged from 13.7-33.3, with a mean of 20.8± 5.7 (s.e.) Isl 1/2 + cells. On the transfected side of EGFP embryos counts ranged from 12.0-31.3, with a mean of 22.5 ± 5.6 (s.e.) Isl1/2 + (Figure 13 D, E; Appendix C3). There was a small but significant difference between transfected and nontransfected sides (paired t-test, mean difference =1.8 Isl 1/2+ cells, p-value = 0.0031, n=3 Appendix C4). In Hoxd10/EGPF transfected embryos, counts of Isl 1/2 + cells on the nontransfected side ranged from 13.3-29.7 with a mean of 23.9± 3.6 (s.e.), while on the transfected side counts ranged from 7.3-14.7 with a mean of 10.9 ± 1.5(s.e.) Isl1/2 + cells (Appendix C5). In contrast to EGFP transfected embryos, Hoxd10/EGPF transfected embryos had a 52.6 % reduction in Isl 1/2+ cells on the transfected side when compared to the nontransfected side of T segments (Figure 13 G,H,) (paired-t-test, mean difference =13.0, p-value = .0175, n=4; Appendix C6). Thus, embryos with Hoxd10 transfections show a large difference between transfected and nontransfected sides. These data indicate that early Hoxd10 expression alters motoneuron cell numbers in the T neural tube as early as stage 18. These results also suggest that Hoxd10 electroporations do not cause precocious motor column formation (Figure 13 H).

At stage 18, Isl1/2+ cells include both presumptive SM and CT neurons (Prasad and Hollyday 1991). To compare the reduction of Isl 1/2 + motoneurons observed in embryos sacrificed at stage 18 and stage 29, stage 29 SM and CT cell counts were combined. Stage 29 EGFP electroporated embryos had a SM + CT total mean of 157.4 ± 22.4 Isl 1/2 + cells per

section on the transfected side (n=10). Stage 29 Hoxd10/EGFP electroporated embryos had a mean of 102.4 ± 31.7 Isl 1/2+ cells per section (n=19). This represents a 34.9 % reduction of Isl 1/2+ cells (Un-paired t-test, p-value = 0.0001; Appendix C7). As mentioned above, we observed a 52.6 % reduction in Isl 1/2 + cells on the transfected sides of Hoxd10/EGFP embryos (n = 4) at stage 18. Although the number comparisons are slightly different (Stage 28-29: EGFP vs HOXD10, Stage18: transfected sides vs nontransfected sides of Hoxd10/EGFP), the data suggest that there is a greater reduction in motoneuron numbers at stage 18 than at stage 29.This observation indicates that the survival of early–born motoneurons is more radically affected than late-born motoneurons and that the decrease in motoneuron numbers seen at stage 29 may have resulted from the early death of motoneurons rather than a slightly early onset of the normal cell death period.

To look for evidence of cell death at early stages, adjacent sections of experimental embryos were immunostained with an antibody to activated-caspase-3. In the EGFP transfected embryos (n=4), there was little or no activated-caspase-3+ cells in the ventral half of the T spinal cord (Figure 13 F). In contrast, Hoxd10/EGFP electroporated embryos (n=5) had small clusters of activated-caspase-3 + cells in the ventral half of the T spinal cord (Figure 13 I). These observations suggest that high and early expression of Hoxd10 causes cell death in ventral progenitor cells and early-born motoneurons

3.2.5 Hoxd10/EGFP transfected thoracic motoneurons express RALDH2

Prior studies suggest that RA signaling plays a significant role in the specification of chick motoneuron subtypes (Sockanathan and Jessell, 1998). After exiting the cell-cycle, all post-mitotic motoneurons express Isl 1 and Isl 2. Motoneurons that settle medially, and extend out to axial (MMC) and ventral limb muscles (LMCm) continue to express Isl1 and Isl2. Late born motoneurons destined to become lateral LMC neurons (LMCl) extinguish Is1 1 expression and begin to express Lim 1. The switch in LIM genes expression appears to be dependent on retinoid signaling by early born LMC motoneurons.

The precise spatiotemporal regulation of RA is determined in part by the expression of enzymes that synthesize and metabolize RA. During chick embryogenesis, retinaldehyde

dehydrogenase-2 (RALDH2) is a major synthetic enzyme that is important in the production of RA. To determine the sites of local RA synthesis in the developing chick embryo, studies have analyzed the expression of RALDH2. Studies of the distribution of RALDH2 in the chick embryo indicate that tissues that express RALDH2 synthesize and/or release RA (Berggren et al., 1999). In the embryonic spinal cord, RALDH2 is selectively expressed in motoneurons in limb innervating regions and has been shown to be a critical determinant in the development of LMCl motoneurons (Sockanathan and Jessell 1998). Previous studies suggest that RALDH2 begins to be expressed by LS motoneurons at stage 19 and that RALDH2 expression becomes restricted to LMCm motoneurons between stages 26-29 (Berggren et al., 1999). Furthermore, few if any, motoneurons in the T segments expressed RALDH2. The difference in RALDH2 expression in T vs LS regions, and evidence suggesting that LIM patterns are established by retinoids, prompted us to ask if the ectopic expression of Hoxd10 in T segments induced RALHD2 expression in motoneurons.

We first characterized the normal expression patterns of RALDH2 in the posterior T and anterior LS spinal cord at stage 29 as prior studies had not detailed the precise distribution of RALDH2 in individual LS segments. We performed double *in situ* hybridization/ immunohistochemistry on sections from normal embryos (n=3) using an *Isl1* probe and a RALDH2 antibody (See Material and Methods section). The use of the *Isl 1* probe allowed us to distinguish MMC and LMCm motoneurons from LMCl motoneurons, since only MMC and LMCm motoneurons are Isl 1+. Transverse sections in the T and LS region showed pronounced RALDH2 immunoreactivity in the roof plate and surrounding meninges, as well as in subsets of LS motoneurons and their processes (Figure 14). A few RALDH2+ cells were present laterally in T7, but no RALDH2+ cells were found in more anterior T segments (Figure 14 A, B). In LS1-3, RALDH2 + cells were located in lateral regions of the spinal cord. In LS 1-2, RALDH2 expression expanded laterally and appeared to be present in all LMCl motoneurons but was absent in the LMCm (Figure 14 C, D). In LS3, RALDH2+ cells appeared as an extreme lateral subset of LMCl motoneurons (Figure 14 E, F). In mid- and posterior LS segments, medial motoneurons (LMCm and MMC) were RALDH2+ and there was a tight overlap between *Isl 1* expression and RALDH2 immunoreactivity labeling (Figure 14 G, H). Together, these observations indicate that motoneurons in the stage 29 LS spinal cord normally express RALDH2 while few, if any, motoneurons in T segments are RALDH2+. There are also clear

differences in the normal RALDH2 expression patterns within the anterior and posterior LS spinal segments.

We screened for RALDH2 in posterior T sections from 22 embryos electroporated with Hoxd10/EGFP. All exhibited RALDH2 expression on the transfected side of T segments. Figure 15 shows a large dorsolateral EGFP+ cluster of cells within the ventral spinal cord which tightly overlaps with the expression of RALDH2. No RALDH2 expression was detected on the non-electroporated side or in T segments of EGFP electroporated embryos (n= 6). To determine if RALDH2+ cells in Hoxd10/EGFP electroporated embryos were motoneurons or interneurons, transverse sections from transfected T segments were double labeled for RALDH2 and Isl 1/2. Most of RALDH2+ cells were Isl 1/2+ motoneurons located in dorsolateral region of the ventral motor column (Figure 16 C). A small number of RALDH2+/ Isl 1/2 (-) cells were found outside the boundaries of the ventral motor column as reported in previous studies (Berggren et al., 1999).

We next asked whether the Lim1+ motoneurons that extended into the motor column of Hoxd10-transfected T segments co-expressed RALDH2. Analysis of transverse sections double labeled for RALDH2 and Lim 1/2 antibodies indicated that a many of the RALDH2+ cells in the motor column were also Lim 1/2 + (Figure 16 D).

We also examined transverse sections from Hoxd10/EGFP electroporated embryos processed via double *in situ* hybridization/ immunohistochemistry, using the *Isl1* probe and a RALDH2 antibody. Our analysis of normal RALDH2 expression patterns at stage 29 indicated that most RALDH2+ cells were located laterally in anterior LS segments and do not appear to express Isl 1 (Figure 14 C, D). Alternatively, all normal T motoneurons are Isl 1 + but do not express RALDH2 (Figure 14 A, B). In Hoxd10/EGFP electroporated embryos, RALDH2 expression was induced on the transfected side of T segments as noted in Figure 16 (E-F). A substantial number of RALDH2+ cells were located in the lateral regions of the motor column and were Isl 1 (-). Taken together, these findings indicate that Hoxd10/EGFP transfected motoneurons can induce RALDH2 expression in the T spinal cord, and that most of these RALDH2+ cells appear to have an LMCl molecular profile characteristic of anterior LS segments (Isl 2+, Lim1+, RALDH2+).

3.2.6 Hoxd10/EGFP transfected T segments have normal Hoxc8 and Hoxd9 expression patterns

There is substantial evidence of auto-, cross-, and para-regulatory interactions among Hox genes that define and maintain their distinct regional expression patterns (Gould et al. 1997, Maconochie et al. 1997, Struder et al. 1998, Gavalas et al. 2003). To determine if the ectopic expression of Hoxd10 in T segments altered the expression of other Hox genes normally expressed in T segments, we analyzed the expression of two endogenous Hox genes, Hoxc8 and Hoxd9.

Hoxc8 is expressed from the brachial spinal cord through posterior T segments. We chose to analyze Hoxc8 because prior studies that transplanted the tailbud (Henson's node) into anterior spinal levels resulted in an induction of Hoxd10 and a coincident repression of Hoxc8 in closely apposed T neural tube cells (Omelchenko and Lance-Jones 2003). Sections from Hoxd10/EGFP electroporated embryos processed for the *Hoxc8* probe, showed that Hoxd10 did not alter the expression patterns of *Hoxc8* (n= 15/15) (Figure 17). This observation raises the possibility that other extrinsic factors emanating from the tail bud may direct the downregulation of Hoxc8, but it is unlikely to be mediated by the induction of Hoxd10.

We also chose to analyze Hoxd9 expression because it is an adjacent Hox gene within the same Hox family. Hoxd9 is expressed from the middle T spinal cord through posterior T segments. Sections from Hoxd10/EGFP electroporated embryos processed for *Hoxd9* probe, showed that Hoxd10 did not alter the expression patterns of endogenous *Hoxd9* (n= 8/9). This finding is compatible with previous analysis of Hoxd10 mutant mice which appear to have normal Hoxd9 expression patterns (Carpenter et al., 1997). Taken together, these findings suggest that neither Hoxc8 nor Hoxd9 are downregulated by Hoxd10. Our data is compatible with recent findings on Hox gene activity in the anterior spinal cord which suggests that cross-repressive interactions are reserved to specific pairs of Hox genes (Dasen et. al., 2004).

3.3 DISCUSSION

To test the hypothesis that Hoxd10 imparts an LS character to the segmental organization of motoneurons, we have assessed motoneuron molecular profiles after ectopically expressing Hoxd10 in the posterior T spinal cord. We have made three major observations. First, Hoxd10 transfected T motoneurons show altered LIM patterns that are consistent with LMCl molecular profile, a normal attribute of the LS spinal cord. Second, though Hoxd10/EGFP electroporated embryos show a reduction in somatic motoneurons, CT motoneurons, which are a distinctive feature of the T spinal cord, show the most severe reduction. Third, Hoxd10 electroporations induce RALDH2 expression in T segments in a pattern which appears similar to normal RALDH2 expression in the anterior LS spinal cord.

3.3.1 Hoxd10 imparts an anterior LMCl phenotype

During normal spinal cord development, Hoxd10 is expressed in the LS spinal cord but not the T spinal cord. Our studies demonstrate that Hoxd10 transfected T motoneurons express Lim1 and RALDH2, two molecules that are distinctively expressed in limb-innervating regions (B and LS). Furthermore, our analysis showed that Hoxd10/EGFP transfected motoneurons were Isl 1(-) and Isl 2+. The presence of Lim 1+, RALDH2 +, Isl 1(-) Isl 2+ motoneurons is consistent with molecular profiles of LMCl motoneurons in anterior LS segments. Taken together, these results demonstrate that a single Hox gene, Hoxd10, can impose LS identity to T motoneurons to generate a distinct motoneuron subtype normally found in one region of the LS spinal cord.

Do Hoxd10- transfected T motoneurons have a strictly LMCl molecular profile or do they have a hybrid (MMC-LMC) identity? Several studies have shown that the disruption of paraxial signals and specific transcription factors during motoneuron development leads to the generation of hybrid motoneurons (Thaler et al., 1999, Lewis et al., 2004). In contrast, misexpression studies of individual Hox genes in the hindbrain have demonstrated that individual Hox genes are capable of generating distinct specified motoneuron subtypes (Jungbluth et al., 1999). Although, Hoxd10 transfected T motoneurons acquire LMCl phenotype, it is possible that these transfected motoneurons have retained some features of T identity. The T

spinal cord consists of MMCl and MMCm motor columns. MMCm motoneurons coexpress Isl1 and Lim3 proteins, while MMCl motoneurons express Isl 1 and Isl 2. Our data suggest that Hoxd10 transfected T motoneurons were Lim 3(-), and our analysis of Islet 1 and Islet 2 expression suggests that these transfected cells were Islet 1(-). These observations indicate that Hoxd10-transfected motoneurons strictly acquire an LMCl molecular profile.

In the process of carrying out these studies we also characterized the expression of RALDH2 in normal LS segments. Our analysis of normal RALDH2 expression after motor column formation revealed clear differences in the distribution of RALDH2+ cells at different AP-levels within the LS spinal cord. In mid -LS and posterior LS segments, RALDH2 expression appears to be restricted to LMCm motoneurons, as previously observed in other expression studies. However, in anterior LS (LS1-2) segments, we noted that most LMCl motoneurons were RALHD2+ and few, if any, LMCm motoneurons expressed RALDH2 at stage 29. This observation raises new questions about the role of RA in motoneuron specification in the anterior LS spinal cord. Prior studies have hypothesized that early born LMCm motoneurons express RALDH2 and generate a non-cell-autonomous retinoid signal that imposes a lateral phenotype to late-born LMCl motoneurons (Sockanthan and Jessell 1998). These authors have shown that RA induces an LMCl molecular profile in developing motoneurons. Our observations raise the possibility that RALDH2 expression in the LMCl itself may also initate or maintain an LMCl molecular profile in anterior LS segments.

Our data also shows that the ectopic expression of Hoxd10 in T segments induces RALDH2 in patterns similar to normal RALDH2 patterns in anterior LS segments. There is evidence suggesting that individual Hox genes predominantly function within the anterior regions of their expression domains (Lufkin et al., 1991). Since the anterior domain of Hoxd10 expression corresponds to the T/LS border, our results support the hypothesis Hoxd10 distinctively imparts an anterior LS identity, instead of a generic LS identity. It is conceivable that RALDH2 is expressed in normal early born LMCm motoneurons in anterior LS segments and these motoneurons downregulate the expression of RALDH2 before stage 29. Since, our analysis of RALDH2 was carried out well after stages of migration, it will be important to further detail the developmental expression pattern of RALDH2 at earlier stages in the anterior LS spinal cord to explore this possibility. Preliminary analysis of RALDH2 expression in normal

stage 24 chick embryos, showed that RALDH2 expression appeared widespread throughout somatic motor regions at anterior LS levels (n=2).

3.3.2 Hoxd10 gene activity and the sequential induction of LMCl molecular profile

How might Hoxd10 induce the observed LIM profile (Lim 1 +, Isl 1-, Isl2 +) in T motoneurons? Our findings show that Hoxd10 induces both RALDH2 and the LMCl LIM profile, hence, Hoxd10 transfected T motoneurons are RALDH2 +, Lim1 +, Isl 2+. These findings can be interpreted in several ways. One possibility is that Hoxd10 induces Lim1, and in turn activates the expression of RALDH2. This model seems unlikely, since ectopic expression Lim 1 in the developing neural tube does not induce RALDH2 expression (Kania et al., 2003).

Most prior evidence suggests a mechanism by which Hoxd10 induces RALDH2 which in turn leads to changes in LIM gene patterns. Studies by Sockanathan and Jessell, (1998) indicate that retinoid signals by early born LMC motoneurons are responsible for the switch from Islet 1 to Lim 1 in late-born LMC motoneurons. As previously mentioned, studies have shown that early-born LMCm motoneurons generate a non-cell-autonomous retinoid signal, via RALDH2 expression, that specifies an LMCl profile to late-born motoneurons. Spinal cord explants grown in RA induce Lim 1 but repress Isl 1 expression (LMCl molecular profile) in developing motoneurons. In addition, excess RA can induce the expression of RARβ, the main retinoic receptor expressed during LMC specification, and the receptor thought to mediate the expression of Lim 1 in LMCl motoneurons (Colbert et al., 1995, Vermot et al., 2005). Lastly, *in vivo* studies that have ectopically expressed RALDH2 demonstrated that RALDH2 expression acts non-cell autonomously to impose an LMCl molecular profile on adjacent motoneurons. Furthermore, Sockanathan and Jessell (1998) also hypothesized that early born LMCm motoneurons are not induced to express Lim1 because they have aged to a point where they are no longer sensitive to RA. Spinal cord explants at later stages of development were unable to respond to retinoids and induce LMCl motoneurons. Collectively, these observations demonstrate the pivotal role of retinoid signaling in the specification of LMCl motoneurons.

Our results are compatible with the possibility that high early levels of Hoxd10 may have precociously induced RALDH2 in T motoneurons, and these transfected cells respond to the

untimely retinoid signals to acquire an LMCl phenotype. To demonstrate that Hoxd10 prematurely induces the expression of RALDH2, it will be important for future studies to examine the expression patterns of RALDH2 during the early stages of motoneuron development in Hoxd10 electroporated embryos.

Recent studies have examined the interactions between Hox genes and retinoid signaling. In the development of brachial LMC motoneurons, analysis of Hoxc8 and RALDH2 knockout mice suggests a cross regulatory interactions between Hox genes and RALDH2 that is functionally linked to RARβ (Vermot et al., 2005). Both the Hoxc8 mutant and RALDH2 mutant mice exhibit a similar reduction of Lim1+ motoneurons and downregulation of RARβ in the brachial spinal cord. Analyses of the Hoxc8 and RALDH2 mutant mice support a model in which RALDH2 provides local RA signals that are transduced by the RARβ to activate the expression of Lim 1 in LMCl motoneurons. Taken together, these findings indicate that Hoxc8 expression and RA signaling direct the development of LMCl motoneurons.

Additional studies in the hindbrain have demonstrated that a bi-directional regulation exists between Hox genes and the RARβ receptor in the establishment of rhombomere boundaries (Serpente et al., 2005). Early RA-mediated signals from the paraxial mesoderm have been shown to induce incongruent expression of Hoxb4 and RARβ in the presegmented hindbrain. The regulatory sequences of both Hoxb4 and RARβ include active RAREs and Hox consensus binding sites. At later stages of hindbrain development, Hoxb4 regulates the expression of RARβ (Hox→ RARβ), which in turn positively feeds back and activates the expression of Hoxb4 in the presence of RA (RARβ→ Hox). These findings describe a complex bi-directional feedback circuit that functions to align and define sharp segmental boundaries at the r6/r7 border. Future studies should further analyze the expression of RARβ in the LS spinal cord. It may be worth considering whether such a bi-directional relationship exists between Hoxd10 and RARβ in the development and boundary formation of LMC motoneurons in the posterior spinal cord.

3.3.3 The timing of Hoxd10 expression on the specification of motoneurons

Expression studies have shown that neural tube progenitor cells in the presumptive LS spinal cord express Hoxd10 mRNA at low diffuse levels at stage 15-16. Previous studies

demonstrated that specification of morphological and LIM patterns are acquired shortly after neural tube closure and before motoneuron birthdates. At stage 11, the B and T spinal cord are labile and sensitive to signals from the surrounding environment; however, by stage 13 these regions become specified (Ensini et al., 1998). Our Hoxd10 electroporations were performed on stage 13-15 chick embryos. Since, Hoxd10 expression was produced in T progenitor cells after stage 13, it appears that motoneuron progenitor fate can be changed after the normal specification period.

How might Hoxd10 confer AP identity to a progenitor cell? One possibility is that the presence of Hoxd10 in T progenitor cells alters the response of T progenitors to extrinsic neural tube patterning signals. Recent studies have shown that the integration of signals from the paraxial mesoderm and Henson's node program the expression of Hoxd10 (Omelchencko and Lance-Jones, 2003). Hoxd10 transfected T motoneurons may be sensitive to certain signals that otherwise normal T progenitor cells would not respond to.

Analysis of normal Hoxd10 expression shows that the LMCl motoneuron maintains a high level of Hoxd10 after progenitors have withdrawn from the cell cycle. This observation raises the possibility that the presence of Hoxd10 in post-mitotic motoneurons is important for the specification of motor columnar identity. Our results suggest that Hoxd10 induces an LMCl molecular profile in T motoneurons. While, the early expression of Hoxd10 (stage 15-16) in T progenitors may impart a general LS identity, it is highly unlikely that this early expression is involved in the specification of motoneuron progenitor cells to a distinct motoneuron subtype like the LMCl. Retroviral lineage studies have shown that motoneuron progenitors cells have not committed to particular motoneuron subtypes even as late as 1-2 cell cycles before motoneurons are born (Leber et al., 1990). Finally, a recent study has provided evidence that suggests Hox activity in the post-mitotic motoneuron is critical for the specification of motor subtypes. Dasen et al., 2003 were able to temporally restrict the expression of Hox-c genes by making a construct that was under the control of the HB9 promoter, a transcription factor expressed only in post-mitotic motoneurons. The ectopic expression of this construct restricted the expression of a single Hox-c gene to post-mitotic motoneurons, and demonstrated that the post-mitotic activity of Hox genes is a major determinant in the specification of motor columnar identity (Dasen et al., 2003).

3.3.4 Hox function and motor columnar identity

Our findings add to a vast amount of work implicating Hox gene function in pattern formation of the central nervous system, however they are most comparable to studies that have ectopically expressed Hox genes in the hindbrain and spinal cord. The individual misexpression of Hoxa2 and Hoxb1 in regions rostral to their normal hindbrain domains of expression results in the generation of ectopic facial and trigeminal branchiomotor neurons, respectively (Jungbluth et al., 1999). Similarly, the ectopic expression of Hoxa3 in the anterior hindbrain, also induces ectopic somatic abducens motoneurons (Guidato et al., 2003). Like the data presented in this chapter, these studies showed that individual Hox genes can actively specify distinct motoneuron subtypes.

Our data is most comparable to recent studies of Hox-c family members and the specification of brachial and T motoneurons (Dasen et al., 2003). In the normal anterior spinal cord, motoneurons expressing Hoxc6 are restricted to the brachial region. The ectopic expression of Hoxc6 in T segments results in the induction of motoneurons with a LIM and RALDH2 molecular profile, demonstrating that Hoxc6 specifies brachial LMCl identity. Further, the gain of brachial identity by motoneurons is accompanied by a loss of CT motoneurons. Our findings indicate that a posterior Hox gene normally confined to the LS spinal cord can also change T segments to a limb level (LS) identity as well. Our data mirrors these Hoxc6 finding, in that the ectopic expression of Hoxd10 not only induces Lim1 and RALDH2, but causes a marked reduction in CT motoneurons.

How do our findings compare to Hoxd10 loss of-of-function experiments? Mice with a targeted disruption of Hoxd10 exhibited distinct hindlimb motor deficits. Analysis of posterior spinal cord development in Hoxd10 mutants revealed a caudal shift in the position of LS LMC and changes indicative of an anterior transformation of the spinal cord. The Hoxd10 mutant phenotype correlates closely with our findings since our ectopic expression results can be interpreted as an anterior shift in LMC identity or a posteriorization of T segmental identity. These complementary observations suggest that the Hoxd10 mutant neural phenotype is largely due to the loss of neural Hox expression as opposed to an indirect effect of Hoxd10 in other tissues.

Do other Hox genes impart an LS identity to motoneurons? Our analyses do not exclude the possibility that other Hox genes are involved in the programming of LS motoneurons. In the chick there are three Hox10 paralogues, and each paralogue has a unique expression pattern that encompasses the LS spinal cord. Further, mice with a targeted disruption of Hoxa10 show alterations that suggest an anterior transformation of L1. Hoxa10/Hoxd10 double mutants exhibit more extensive shifts in LMC motoneurons than either single mutant. These last observations suggest that Hoxd10 and Hoxa10 work synergistically to pattern the LS spinal cord. Future studies might seek to determine if the misexpression of paralogues of Hox10 can specify LS motor column identity and if they have unique effects on different motoneuron subtypes.

3.3.5 The effect of Hoxd10 on motoneuron survival and early development

Our results indicate that the ectopic expression of Hoxd10 in T segments leads to a substantial reduction in motoneuron numbers present at stage 28-29 embryos. In the transfected motor regions, Hoxd10/EGFP electroporated embryos show a 30% reduction in Isl 1/2 + cells when compared to EGFP electroporated embryos. In the transfected CT regions there is an even greater reduction (44%). In addition, our analysis at early stages demonstrates reduced motoneuron numbers and evidence of cell death, suggesting that Hoxd10 prominently exerts an early influence on motoneuron survival.

Some prior studies raise the possibility that Hox genes have negative effects on cell survival. Hoxd13 knockout mice exhibit overgrowth in all structures in the tail bud, secondary NT, caudal spinal ganglia, and caudal vertebrae (Economides et al., 2003). Studies in *Drosophila* have also shown that the ectopic expression of abdominal Hox genes in the T regions is able to activate neuroblast –specific apoptosis (Bello et al., 2003). However, the vast majority of studies in the hindbrain and spinal cord provide evidence that Hox genes have a positive effect on cell proliferation and/or cell survival, especially among motoneuron populations. For example, the targeted inactivation of Hoxc8 leads to increased apoptosis in cervical motoneurons of mutant animals (Tiret et al., 1998). Similarly, the expression of Hox genes appears to increase cell proliferation and/or survival in other tissue types, including epidermal (Hoxb4) and hematopoetic (Hoxa10) cells (Komuves et al., 2002, Bjornsson et al., 2001). Most striking are

observations that Hoxd10/Hoxa10 double mutants show a 35% and 39% decrease in the number of motoneurons in the MMC and LMC, respectively (Lin and Carpenter, 2003). Why then did we find a decrease in motoneuron numbers when Hoxd10 was ectopically expressed in the T spinal cord.

Hoxd10 induces an LMC molecular profile in T motoneurons, these LS-like motoneurons may die because they find themselves in a foreign environment and are unable to sustain their survival. This explanation has been given to account for results of Hoxa3 misexpression in the hindbrain (Guidato et al., 2003). The ectopic expression of Hoxa3 induces abducens motoneurons in anterior hindbrain segments, however, only abducens motoneurons next to the floor plate continue to survive beyond early stages. It was hypothesized that many induced abducens motoneurons were located too far from the floor plate to receive appropriate survival factors. Since Hoxd10/EGFP electroporated embryos show early cell death, the effect of the foreign environment would have to have a very early negative effect. It would be interesting to look at electroporated embryos at later stages to see if there is also more cell death.

In Hoxd10/EGPF electroporated embryos, we consistently observed that the EGFP+ transfected cells were located laterally. The reduced motoneuron numbers and lateral bias of Hoxd10 transfected motoneurons indicate that Hoxd10 may have an effect on the development of early-born motoneurons. Between stages 17-18, roughly 6-12 hours after we performed our electroporation, T and LS motoneurons begin to exit the cell cycle. As motoneurons withdraw from the cell cycle, the early –born motoneurons settle medially and the late-born motoneurons settle in more lateral position in the somatic motor region (Hollyday and Hamburger, 1977). During our Hoxd10 electroporations, the early-born motoneurons may be more substantially affected since they undergo the least number of cell cycles after electroporations, therefore, maintaining a high level of Hoxd10. Consequently, a majority of the nontransfected cells would settle in ventral medial sections. Given that the observed lateral position of Hoxd10 transfected motoneurons resembles the normal expression of Hoxd10 in the LS somatic motor column at stage 29, we do not exclude the possibility that Hoxd10 participates in the lateral settling of motoneurons in the somatic motor region.

How might the early high level of Hoxd10 expression affect MN development? One interpretation of our data is that the observed LMCl phenotype is acquired by the immediate activity of Hoxd10 in T progenitor cells that exit the cell cycle. Therefore, newly emerging post-

mitotic motoneurons with high levels of Hoxd10 are inducing the expression of RALDH2 and Lim1, which repress the expression of Isl 1 and Lim3. Islet 1 knockout studies have demonstrated that the early presence of Isl 1 in newly post-mitotic motoneurons is required for the generation of motoneurons, and that the expression of Isl 2 can not compensate for this loss. Therefore, if early Hoxd10 expression represses the expression of Islet 1, by the induction of Lim 1 and Raldh2, this could substantially affect the number of motoneurons generated.

Our analysis of Hoxd10 electroporated embryos revealed that transfected T segments developed a severely depleted CT. How might Hoxd10 expression lead to a specific reduction in CT (visceral) motoneurons? One explanation for a more specific reduction in the CT is that CT motoneurons make up a large preponderance of the early-born neurons that are adversely affected in our Hoxd10 electroporations. However, this outcome is unlikely because studies suggest that most CT motoneurons are born between stages 18-24, with a peak between stages 20-24 (Prasad and Hollyday 1992).

A more likely explanation for the reduction in CT motoneurons is that the high levels of Hoxd10 cause an early loss of Isl 1 which disrupts the competence of these transfected cells to acquire visceral motoneuron identity. In the early phases of maturation, all motoneuron subtypes express Isl 1 and Isl 2. Genetic manipulations that have depleted Isl 1 and Isl2, suggest that high levels of Islet (Isl 1 and Isl 2) activity serve a permissive role in the acquisition of visceral motoneuron identity (Thaler et al., 2004). In these mice, T motoneurons with a low Islet levels appear to undergo a cell autonomous switch from a visceral to somatic motoneuron identity. Two sets of observations support this outcome. First, analyses of the Lim 1 mutant suggest that retinoid signaling has a primary role in repressing Isl 1 expression (Kania et al., 2004). In addition, cell explant experiments support the idea that retinoid signaling inhibits the expression of Isl1. Secondarily, Isl1 and Lim1 expression have been shown to be mutually and selectively cross-repressive. In our experiments early Hoxd10 expression may lead to early and abnormally high levels of RALDH2 and Lim 1, a subsequent selective repression of Isl 1, with an early decrease in net Islet proteins, and consequently a selective loss of CT motoneurons.

4.0 ECTOPIC EXPRESSION OF HOXD10 IN THORACIC SEGMENTS ALTERS NERVE PATTERNS TO LS TARGETS

4.1 INTRODUCTION

Motoneurons exit the spinal cord as spinal nerves and subsequently project axons to the periphery in a proximo-distal sequence. In the LS spinal cord, spinal nerves from each segment converge at the base of the limb to form one of two plexi, the crural and sciatic (Lance-Jones and Landmesser, 1980). In the anterior LS region, LS1-3 and a small fraction of the T7 spinal nerves meet to form the crural plexus. Posteriorly, LS 4-8 and a portion of LS3 spinal nerves join to form the sciatic plexus. At the plexi, motor axons undergo a period of rearrangement and segregation, and divide into the dorsal and ventral nerve trunks (Tosney and Landmesser, 1985). The dorsal and ventral nerve trunks will innervate the dorsal and ventral muscles, respectively. The general nerve pattern in the vertebrate limb is consistent and highly reproducible from animal to animal.

Somatic motoneurons that innervate limb muscles are found within the LMC. The LMC is a distinctive feature of limb-innervating regions (B and LS segments) in the spinal cord. Within the LMC, motoneurons that innervate specific limb muscles are functionally grouped together in discrete clusters termed motor pools. Retrograde labeling of motoneurons that innervate each hindlimb muscle has demonstrated that LS motoneurons are arranged in stereotyped motor pool positions within the LMC (Landmesser, 1978). In the hindlimb, the A-P location of motor pools approximately coincides with A-P position of target limb muscles. Individual motor pools span 2-4 segments.

Experiments that have manipulated motoneuron and/or muscle target positions suggest that positional identity is acquired at early neural tube stages (prior to axonal outgrowth), and that developing motor axons from different regions in the spinal cord respond distinctively to

specific guidance cues in the periphery (O'Brien and Oppenheim, 1990; Ensini et al., 1998; Lance-Jones and Landmesser, 1981; Ferguson, 1983) . What molecules are responsible for programming motoneuron target identity to developing axons? Along the D-V axis, many studies have shown that LIM proteins are important for the ability of motor axons to select a dorsal or ventral projection into the limb (Kania et al., 2000; Kania et al., 2003). In contrast, few studies have identified molecules that determine the selection of limb targets on the AP axis, however, Hox proteins are a likely candidate.

Many studies that have examined the role of Hox genes in the nervous system have concentrated on their function in the hindbrain. Analysis of nerve patterns in anterior or 3' Hox mutants revealed complex deficits including failure of nerve fasciculation, loss of nerves, and abnormal projections of motoneurons in the hindbrain (Carpenter et al., 1993; Goddard et al., 1996; Gavalas et al., 1998). A small number of studies have analyzed nerve patterns in posterior or 5' Hox mutants (Tiret et al., 1998; Carpenter et al., 1997; Wahba et al., 2001). Similar to 3' Hox mutants, nerve patterns of 5' Hox mutants are difficult to interpret because they do not conclusively match changes observed in segmental identity. Difficulties in interpreting the nerve patterns of Hox mutants may also be compounded by the fact that the majority of these studies have globally manipulated Hox gene expression. In normal development, Hox genes are expressed centrally in motoneurons and in peripheral tissues that motor axons traverse en route to their respective targets. Therefore, it is unclear whether the altered nerve patterns in Hox mutants are due to a central loss of Hox expression from motoneurons or the indirect loss of Hox expression in peripheral tissue. One way to separate the central and peripheral effects of Hox gene activity is to ectopically express a Hox gene in a tissue- restricted manner. Studies that have ectopically expressed 3' Hox gene in more anterior regions of the hindbrain, have demonstrated that a posterior Hox gene can "posteriorize" the segmental identity and corresponding axon projections of motoneurons (Bell et al., 1998; Guidato et al., 2003). Similarly, only one study has misexpressed 5' Hox genes in the developing spinal cord; the authors, Dasen et al. 2003 did not, however, analyze motor axon projections. Since the misexpression of Hoxd10 changed the molecular profile of a subset of T motoneurons to an LS identity, we wanted to determine whether transfected motoneurons also showed altered axon pathfinding.

4.2 RESULTS

4.2.1 Hoxd10 transfected thoracic motoneurons project to dorsal limb muscles

We used standard retrograde HRP labeling to determine if Hoxd10/EGFP transfected T motoneurons were projecting axons to limb muscle targets at stage 29 (See Methods section, Landmesser and Lance-Jones, 1981; Matise and Lance-Jones, 1996). The sartorius and anterior iliotibialis motor pools were chosen for HRP labeling because they are dorsal hindlimb muscles that are in close proximity to posterior T segments. We specifically chose dorsal rather than ventral limb muscles because these muscles are normally innervated by Lim 1/2 + cells (LMCl) and our analyses of LIM patterns indicated an induction of Lim 1/2 + cells. Hoxd10/EGFP electroporations were performed on stage 12-15 chick embryos. HRP was injected into either the sartorius or the anterior iliotibialis muscle in both hindlimbs of experimental embryos at stage 29. Horizontal and transverse sections from experimental embryos were double-labeled with EGFP and HRP antibodies. The sartorius is normally innervated by motoneurons in LS 1-2 segments with a few in T7 (Figure 18). In 11/ 15 Hoxd10/EGFP electroporated embryos, HRP + cells were found outside this domain on the transfected side of the spinal cord (Figure 18 A, B). HRP+ cells were found in T5-T6 as well as T7-LS2. In transverse sections at the posterior T level, HRP+ cells were consistently found in a dorsolateral portion of the somatic motor region on the transfected side, a position which is similar to EGFP+ distribution of Hoxd10/EGFP electroporated embryos and the normal position of the sartorius pool in anterior LS segments (Figure 19). On the transfected side, few, if any, cells were HRP+/EGFP- in the somatic motor region. On the nonelectroporated side, HRP+ cells were found only in T7-L2 segments.

The anterior iliotibialis is normally innervated by motoneurons in the L1-L3. In 2/3 of the Hoxd10/EGFP electroporated embryos, HRP + cells extended anteriorly out of this domain (Figure 18 D, E). For embryos with both sartorius and anterior iliotibialis muscle injections, double-labeling indicated a tight overlap between EGFP+ and HRP+ cells in T segments (Figure 18 C, F). The presence of HRP+ cells in more anterior T segments, and the close correspondence of EGFP+ and HRP+ cells indicate that transfected T motoneurons are projecting to dorsal limb muscles.

4.2.2 Hoxd10 transfected thoracic motoneurons are likely to reach limb muscles by proximal connectives.

Our retrograde labeling data suggest that Hoxd10/EGFP transfected motoneurons make novel projections to dorsal limb muscles. However, it is unclear what path or route these novel projections take to reach limb targets. To identify these novel projections, we took images of the trunk and limb region of EGFP and Hoxd10/EGFP electroporated embryos as wholemounts just after sacrifice and before sectioning. In these preparations, we observed proximal nerves that connected thoracic spinal nerves to the LS1 spinal nerve (large arrow, Figure 20 A, B). These proximal connectives were often larger in the Hoxd10/EGFP embryos than the EGFP embryos, and no aberrant nerves were observed (n= 13). Hoxd10/EGFP electroporated embryos also had truncated distal thoracic nerve branches (smaller arrow, Figure 20 A, B). The presence of large EGFP-labeled proximal connectives that link up thoracic and LS1 spinal nerves suggest a likely pathway for Hoxd10-transfected T motoneurons to reach the limb.

We also examined wholemount Hoxd10/EGFP electroporated embryos after staining with a neurofilament antibody. Embryos were sacrificed at stage 27 to better visualize developing motor axons and avoid background staining observed in later staged embryos. In each embryo, we compared neurofilament stained nerve patterns in experimental embryos on the transfected side to the nontransfected side, since they are ideally at similar points in development. In 3/4 embryos, we observed larger proximal connectives that linked thoracic spinal nerves to the LS1 spinal nerve on the transfected side when compared to the nontransfected side of Hoxd10/EGFP electroporated embryos (Figure 21, B, D). This finding further supports the hypothesis that Hoxd10/EGFP transfected T motoneurons are reaching limb muscles by proximal connectives.

4.2.3 The ectopic expression of Hoxd10 in T segments leads to the induction of the c-met receptor and Pea3 transcription factor

Our data shows that Hoxd10/EGFP transfected T motoneurons develop novel axon projections to two dorsal muscles in the hindlimb. This finding suggests that Hoxd10-transfected

T motoneurons are responsive to long range guidance cues emanating from the limb. It is unknown which guidance cues are involved in the trajectory of these novel projections; however, there is evidence that the limb mesenchyme can attract developing motor axons (Ebens et al., 1996). HGF is a long-range chemoattractant found in the vertebrate limb that could be responsible for the attraction of Hoxd10/EGFP transfected T motoneurons. The HGF receptor, c-met, is a tyrosine-kinase receptor that is selectively expressed by motoneurons (Sonnenberg et al.,1993; Ebens et al.,1996). Previous *in situ* hybridization studies have reported that c-met is expressed in motoneurons in the lumbar spinal cord, but not in the T spinal cord (Novack et al., 2000). To determine if HGF/c-met signaling may be involved in the long-range axon pathfinding of Hoxd10 transfected T motoneurons, we asked if Hoxd10 transfections in T segments induced c-met expression.

We first sought to precisely define the normal expression of c-met in LS segments at stage 29. Transverse sections from the T and LS spinal cord of a stage 29 chick embryo were stained for *c-met* mRNA. C-met staining was scarce or absent in the T spinal cord at stage 29 (Figure 22 A, B). We observed distinct differences in the expression patterns of c-met in anterior and middle LS segments. In anterior LS segments (LS 1-2), c-met is expressed in the LMCm but also extends into a region at the dorsolateral edge of the ventral motor column which corresponds to part of the LMCl (arrow, Figure 22 C,D). In middle LS segments (LS 3-5), c-met expression appears to be restricted to the medial region of the LMC or LMCm motoneurons (Figure 22 E,F). We observed that c-met was expressed in a majority of LMC motoneurons in posterior LS segments (Figure 22 G,H).

To determine if Hoxd10 induces c-met expression in the T spinal cord, transverse sections from Hoxd10/EGFP electroporated embryos were processed for c-met mRNA. While, c-met expression is either scarce or absent in the normal T spinal cord at stage 29, 8/10 Hoxd10 electroporated embryos showed c-met expression on the transfected side in posterior T segments (Figure 23). Adjacent sections stained for either EGFP or double labeled for Lim1/2 protein and Isl 1 mRNA showed that regions with high EGFP closely overlapped with a cluster of cells that were Lim1 (+) and c-met(+) (Figure 23 A-C). This finding raises the possibility that HGF/c-met signaling participates in the axon pathfinding of Hoxd10-transfected T motoneurons.

Our observation of large EGFP-labeled proximal connectives suggested that Hoxd10-transfected T motoneurons may have been responsive to guidance cues from the limb during

early stages of axon outgrowth. Previous studies reported that c-met is first expressed in the chick lumbar LMC motoneurons at E5 (stage 25-26) (Novak et al., 2000). We found that c-met is expressed in the normal lumbar spinal cord as early as stage 24, however, we also observed some c-met staining in the normal T spinal cord at stage 24 (n=3; data not shown). While, the data is limited, these observations suggest that either temporal of quantitative differences in c-met expression would have to be critical if HGF/c-met signaling is to implicated in axon growth towards the limb.

In the spinal cord, the differentiation of specific motor neuron pools is associated with the expression of ETS class transcription factors (Lin et al., 1998). The initiation of ETS gene expression coincides with the arrival of motor axons to muscle targets, and this expression is blocked by early limb bud removal. This observation suggests that the expression of an ETS gene is coordinated by signals from the periphery. Recent studies have shown that peripheral signals from the limb initiate the onset of Pea3 expression in limb innervating regions of the spinal cord (Haase et al., 2002). This is followed by an expansion of the Pea3 domain in which more neurons are recruited to express Pea3. Recent studies have linked c-met signaling with the regulation of Pea3 expression (Helmbacher et al., 2003). This study demonstrated that the rostral expansion of the Pea3 domain to anterior segments is dependent on c-met signaling. Given that Hoxd10 induced c-met expression in T segments at stage 29, we asked if the misexpression of Hoxd10 also induced Pea3 expression. To determine if Hoxd10/EGFP transfected T motoneurons express Pea3, transverse sections from Hoxd10 electroporated embryos were immunostained with a Pea3 antibody. At stage 29, Pea3 is normally expressed in the LMCl motor column in the LS spinal cord, but is not expressed in the T spinal cord. Transverse sections through the T spinal cord of stage 29 Hoxd10/EGFP electroporated embryos were immunostained for Pea3. In 5/7 Hoxd10/EGFP electroporated embryos, a small cluster of Pea3(+) cells (4-7 cells) were induced on the transfected side. Figure 24, shows adjacent slides stained for EGFP and Pea3, and suggests a spatial overlap of Hoxd10/EGFP expression and the location of Pea3(+) cells. The presence of Pea3(+) motoneurons in the T spinal cord is compatible with the observation that Hoxd10 transfected motoneurons are reaching limb muscle targets.

4.3 DISCUSSION

The experiments described in this chapter provide direct evidence that the misexpression of a single Hox gene in the spinal cord can alter motor axon trajectories to specific limb muscles. In particular, we have made four major observations. First, retrograde labeling of Hoxd10/EGFP electroporated embryos demonstrates that transfected T motoneurons make novel projections to two anterodorsal limb muscles, the sartorius and anterior iliotibialis. Second, analyses of gross nerve patterns suggest that Hoxd10 transfected T motoneurons appear to reach the limb by proximal connectives. Third, Hoxd10 transfected T motoneurons induce the expression of c-met, a receptor known to mediate long-range chemoattraction into the limb. Fourth, the misexpression of Hoxd10 in the T spinal cord induces Pea3 expression; a transcription factor normally expressed when LS motor axons reach limb muscle targets.

4.3.1 Misexpression of Hoxd10 in T segments results in altered AP nerve patterns

Our experiments demonstrated that Hoxd10 transfected thoracic motoneurons alter their axon projections in parallel with their induced LMCl molecular profile. In the previous chapter, we provided evidence that the ectopic expression of Hoxd10 in the T spinal cord induces anterior LMCl identity in T motoneurons. Normally, LMCl motoneurons are found in the LS spinal cord, and innervate dorsal limb muscles. Using retrograde HRP nerve tracing techniques, we have shown that Hoxd10 transfected T motoneurons make novel axon projections to two anterior dorsal muscles. When we mapped the sartorius motor pool in Hoxd10 electroporated embryos, we observed the presence of EGFP+ /HRP+ cells in the posterior T segments (T5-6), which normally never innervate these muscles. Similar results were observed when we mapped out the anterior iliotibialis motor pool. Our data clearly demonstrate that the misexpression of a single posterior Hox gene in spinal motoneurons leads to the "posteriorization" of AP segmental identity and corresponding motor projections. Our findings are most comparable to one previous study that has analyzed AP segmental identity and the projection of motoneurons after the selective manipulation of neural Hox gene expression. Using retroviruses, Bell et al. (1999) ectopically expressed Hoxb1 in anterior regions of the hindbrain. Normally, Hoxb1 is expressed in r4 and r4 motoneurons innervate the 2nd branchial arch. The misexpression of Hoxb1 in r2

results in an r2 to r4 conversion of segmental identity of branchiomotor neurons and a corresponding change in axon trajectories. R2 motoneurons now innervate the 2nd branchial arch, rather than the 1st branchial arch.

We considered two alternate explanations for the anterior shift in the sartorius and anterior iliotibialis motor pools in Hoxd10/EGFP electroporated embryos. First, the reduction in T motoneurons observed in our experimental embryos may have caused a compensatory migration of LS motoneurons into the posterior T spinal cord to fill in these gaps. Alternatively, our electroporations may have reduced the number of LS motoneurons, and the lack of innervations of these target muscles might have resulted in the recruitment of adjacent T motoneurons to these targets. We think that these outcomes are unlikely, as there was a correspondence between the positions of HRP+ cells and EGFP+ cells in Hoxd10/EGFP transfected T segments. Numerous HRP+/EGFP- cells would have been expected for these other explanations to be valid.

In addition to motoneuron progenitors, our electroporations clearly transfected other cells in the neural tube, for example, we transfected neural crest progenitors. Hoxd10/EGFP transfected neural crest cells (NCCs) that leave the spinal cord and migrate into the periphery may have been responsible for the novel axon trajectories made by T motoneurons. We think this explanation is also unlikely for several reasons. During normal embryonic development, a subset of NCCs give rise to Schwann cells that eventually migrate and populate peripheral nerves. It was hypothesized that Schwann cells may precede developing peripheral nerves into the periphery and operate as guidepost cells (Noakes and Bennett, 1987). Using chick-quail chimeras, prior studies have examined the distribution of Schwann cells in the developing peripheral nerves of the chick forelimb and have shown that neural crest cell-derived Schwann cells do not act as guidepost cells for spinal motoneurons (Carpenter and Hollyday, 1992). Schwann cells were never positioned in advance of growing peripheral nerves and do not appear to lead peripheral nerves into the periphery. Therefore, these findings indicate that NCCs are not involved in axon pathfinding of spinal motor nerves. Furthermore, in our data, we observed a conspicuous tight overlap between EGFP(+) and HRP(+) cells in T segments of Hoxd10 electroporated embryos. One would not predict this outcome if NCCs had a prominent influence on motor axon decision making. Lastly, retrograde labeling of Hoxd10 electroporated embryos, where the transfections were restricted to the intermediate and dorsal spinal cord (n=3),

had normal motor pools. This finding also suggests that the expression of Hoxd10 by other cell populations in the T spinal cord does not influence the trajectories of T motoneurons. In contrast, it strengthens the hypothesis that the expression of Hoxd10 in T motoneurons is responsible for the novel axon projections.

If the expression of Hoxd10 in T motoneurons is sufficient to make novel axon projections to dorsal limb muscles, what contribution do peripherally expressed Hox genes have in axon pathfinding? 5' Hox genes expressed in paraxial mesoderm and lateral mesoderm play an important role in vertebral morphology and limb patterning (Burke et al., 1995; Nowicki et al., 2000). For example, mice with single mutations in Hoxa10 or Hoxd10 exhibit homeotic transformations in vertebral axial identities and limb skeletal abnormalities. Furthermore, triple mutants for Hox10 genes show a transformation of all LS vertebrae to T identity, and more severe proximal limb defects (Boulet and Capecchi, 2004).

There are a few lines of evidence suggesting that Hox genes are important in establishing regional guidance cues for motoneuron pathfinding. In Hoxc8 mutants, subsets of cervical C5-C6 motoneurons that normally do not express Hoxc8 have misrouted projections. This observation raises the possibility that the misrouting of these motoneurons is due to a loss of peripheral Hoxc8 expression (Tiret et al., 1998). Hox genes have also been ectopically expressed in mesenchymal tissues in anterior regions outside their normal expression domain. The ectopic expression of Hoxb1 in the 1st branchial arch results in a truncation of adjacent cranial nerves (Bell et al., 1999). Similarly, the ectopic expression of Hoxc6 in cervical mesoderm, leads to the truncation of cervical spinal nerves (Burke and Tabin, 1996).

To distinguish central versus peripheral effects of Hoxd10 on axon pathfinding, we compared our data with the phenotype of the Hoxd10 mutant. Our findings strongly complement the altered nerve patterns of Hoxd10 mutant mice (Carpenter et al., 1997). In Hoxd10 mutant mice, the dorsal nerve trunk or peroneal nerve was often absent, while the ventral nerve trunk or tibial nerve was expanded (Wahba et al., 2001). Our results can be interpreted as a complementary promotion of ectopic dorsally-projecting axons to dorsal limb muscles. The matching nerve patterns of the Hoxd10 mutant and our misexpression experiments suggest that the expression of Hoxd10 in motoneurons is the primary determinant of motor axon pathfinding.

Our data suggest that Hoxd10 expression in motoneurons prominently influences axon pathfinding choices; however, it does not exclude the possibility that peripheral Hoxd10 expression influences developing axons. Potential targets for peripherally expressed Hox genes are the EphA/ephrin guidance molecules. There is evidence that Hoxa13 and Hoxd13 can regulate EphA receptor signaling in the developing limb (Stadler et al., 2001; Caronia et al., 2003). Furthermore, recent studies have demonstrated that Eph/ephrins interactions are important for motor axons to form topographic maps on developing muscles (Feng et al., 2000).Other possible targets of peripherally expressed Hox genes are members of the Meis family of transcription factors. Misexpression studies have shown that Hox genes can regulate the expression of Meis homeodomain proteins. In the limb, Meis proteins are involved in the differentiation of the proximal limb bud regions, an area where motor axons segregate, sort out, and make initial pathfinding decisions (Capdevila et al., 1999, Mercador et al., 2000). Future studies might misexpress Hoxd10 in the developing hindlimb and assess nerve patterns as well as the distribution of Meis and Eph/Ephrin molecules in limb mesodermal cells.

4.3.2 Evidence that Hoxd10 expressing T motoneurons respond to specific guidance cues

Our wholemount analysis of EGFP and neurofilament labeling of electroporated embryos suggests that axons of Hoxd10 expressing T motoneurons make their way to the limb by proximal connectives. We found no evidence of aberrant axon projections from Hoxd10 transfected T segments to dorsal limb muscles. Instead, Hoxd10 embryos appeared to have a grossly normal nerve patterns in the hindlimb. This finding is consistent with a vast amount data that suggest that developing motor axons are constrained to grossly defined anatomical nerve patterns (Lance-Jones and Landmesser, 1981; Whitelaw and Hollyday, 1983). In many ways, our Hoxd10 misexpression experiments parallel previous displacement experiments. The ectopic expression of Hoxd10 induces an LMCl molecular profile in T motoneurons, which then confront a foreign environment. Previous experiments have manipulated the position of motoneurons and demonstrated that motor axons alter their trajectories to reach their appropriate targets; however, the gross anatomical pattern of the plexus and nerve trunks are largely indistinguishable from normal embryos (Lance-Jones and Landmesser, 1981; Summerbell and

Stirling, 1981; Whitelaw and Hollyday, 1983). This is due primarily to the presence of passive or non-specific guidance cues, mainly inhibitory, that limit developing axons to a defined anatomical pathway or 'highway'. It is within this pathway that motoneurons have the capacity to respond to specific guidance cues and alter their projections. For Hoxd10- transfected motoneurons, the proximal connectives appear to provide a conduit for developing axons that have the ability to respond to specific guidance cues from the limb.

Lastly, we noted that the large proximal connectives were most apparent between posterior T segments (T4-T7) even though Hoxd10 transfections often extended into middle and anterior T segments. In middle and anterior T regions, T spinal nerves appear to have normal trajectories and a lack of large proximal connectives. This observation is consistent with data from large anterior-posterior rotation experiments. Motoneurons displaced far from their normal environment are unable to detect guidance cues in the new (or foreign) environment and consequently are constrained to enter a pathway at their new location (Lance-Jones and Landmesser, 1981; Whitelaw and Hollyday, 1983). Our observations suggest that Hoxd10 transfected T motoneurons in posterior T segments have the ability to respond to specific guidance cues from the limb due to their close proximity; however, transfected T motoneurons in middle/anterior T segments appear too remote to sense these cues. This line of reasoning is also supported by our retrograde labeling experiments, where HRP(+) cells on the transfected side were found in posterior T segments but few, if any, extended into middle/anterior T segments.

What guidance cues are involved in steering developing axons of Hoxd10 transfected T motoneurons to dorsal limb muscles? The existence of proximal connectives in posterior T, but not anterior T segments, suggests the presence of a diffusible long-range chemoattractant that draws axons of Hoxd10 expressing T motoneurons into the limb. HGF is a long-range chemoattractant identified in the vertebrate limb. In the chick embryo, RT-PCR studies have shown that HGF is expressed in peripheral muscle progenitor cells in the LS region but not in the T regions. The exact distribution of HGF in the developing chick hindlimb is unknown (Novack et al 2000). Yet, radioactive *in situ* hybridizations of HGF in the mouse embryo have placed HGF in the proximal limb during early stages of axonal outgrowth (Ebens et al. 1996). LS motoneurons express the HGF receptor, c-met, during stages when their axons project into the limb (Novack et al., 2000). We found that ectopic expression of Hoxd10 in T segments induced c-met expression in motor column regions. The presence of the c-met receptor

in transfected cells suggests that c-met/HGF interactions participate in establishing the dorsal limb trajectory of the Hoxd10 transfected T motoneurons. Our data parallels findings from the studies of HGF and c-met mutants. Both c-met and HGF mutant mice are missing specific dorsal nerve branches in the forelimb (Ebens et al., 1996). These observations support the role of HGF/c-met guidance system in promoting dorsal nerve projections in the developing limb.

We also found that misexpression of Hoxd10 in T segments leads to an induction of Pea3+ cells. Pea3 is an ETS transcription factor that is a marker for distinct motor pools in the LMCl, and is never expressed in the normal T spinal cord. The initial expression of Pea3 coincides with the arrival of motor axons that have reached their muscle targets. The removal of the limb blocks the expression of Pea3 by LMC motoneurons, suggesting that limb-derived signals coordinate pea3 expression in the spinal cord (Lin et al., 1998). In the anterior LS spinal cord, Pea3 is specifically expressed by LMCl motoneurons that make up the anterior iliotibialis motor pool. In our experiments, the presence of Pea3(+) cells provides additional evidence that Hoxd10 transfected motoneurons are reaching limb muscles (in particular the anterior iliotibialis muscle) and responding to limb-derived signals.

Recent studies have also demonstrated that c-met/HGF signaling is required for a late rostral expansion of Pea3(+) motoneurons in the spinal cord (Helmbacher et al. 2003). These studies suggest that c-met signaling functions in a non-autonomous manner to recruit more anterior motoneurons to express pea3 (Helmbacher et al. 2003). In our experiments, it is unclear if c-met signaling functions in a non-autonomous manner to recruit more anterior pea3(+) cells since we did not double label experimental sections for pea3 and c-met, and we did not analyze pea3 expression at more anterior T segments. To test the hypothesis that Hoxd10 induction of c-met causes an expansion of Pea3(+) cells into the T spinal cord, future experiments may take horizontal sections from experimental embryos and perform a double *in situ* hybridization/ immunohistochemistry using the c-met probe and a pea3 antibody.

It is well-known that axon pathfinding is a complex process involving multiple guidance cues at many different stages of development. As a transcription factor, Hoxd10 may be targeting many downstream guidance molecules. One likely target is the EphA/Ephrin guidance system. We have showed in Chapter 3 that Hoxd10 induces the expression of Lim1 in T motoneurons. Misexpression studies have shown that Lim1 induces the expression of the EphA4 receptor in spinal motoneurons (Kania and Jessell, 2003). Evidence suggests that EphA/ephrin interactions

primarily mediate contact inhibition events (Flanagan and Vanderhaeghen, 1998; Wang et al., 1997). EphA4 is normally expressed in dorsally-projecting LMCl motoneurons in the LS spinal cord. Mice carrying mutations in EphA4 lack a dorsal nerve trunk, and all LMCl motor axons project to ventral regions of the limb (Helmbacher et al., 2000). Similarly, the misexpression of EphA4 in LMCm motoneurons leads to their aberrant projections into the dorsal nerve trunk (LMCm normally project to the ventral nerve trunk; Eberhart et al., 2002). Further studies may seek to determine if Hoxd10 induces or alters the expression of the EphA4 receptor in the spinal cord.

5.0 ECTOPIC EXPRESSION OF HOXD10 IN THORACIC SEGMENTS AT THE ONSET OF MOTONEURON DIFFERENTIATION INDUCES LS MOTONEURON SUBTYPES

5.1 INTRODUCTION

In the previously described experiments, we carried out Hoxd10 electroporations on chick embryos staged 12-15 (47-52.5 hours) which is prior to normal motoneuron birthdates and motor column formation. In the T spinal cord, motoneuron birthdating experiments have demonstrated that most CT and MMC motoneurons are born between stages 18-24 with a peak period between stages 20-24 (Prasad and Hollyday, 1991). Therefore, electroporations performed on stage 12-15 chick embryos were roughly 14.5-20 hours before the first group of T motoneurons exit the cell cycle at stage 18 (67 hours). Prior studies have demonstrated that the cell cycle time of ventral progenitor cells of the neural tube is approximately 8 hours (Langman and Haden., 1970). It takes approximately 3 hours for cells in the neural tube to express the Hoxd10/EGFP construct at high levels (personal observation). Collectively, these observations suggest that Hoxd10 expression is initiated at a time when a vast majority of motoneuron progenitors are undergoing cell division, and are not exiting the cell cycle.

Our previous results are compatible with the hypothesis that the early expression of Hoxd10 plays a role in the development of an LS molecular profile in T motoneurons. It is, however, important to conduct electroporations at later timepoints for two reasons. First, there are several pieces of evidence that suggest that the expression of specific genes during the final cell cycle of progenitor cells is important in determining the fate of post-mitotic cells (Tanabe et al., 1998, Novitch et al., 2001). For example, MNR2 is a transcription factor that is first expressed in motoneuron progenitor cells in their final cell cycle. Although transiently expressed, misexpression studies have shown that MNR2 is sufficient to direct the differentiation of

motoneurons (Tanabe et al., 1998). These observations raise the question of whether transfections of motoneurons during their last cell cycle would amplify or alter the development of an LS identity.

The normal temporal pattern of Hoxd10 expression provides a second reason for conducting electroporations at later timepoints. Hoxd10 is normally expressed at low and diffuse levels in neural tube progenitors at stage 15-16. High levels of Hoxd10 expression are observed in the ventral motor column at stage 19-21, when motoneurons are born and initiate axon outgrowth (Lance-Jones et al., 2001). Later transfections may more closely match the normal temporal upregulation of Hoxd10.

To address these issues and determine whether the very early expression of Hoxd10 is required for the induction of an LS identity, we performed later transfections during stages of early motoneuron birthdates and motor column formation (stage17-18). We asked if late Hoxd10 electroporations (stage17-18) in the T spinal cord altered LS phenotype and cell numbers as previously seen following early Hoxd10 electroporation (stage 12-15).

5.2 RESULTS

We ectopically expressed Hoxd10/EGFP in T segments by *in ovo* electroporation in stage 17-18 (> 29 somites) chick embryos. Electroporated embryos were sacrificed at stage 28-29, when motoneurons have terminally settled and prior to the normal motoneuron cell death peak. Transfected embryos were first assessed for changes in LIM expression patterns. Adjacent transverse sections through T segments were immunostained with EGFP, Isl 1/2, and Lim 1/2 antibodies. As with early Hoxd10/EGFP electroporations, the majority of EGFP+ cells were found in the dorsolateral portion of the somatic motor region (Figure 25 A and D). On the transfected side of Hoxd10/EGFP electroporated embryos, we noted that Lim 1/2 + cells extended ventrally into the somatic motor region (n= 6/7, Figure 25 B-C). The position of these cells corresponded to the position of EGFP+ cells in the ventral motor region. This Lim 1/2+ extension of cells was present in the lateral portion of the motor region, like the LMCl of normal

LS segments. No Lim1/2 + cells were present in ventral motor region on the nontransfected side. These observations suggest that Hoxd10/EGFP electroporations at later stages (stage 17-18) induce Lim1+ motoneurons in a manner similar to electroporations at earlier stages.

In Isl 1/2 stained T sections, we consistently noted the presence of Isl 1/2 + cell clusters in ectopic regions dorsal to the normal position of the somatic motor region (n=5/6). These clusters were best visualized in sections incubated with the Isl 1/2 antibody and then processed with an ABC kit and DAB staining (see Methods and Figure 25 E and F). These ectopic Isl 1/2 + cells were only lightly stained with Isl 1/2, suggesting that they lacked Isl 1 expression, like normal LMCl motoneurons (Figure 25 F). Their position also matched the position of EGFP+ cells found outside the somatic motor region in adjacent sections. This observation raises the possibility that late Hoxd10/EGFP electroporations led to the induction of more cells with an LMCl phenotype than earlier electroporations. Alternatively, these Isl 1/2 + cells may represent or include a small population of Isl 1/2 + interneurons. Such a population is present in an intermediate and lateral position in a normal T segment (see Figure 25E, arrowhead).

5.3 DISCUSSION

We report here that Hoxd10/EGFP electroporations of T spinal segments at stages 17-18 induce one characteristic normally found in LS segments. We consistently found Lim 1/2+ cells that extended ventrally into the somatic motor column, and overlapped with EGFP+ cells. This observation suggests that the presence of Hoxd10 during periods of motoneuron birthdates and early motor column formation as well as earlier stages can establish an LS-like identity in motoneurons. This finding is also compatible with the hypothesis that an early initiation of Hoxd10 expression is not necessary for T motoneurons to develop an LS molecular profile.

We also found that late electroporations of Hoxd10/EGFP in the T spinal cord led to the appearance of ectopic Isl 1/2+ cells above the normal position of the somatic motor region. These cells were lightly stained with the Isl 1/2 antibody and often reached as far dorsally as the CT. While, lightly stained Isl 1/2 + cells were present at the dorsolateral edge of embryos with stage 12-15 transfections, these cells never extended far dorsally. This finding raises two questions. What are these cells? Why the difference between early and late electroporations?

Our late electroporations may have affected interneuron progenitor cells. During early spinal cord development, ventral progenitor cells express specific transcription factors that determine whether these progenitor cells are directed towards generating interneuron or motoneuron progeny (Tanabe et al., 1998, Novitch et al., 2001). The late electroporation of Hoxd10 expression may have perturbed interneurons progenitor cells and led to the induction of abberant Isl 1/2 + interneurons in a normal location dorsal to the somatic motor column.

Alternatively, our late electroporations may have caused errors in the migration patterns of normal Isl 1/2+ interneurons. D2 neurons are a distinct subclass of dorsal interneurons that express Isl 1. D2 neurons are generated close to the roof plate at stage 19, and undergo a ventral migration between stages 24-27 (Liem et al. 1997). Figure 25 (arrowhead) shows that D2 neurons settle in lateral positions in the dorsal spinal cord, just adjacent to the top of the CT. In our electroporations, we often transfect the dorsal spinal cord and high levels of Hoxd10 may have caused D2 interneurons to migrate to more ventral positions than they normally do.

An alternative explanation is that the observed ectopic Isl1/2 + cells are motoneurons. We favor this explanation for two reasons. The position of Isl 1/2 + cells are more indicative of a dorsal extension of Isl 1/2 + motoneurons outside the somatic motor region rather than a ventral invasion of Isl 1/2 (+) interneurons. Studies of motoneuron migratory patterns have shown that somatic motoneurons can migrate dorsally, and this migration accounts for the dorsal expansion of the motor column (Leber and Sanes, 1995). It should also be noted that the antibodies we used to identify Isl 1/2 cells generally stain cells expressing Isl 1 and Isl 2 more darkly than cells that express only Isl 2. Although not definitive, this observation suggests that the lightly stained Isl 1/2 + ectopic cells lacked Isl 1 expression like normal LMCl motoneurons and unlike dorsal interneurons. Despite these hints that these cells are motoneurons it is clear that additional analyses with motoneuron markers are needed.

How might changes in the temporal patterns of Hoxd10 alter outcomes? In the normal avian embryo, Hoxd10 expression is low and diffuse in neural progenitors at stage 15-16, however, it is high in post-mitotic cells that begin to differentiate between stages 19-21 (Lance-Jones et al., 2001). Late transfections of Hoxd10/EGFP (stage 17-18) into T segments may more accurately mimic the normal upregulation of Hoxd10, and therefore, enhance the effect of Hoxd10 on motoneurons. Stage 17-18 Hoxd10 electroporation is also very likely to have resulted in the transfections of many motoneuron progenitors during their last cell cycle. The peak period

of MMC and CT motoneuron birthdates occurs at stage 19-20 (Prasad and Hollyday, 1992). As result these progenitors may have contained particularly high levels of Hoxd10 when compared to progenitors transfected earlier. It would be of interest to see if the size of the ectopic Isl 1/2 + cluster increases with even later electroporations.

6.0 MISEXPRESSION OF HOXD9 IN THORACIC SEGMENTS AT EARLY NEURAL TUBE STAGES DOES NOT INDUCE LS MOTONEURON SUBTYPES

6.1 INTRODUCTION

We have demonstrated that Hoxd10 electroporations can alter molecular profile and axonal trajectories of T motoneurons to resemble that of LS motoneurons. However, the possibility remains that the observed LS phenotype in Hoxd10 transfected T segments is a nonspecific effect of the overexpression of high and early expression of any single Hox gene. To address this possibility, we misexpressed another Hox gene in the T spinal cord. We specifically chose Hoxd9 because it is normally expressed in both posterior T as well as in LS spinal segments. Thus, it is not likely to participate in encoding an LS spinal cord identity (Burke et al., 1995; Carpenter, 2003). Hoxd9 and Hoxd10 are found within the same linkage group. Hoxd9 is the adjacent 3' neighbor of Hoxd10 on the same chromosome (Nelson et al., 1996). In this chapter, we describe the organization of motoneuron subtypes after misexpressing Hoxd9 in both anterior and posterior T segments.

6.2 RESULTS

6.2.1 Normal development of neural Hoxd9 expression

Previous studies have mapped the expression of Hoxd9 in mesodermal and endodermal tissues in the avian embryo, but have not fully mapped its expression in neural tissue (Burke et al., 1995; Nelson et al. 1996; Roberts et al., 1995). We, therefore, began by characterizing the normal Hoxd9 expression patterns in the chick spinal cord between stages of early motor column

formation (stage 22) through stage 29. We performed *in situ* hybridizations using a *Hoxd9* probe on both transverse sections and wholemount processed embryos. Prior data indicated that Hoxd9 was expressed in the posterior T region (Burke et al., 1995). At stage 22-23 (n=3), the majority of T and LS motoneurons are born, begin to migrate to future ventral motor regions, and initiate axon outgrowth. Hoxd9 expression is evident in the stage 22-23 ventral spinal cord from posterior T through LS spinal segments (Figure 26, A,B). Hoxd9 expression was also observed in the mesonephric duct, somites, limb bud, and gut mesoderm (data not shown) at stage 22-23.

Between stages 23-27, the T and LS motor columns grow in size and LS motor axons enter the limb. In transverse sections of a stage 25 embryo (n=3), we noted differences in Hoxd9 expression within motor column regions of posterior T and LS segments. In the posterior T sections, Hoxd9 was expressed in the most medial and lateral subset of cells in the ventral spinal cord (Figure 26 C). However, a central group of cells appears not to express Hoxd9. In LS segments, we noted expression in a medial subset of cells and a group of cells that extend laterally at the ventral and dorsal edges of the motor column (Figure 26 D).

At stage 29, motoneurons have terminally settled into their respective motor columns and their motor axons have innervated individual muscles. In transverse sections of stage 29 embryos (n=4), we observe clear A-P differences in Hoxd9 expression patterns within the motor column region. Few, if any, cells express Hoxd9 in anterior T segments (T2-3) (Figure 27 A, B). In posterior T segments (T5-T7), Hoxd9 expression appears to be expressed in almost all post-mitotic cells in the entire spinal cord (Figure 27 C, D). This expression pattern is different from the expression pattern in posterior T segments at stage 25, where there is a lack of Hoxd9 expression in the center of the developing motor column region. These differences suggest temporally dynamic expression patterns of Hoxd9 during motor column formation.

In anterior LS segments of stage 29 embryos, Hoxd9 expression is high in the MMC region and in a small crescent-shaped cluster of cells that extend ventrolaterally within the LMC region (Figure 27 E, F). Cells in the lateral and central LMC regions did not appear to express Hoxd9. At posterior LS levels, expression was similar but included LMCl cells (Figure 27 G, H). From posterior T segments through LS segments, post-mitotic cells in intermediate and dorsal spinal cord region also appeared to express Hoxd9 at stage 29.

6.2.2 Ectopic and overexpression of Hoxd9 in the T spinal cord

The above results indicate that Hoxd9 is expressed in motor column regions of posterior T and LS segments during motor column formation. We used *in ovo* electroporation to ectopically express Hoxd9 in anterior T segments and overexpress it in posterior T segments. The Hoxd9/EGFP construct used was made by placing a full-length chick Hoxd9 into the EGFP construct. The Hoxd9 DNA was provided by C. Tabin. Hoxd9/EGFP DNA (0.625 -1.25 μg/μL) was injected into the neural tube of stage 13-15 chick embryos. Electroporated embryos were sacrificed at stage 28-29 after the normal period of motor column formation and early axon outgrowth. All embryos were immediately examined under a compound or inverted microscope for evidence of GFP expression in T segments. Embryos with good transfections were selected, fixed, and transversely sectioned as previously described. Adjacent transverse sections were first processed to detect EGFP and *Hoxd9* (n=7). Shown in Figure 28 (A, B) are photos of anterior T sections from one Hoxd9/EGFP electroporated embryo. The unilateral EGFP distribution matches the patterns of Hoxd9 mRNA distribution.

Shown in Figure 28 (C,D), are photos of a posterior T sections from a second Hoxd9/EGFP electroporated embryo. The transfected side of the spinal cord shows higher levels of Hoxd9 staining than the nontransfected side of the posterior T spinal cord (n=7).

Unlike Hoxd10/EGFP electroporated T segments, the EGFP distribution of Hoxd9/EGFP transfections appears to be widespread in the motor column region suggesting a lack of a differential effect on early and late born motoneurons. Like Hoxd10/EGFP electroporated T segments, there appears to be a reduction in the number of motoneurons on the transfected side. This observation is compatible with idea that overexpression of any Hox gene has general effects on motoneuron survival.

6.2.3 Ectopic expression and overexpression of Hoxd9/EGFP in T segments does not induce Lim1 expression

Our previous experiments have demonstrated that the ectopic expression of Hoxd10/EGFP in T spinal segments induces an LS identity among motoneurons. Hoxd10/EGFP transfected T

motoneurons express Lim1, and do not appear to express Isl 1. This molecular profile is normally shown by LMCl motoneurons. To determine if similar changes accompany Hoxd9/EGFP transfections, sections from anterior T and posterior T spinal segments of 8 embryos were stained with EGFP, Lim 1/2, and Isl 1/2 antibodies. On the transfected side of the Hoxd9/EGFP embryos, we noted that the EGFP distribution was widespread in the motor column region (n=7, Figure 29 A-B). Isl 1/2 staining indicated that the motor column region was reduced on transfected side when compared to the nontransfected side, as had been found with Hoxd10/EGFP electroporations. However, in Hoxd9/EGFP electroporated embryos, no Lim1/2 (+) cells were noted in the somatic motor column on the transfected side. This was true following the ectopic expression of Hoxd9 at anterior T levels (n=6/7) and the overexpression of Hoxd9 at posterior T levels (n=6/7) (Figure 29 C).

6.2.4 Ectopic and Overexpression of Hoxd9/EGFP in T segments does not induce RALDH2

At stage 29, motoneurons in the LS spinal cord normally express RALDH2, while motoneurons in T segments do not. Transverse T sections from embryos electroporated with Hoxd9/EGFP were double-labeled for EGFP and RALDH2 antibodies (n=3, Figure 29 E-F). On the transfected side of posterior T segments, there was no RALDH2 expression. We also performed double *in situ* hybridization/ immunohistochemistry on sections from Hoxd9/EGFP electroporated embryos using an *Isl1* probe and a RALDH2 antibody (n=3, Figure 29 D). No RALDH2 expression was observed on the transfected side. Similar results were obtained in embryos with ectopic expression of Hoxd9/EGFP in anterior T segments (n=3).

6.2.5 Nerve patterns appeared normal in T segments of Hoxd9/EGFP electroporated embryos

To determine if electroporation of Hoxd9 alters gross nerve patterns in segments from the T spinal cord, we compared EGFP+ nerve patterns in Hoxd9/EGFP electroporated embryos and EGFP embryos. Trunk and posterior limb regions were examined as wholemounts immediately

after sacrifice and before sectioning (n=7). In these preparations, we observed no gross alterations in the thoracic nerve patterns in Hoxd9/EGFP electroporated embryos. Unlike nerve patterns in Hoxd10/EGFP electroporated embryos, we did not see clearly large EGFP-labeled proximal connectives that linked thoracic and LS1 spinal nerves (Figure 30).

6.3 DISCUSSION

The aim of the experiments described in this chapter was to determine if the molecular phenotype and nerve pattern alterations observed with Hoxd10 electroporations were a non-specific effect of the early and high expression of any Hox gene in the posterior T spinal cord. A preliminary characterization of the normal expression patterns of Hoxd9 in the chick embryonic spinal cord indicated that Hoxd9 is expressed in the posterior T spinal cord as well as the LS spinal cord. We then ectopically expressed and overexpressed Hoxd9 in anterior and posterior T segments, respectively. We found no evidence of an induction of LS-like motoneurons with either the overexpression or ectopic expression of Hoxd9 in the T spinal cord. The expression of Hoxd9 in the T spinal cord did not induce either the expression of Lim 1 or RALDH2. These findings suggest that the induction of an LS phenotype in the T spinal cord is a specific attribute of Hoxd10 expression.

Prior studies have characterized the effects of Hoxd9 in loss-of-function mice. Hoxd9 mutants do not have specific limb gait defects like Hoxd10 mutants (Fromental-Ramain et al., 1996). No central or peripheral nerve phenotypes have been reported in the Hoxd9 mutants, although, specific studies of motoneuron development have not been made. Studies have also targeted the disruption of multiple Hox9 paralogues, including Hoxa9/Hoxd9 and Hoxa9/Hoxb9/Hoxd9 (Chen and Capecchi, 1997; Chen and Capecchi, 1999). While, mesodermal patterning defects in the T region are present there are no reported alterations in neural phenotypes. It may be difficult to identify segmental differences in the T region because the somatic motor columns and nerve patterns appear uniform along the A-P axis. However, preganglionic sympathetic neurons in the T spinal cord do exhibit segment-specific patterns. Most preganglionic sympathetic motoneurons found in anterior T segments project rostrally, whereas, preganglionic sympathetic motoneurons in posterior T segments project caudally

(Forehand et al., 1994). Since our findings with Hoxd10 suggest that this gene has a prominent influence on the axon pathfinding of motoneurons, future studies may ectopically express Hoxd9 in anterior T segments and determine if preganglionic sympathetic motoneurons alter their trajectories to more caudal targets.

Hoxd9/Hoxd10 double mutants do display altered peripheral nerve phenotypes that suggest synergistic interactions. In Hoxd10 mutants, the peroneal nerve or dorsal nerve trunk is reduced by 20% in adult mice and missing in 30 % of embryos. In Hoxd9/Hoxd10 double mutants, the peroneal nerve is reduced or missing in 61% of adult mice and reduced in all embryos (de la Cruz et al., 1999). This observation suggests that Hoxd9 normally operates with Hoxd10 to pattern hindlimb peripheral nerves, and supports the hypothesis that there is a functional interaction between these two adjacent Hox genes. Future experiments might ask whether adjacent Hox genes from the same family have combinatorial effects on molecular profiles. Co-transfection experiments with Hoxd9 and Hoxd10 might be used to determine if there is a more pronounced change in molecular phenotype than with Hoxd10 transfections alone.

7.0 OVEREXPRESSION OF HOXD10 IN LUMBOSACRAL SEGMENTS CHANGES THE PROPORTION OF LATERAL AND MEDIAL MOTONEURON SUBTYPES

7.1 INTRODUCTION

We have used *in ovo* electroporation to ectopically express Hoxd10 in T segments at early neural tube stages. Analyses of experimental embryos at stages after motor column formation and axon outgrowth have shown that transfected motoneurons develop an anterior LMCl molecular profile and project axons to dorsal limb muscles. In particular, our data have demonstrated that the ectopic expression of Hoxd10 leads to the development of Lim1 (+) and RALDH2 (+) motoneurons in the T spinal cord. Since Hoxd10 is endogenously expressed in the LS spinal cord, we asked if increasing the expression of Hoxd10 in anterior LS segments would increase the number of Lim 1(+) and RALDH2 (+) cells in the LS spinal cord.

7.2 RESULTS

7.2.1 Overexpression of Hoxd10 promotes the development of LMCl motoneurons

To assess the effect of Hoxd10 overexpression on the development of the LS spinal cord, we targeted our electroporations to overexpress Hoxd10/EGFP or EGFP DNA in LS segments of stage 13-15 chick embryos. Electroporations were carried out with DNA concentration ranging from 0.625-1.25 μg/μL. Electroporated embryos were sacrificed at stage 28-29, fixed, and sectioned as performed in previous experiments. To determine if Hoxd10 mRNA levels were increased at stage 28-29, we first stained adjacent transverse sections from anterior LS segments

of Hoxd10 electroporated embryos (n=3) with either an EGFP antibody or a probe for *Hoxd10* mRNA. We consistently noted an increased intensity of *Hoxd10* staining that tightly coincided with the distribution of EGFP(+) cells on the transfected side of the spinal cord (Figure 31 A-B).

We next compared the LIM expression profiles on the transfected and nontransfected sides of both Hoxd10/EGFP and EGFP embryos. Adjacent transverse sections from anterior LS segments were antibody stained with EGFP, Isl1/2, and Lim 1/2 antibodies. On the transfected side of EGFP electroporated embryos, EGFP+ cells were found extensively in the somatic motor region, and the somatic motor region appeared normal in size when compared to the nonelectroporated side (Figure 32 A) (n=8/9). In addition, the number of Lim 1+ cells in the somatic motor region appeared similar on the transfected and nontransfected side of EGFP embryos (Figure 32 B).

In Hoxd10/EGFP electroporated embryos, the majority of EGFP+ cells in the somatic motor region were located in a dorsolateral position, and there was a reduction in the size of the somatic motor columns (Figure 32 C). Despite the size of the reduction we noted that the number of Lim1/2(+) cells in the transfected somatic motor region appeared to be equivalent or larger on the transfected side when compared to the nontransfected side (Figure 32 D). Figure 32 shows a high magnification view, comparing the transfected and nontransfected somatic motor regions. The number of Lim1/2+ Isl1/2 + cells appears greater on the transfected side than the nontransfected side of Hoxd10/EGFP electroporated LS segments, yet, the overall size of the somatic motor region appears to be reduced on the transfected side (n=8/9; Figure 32 E,F). While, the overexpression of Hoxd10 in LS segments results in a reduction of motoneuron number on the transfected side, a greater proportion of the remaining motoneurons are Lim1 (+). These observations are compatible with the hypothesis that the effect of overexpressing Hoxd10 in anterior LS segments specifically promotes the development of Lim1 (+) motoneurons.

If Hoxd10 is promoting the development or survival of Lim 1+ motoneurons (LMCl), then a proportional reduction in Isl 1+ motoneurons (LMCm and MMC) might be predicted. To determine if the overexpression of Hoxd10 leads to a decrease in Isl 1+ motoneurons, transverse sections were either double –labeled with an EGFP and Isl 1/2 antibody, or processed with a probe for Isl 1 and stained with Isl 1/2 antibody (n=5). Figure 33 is a high magnification view of the transfected and nontransfected somatic motor region. On the transfected side, there were disproportionately fewer Isl 1+ cells when compared to the

nontransfected side (Figure 33 B and C). These findings suggest that the effect of overexpressing Hoxd10 in anterior LS segments impedes the development of Isl 1+ motoneurons.

7.2.2 Overexpression of Hoxd10 in LS spinal segments promotes RALDH2 expression

In anterior LS segments of stage 29 chick embryos, RALDH2 (+) cells are normally located laterally in the position of the LMCl, and do not appear to express Isl 1. To determine whether the overexpression of Hoxd10 in LS segments enhances RALDH2 expression, we performed double *in situ* hybridization/ immunohistochemistry on LS sections from Hoxd10/EGFP electroporated embryos using an Isl1 probe and a RALDH2 antibody. While, the somatic motor region appears to be reduced on the transfected side of experimental embryos, a large number of the cells in this region appear to be RALDH2 (+) (Figure 34 A-C, n=3/3). These findings suggest that Hoxd10 overexpression in LS segments proportionately increases the number of RALDH2(+) cells in the somatic motor region.

To examine the relationship between transfected cells (EGFP+) and RALDH2 expressing cells, transverse sections through the anterior LS segments of Hoxd10/EGFP and EGFP electroporated embryos were double-stained with EGFP and RALDH antibodies.

In Hoxd10/EGFP electroporated embryos, EGFP(+) cells were found in the dorsolateral portion of the somatic motor region and tightly overlapped with cells that showed increased RALDH staining intensity(n=3/4, Figure 35 A-B). Isolated clusters of EGFP+ cells were more intensely stained for RALDH2, suggesting that Hoxd10 induces RALDH2 in a cell autonomous manner. No increase in RALDH2 expression was observed on the nontransfected side of Hoxd10/EGFP embryos (n=4/4) or the transfected side of EGFP electroporated embryos (n=4/4, Figure 35 C, D, and E). This observation is compatible with the hypothesis that LS motoneurons with higher levels of Hoxd10 express higher levels of RALDH2.

7.3 DISCUSSION

In this chapter we made two major observations. First, the overexpression of Hoxd10 in anterior LS segments leads to changes in the proportion of LMCl and LMCm/MMC motoneurons. Second, Hoxd10/EGFP transfected LS motoneurons show an increase in the intensity of RALDH2 expression.

We found that the Hoxd10 overexpression in the LS spinal cord leads to a disproportionate increase in the number of Lim 1+ and RALDH2+ motoneurons. This molecular profile is normally shown by LMCl motoneurons in the anterior LS spinal cord. These findings are compatible with our results following the ectopic expression of Hoxd10/EGFP in T segments, where Hoxd10 appears to promote the development of anterior LS LMCl motoneurons.

Hoxd10 overexpression in LS segments also led to a proportional reduction in Islet1 + motoneurons (MMC and LMCm motoneurons). One explanation for this reduction is that LMCm or MMC motoneurons were induced early but did not survive to stage 28-29. During motor column formation, Hoxd10 expression normally declines in LMCm cells but is highly expressed LMCl cells. This decline in Hoxd10 expression might be important for survival of Isl 1+ motoneurons. An alternative hypothesis is that Hoxd10 specifically promotes an LMCm/MMC to LMCl fate change. This hypothesis might be addressed by examining Hoxd10 electroporated embryos with different motoneuron subtype markers at earlier stages of development when motoneurons are first beginning to differentiate.

We observed that LS motoneurons expressing high levels of Hoxd10/EGFP appeared to express higher levels of RALDH2. Even isolated clusters of Hoxd10/EGFP transfected cells showed increased RALDH2 staining intensity, suggesting that Hoxd10 induces RALDH2 in a cell autonomous manner. The analysis of Hoxc8 and RALDH2 mutants also suggest a dual role for Hox genes and RALDH2 in the specification of LMC cell fates (Vermot et al. 2005). Hoxc8 and RALDH2 mutant mice exhibit a loss of Lim1+ and RALDH2+ cells in the brachial spinal cord. Vermot et al. (2005) and Sockanathan et al. (1998) have hypothesized that RALDH2 produced by LMC motoneurons provides local RA signals which are then transduced by RARβ receptors to activate Lim1 expression in adjacent LMC motoneurons. Other studies have shown that excess RA can ectopically induce the expression of RARβ receptor in the spinal cord

(Colbert et al., 1995). In light of these studies, our data is compatible with the hypothesis that Hoxd10 may be involved in autocrine signaling. Hoxd10 may regulate the expression of RALDH2, and possibly the RARβ receptor (via local RA levels), to activate Lim 1 expression. Future studies might determine if RARβ receptor levels change following Hoxd10 overexpression in the LS spinal cord.

Both the Hoxd10 and the Hoxd10/Hoxa10 mutant mice have reduced numbers of LMC motoneurons in the LS spinal cord; however, no molecular distinction was made in terms of a loss in specific motoneuron subtypes (Wahba et al., 2001, Carpenter et al., 1997). Our data suggest that it would be worthwhile for future studies to re-examine the Hoxd10 mutant mice for specific losses in Lim1 + and RALDH2 + motoneurons.

As with the ectopic expression of Hoxd10 in the T spinal cord, the overexpression of Hoxd10 in LS segments results in a reduction in cell numbers. This observation strongly conflicts with a previously mentioned hypothesis for the reduction of motoneurons in the T spinal cord, in which Hoxd10 transfected motoneurons found in an abnormal environment die prematurely due to a lack of survival factors. Following this reasoning, one might expect that the overexpression of Hoxd10 in the normal LS environment could lead to an increase in motoneuron numbers. Instead, we found that the effect of overexpressing Hoxd10 results in proportionate changes in motoneuron numbers, with no apparent enlargement of the somatic motor regions. These observations are compatible with the idea that region-specific differences in proliferation patterns are established early, and suggest that Hoxd10 is not involved in this process (Oppenheim et al., 1989). It also appears that the overexpression of Hoxd10 has general effects on motoneuron numbers in both the T and LS spinal cord, and supports our previous conclusion that early and high levels of Hoxd10 may adversely affect motoneuron survival.

8.0 GENERAL DISCUSSION

8.1 THE ROLE OF HOXD10 IN MOTOR COLUMN DEVELOPMENT.

Hoxd10 is expressed at high levels in the LS spinal cord from early stages of motor column formation to the late stages of motor neuron outgrowth, suggesting that Hoxd10 may have multiple roles in motoneuron development. Our findings have shown that Hoxd10 imparts an LS identity to the developing neural tube (see Figure 36). Specifically, Hoxd10 induces Lim1 and RALDH2 expression in motoneurons, in a pattern like that normally found in the LMCl of anterior LS segments. These findings raise the question of whether Hoxd10 imparts a generic LS identity or a specific LMCl profile. Is the LMCm induced in T segments? Data from ectopic expression of Hoxd10 in T segments were unclear, since LIM patterns did not distinguish the LMCm and MMCl motoneurons. To determine if Hoxd10 expression promotes a LMCm motoneuron phenotype, future studies might ectopically express Hoxd10 in T segments and perform retrograde labeling of ventral limb muscle that are normally innervated by LMCm motoneurons.

Data from the overexpression of Hoxd10 in LS segments indicated a proportional increase in Lim 1+ and RALDH2+ (LMCl) motoneurons, and decrease in Isl 1+ motoneurons (LMCm and MMC). The reduction of Isl 1+ cells raises the question of whether Hoxd10 is having a unique effect on LMCm, MMC, or on both subpopulations of motoneurons. To address this question one might stain slides from our Hoxd10 overexpression experiments with a Lim3 antibody, to distinguish the LMCm and MMC subpopulations (Tsuchida et al., 1994).

Data from the ectopic expression of Hoxd10 in T segments performed at later stages (stages 17-18) showed that late electroporations induced more Isl 1/2 + (ectopic Isl 1/2+) cells. Recent studies in zebrafish showed that Hox genes can regulate the expression of HB9, a transcription factor that directs motoneuron-specific gene expression during early stages of motoneuron development (Nakano et al., 2005). This finding raises the question of whether our

late electroporations are having effect on the motoneuron vs. interneuron fate decision, or whether they are having a specific effect on the specification and/or survival of LMCl motoneurons. To address theses issues we propose two potential experiments. First, future studies can perform even later electroporation of Hoxd10 in T segments to see if there are an even greater number of Isl 1/2 cells. If there is a greater number of Isl 1/2 + cells, further analyses with motoneuron and interneuron markers are needed to determine if later electroporations enhance the LMCl motoneuron phenotype. Second, experiments in which Hoxd10 is conditionally ablated would be useful in dissecting the function of the early expression patterns of Hoxd10 in the spinal cord (see Figure 36). In order to examine the function of Hoxd10 in the LS spinal cord, previous studies have inactivated the expression of Hoxd10 (Carpenter et al., 1997). The Hoxd10 knockout model, however, is not useful fro gaining an understanding of the temporal patterns of Hoxd10. An ideal approach to resolve this issue is to conditionally inactivate Hoxd10 expression at different stages during the development of the LS spinal cord. Until recently, a reliable method to ablate target genes in the avian embryo was not available. The development of RNA interference (RNAi) provides a loss-of-function tool for developing chick embryos (Pekarik et al. 2003, Katahira and Nakamura 2003). To determine if the early expression of Hoxd10 is important in the progression of progenitor cells to a motoneuron fate, future studies should use RNAi technology and conditionally silence the expression of Hoxd10 in the avian neural tube at different stages of motoneuron development.

Our findings also showed that Hoxd10 expression in T segments leads to the induction of Pea3, a specific limb motor pool marker. This observation raises the possibility that Hoxd10 functions at later stage to establish specific motor pool identities. The latest stage we examined Hoxd10 electroporated embryos was stage 29, however, previous studies have shown that the LS spinal cord normally expresses Hoxd10 to at least stage 35 (Lance-Jones et al., 2001). Further studies might examine the expression of other motorpool specific markers to determine if Hoxd10 also encodes motorpool specific identity in the LS spinal cord. In addition, studies have shown that GDNF from the limb induces the expression of Pea3 in a subset of motoneurons at limb levels (Haase et al., 2002). GDNF is a neurotrophic factor that binds to the RET and GFRα1 receptor complex. The activation of this pathway prevents cell death during the normal cell death period (Pachnis et al., 1993; Garces et al., 2000; Cacalano et al., 1998; Moore et al., 1996). Do high levels of Hoxd10 promote the survival of motoneurons during the normal cell death period?

It might also be worthwhile to examine Hoxd10 electroporated embryos at later stages (after stage 29) to determine if Hoxd10 has a later role during the normal cell death period.

8.2 THE ROLE OF HOXD10 IN OTHER CELL POPULATIONS.

It is clear from our electroporations that we transfected various cell types in the neural tube, including interneurons and neural crest cells (NCCs). Hox genes are normally expressed by interneurons and NCCs suggesting that Hox proteins may be involved in establishing molecular identity and target connectivity among these other cell populations. The diversity of interneurons and the patterns of their local circuits are not well characterized. Future experiments might ask if the misexpression of Hox genes alters the connectivity and the distribution of specific interneuron populations along the A-P axis (limb innervating region vs. nonlimb region).

In Hoxd10 electroporated embryos, we consistently observed migrating NCCs expressing Hoxd10 at high levels. NCCs are pluripotent cells that emerge from the dorsal spinal cord, to give rise to bones, tendons, adipose tissue and several types of neuronal, glial, and endocrine cells (Le Douarin and Teillet, 1974; Le Lievre et al., 1980; Sieber-Blum and Cohen, 1980). In craniofacial development, Hox genes have a prominent role in patterning head neural crest derivatives. For example, facial bone cells arise only from Hox-negative skeletogenic NCCs, whereas cartilage cells stem from both Hox-positive and Hox-negative NCCs (Crezet et al., 2002; Abzhanov et al., 2003). Evidence suggests that the developmental potential of the NCCs are restricted by Hox gene expression (reviewed by Le Douarin et al., 2004). In the trunk region, NCCs give rise to a number of structures including sensory neurons and parasympathetic ganglion (Le Douarin and Teillet, 1974). Little is known about the function of Hox genes in the development of posterior structures. It may be worthwhile to determine if Hoxd10 transfected NCCs emerging from the posterior spinal cord have altered identity, migration patterns, or differentiation.

8.3 THE RELATIONSHIP BETWEEN HOXD10 AND OTHER HOX PROTEINS.

Our findings demonstrate that the misexpression of a single Hox gene in the posterior spinal cord alters molecular profiles of motoneurons that are matched by changes in their connectivity. Recent studies by Dasen et al. (2005) showed that coordinate activities of multiple Hox genes establish A-P motor pool identity and the intrasegmental diversification of motor pools. In a tour de force effort, Dasen and colleagues examined 11 Hox proteins in the development of the LMC in the brachial spinal cord. They provide evidence that different Hox proteins form a "regulatory network" in which specific Hox protein interactions assign 1) LMC motor columnar identity (motor axons are directed to the limb, 2) the intrasegmental division of motor pools (assigning LMC motoneurons with medial or lateral identities such that motor axons are directed to ventral or dorsal muscles) and 3) motor pool identity (to direct motor axons to specific muscles along the AP axis). Moreover, experimental manipulations of Hox gene expression, via *in ovo* electroporation, can readily change the identity of motor pools and this identity change is matched by predicted alterations in peripheral connectivity. Findings from these studies raise the question of whether a "regulatory network" of Hox proteins operates to pattern LS motoneurons (Dasen et al., 2005). Only a small number of studies have examined a combination of Hox genes in the development of the posterior spinal cord (Wahba et al., 2001, de la Crux et al., 1999).

What is the relationship of different Hox genes in the same linkage group? How do adjacent Hoxd genes interact to pattern the posterior spinal cord along the A-P axis? The majority of the loss-of-function studies suggest that adjacent Hox genes largely function independently, however, there is some data suggesting that adjacent Hox genes work coordinately to pattern the LS spinal cord (de la Crux et al., 1999). For example, the double Hoxd9/Hoxd10 mutant mice exhibit a phenotype that is different from the combination of the Hoxd9 and Hoxd10 mutant phenotypes. Hoxd9 and Hoxd10 appear to function together to provide more patterning information to the LS spinal cord than either Hoxd9 or Hoxd10 alone. Future experiments may seek to determine if adjacent Hox genes with overlapping expression patterns interact to impart patterning information to the same region along the A-P axis. In addition, it is clear from Dasen et al. (2003) that specific subsets of Hox protein in the anterior spinal cord are mutually repressive. This raises the question of whether other Hox proteins

regulate and/or restrict the expression of Hoxd10 in the LS spinal cord. Further studies need to examine the expression patterns of neighboring 5' Hox genes (i.e. Hoxd8 and Hoxd11) and determine if repressive interactions exist between them.

What is the relationship of Hox genes in different linkage groups? How do Hoxa, Hoxb, Hoxc, and Hoxd genes interact to pattern the posterior spinal cord along the A-P axis (see Figure 36)? Prior studies suggest that Hox genes from different families that are expressed in the similar positions along the AP axis (i.e. paralogues Hoxa10 and Hoxd10), have distinctive, redundant and synergistic activities. Comparisons of gross spinal cord and limb morphology in single and double mutants suggest that paralogue genes cooperatively function to pattern the spinal cord (Rijli et al., 1995; Carpenter et al., 1997; Wahba et al., 2001). How the combinatorial expression of Hox genes defines the segmental identity of motoneurons and dictates their peripheral nerve projections is not well understood. Future studies may seek to investigate the specific and cooperative effects of Hoxa10, Hoxc10, and Hoxd10. For example, it would be useful to ectopically express Hoxa10 and compare the outcome to our results following the ectopic expression of Hoxd10. Further experiments might co-express Hoxa10 and Hoxd10, and determine if Hoxa10 and Hoxd10 function cooperatively in the specification of motoneuron subtypes.

In our experiments, we consistently observed a lateral bias in the settling of Hoxd10 transfected motoneurons. Regardless of the stage of electroporation (early vs late) or the level of the spinal cord (T vs. LS), transfected motoneurons were found in the dorsolateral portion of the somatic motor column. The lateral-medial restriction of Hox gene expression has not been studied in the normal developing spinal cord. Do other Hox genes lead to a medial bias in motoneuron specification and settling? The expression patterns of other 5'Hox genes should be examined to determine if other Hox genes have restricted expression patterns in the medial portion of the somatic motor region. Future experiments might ectopically express these other 5' Hox genes to determine if these genes distinctively direct the development of lateral and medial motoneuron subtypes.

8.4 HOXD10 AND THE INDUCTION OF CELL ADHESION AND GUIDANCE MOLECULES.

Our experiments have identified a role for Hoxd10 in motoneuron specification and axon pathfinding, and suggest that Hoxd10 regulates genes involved in the process of cell migration, differentiation, and axon pathfinding. Understanding the exact mechanism through which Hox genes mediate segment-specific identity requires the identification of their downstream targets.

As newly born motoneurons acquire motor columnar identity, they simultaneously undergo axogenesis and migrate to their respective positions in the somatic motor region.

Many of the molecules that are likely to be involved in processes like migration and differentiation are cell adhesion molecules. Recent studies showed that Type II cadherins exhibit restricted expression patterns in specific motor pools. Type II cadherins are potential downstream candidates of Hox genes. They are uniquely upregulated in migrating cells and may have a role in the segregation of LMCm and LMCl motoneurons. The misexpression of specific cadherins during motoneuron development disrupts the normal segregation of motor pools (Price et al. 2002). Specific motorpools in the dorsolateral somatic region appear to express Cad6b, a likely target of Hoxd10. In addition, analyses of Hoxa1 mutants exhibited a lack of Cad6 expression in the region of rhombomeres 4 to 6 (Inoue et al., 1997), suggesting a link between Hox proteins and Cad6 expression. Future experiments should seek to determine if Type II cadherins are a downstream target of 5' Hox genes.

The experiments in this thesis have linked a single posterior Hox gene to several downstream guidance molecules. Our findings have linked Hoxd10 to the induction of Lim 1 expression. Recent studies demonstrated that Lim1 can induce the expression of EphA4 (Kania and Jessell, 2003). EphA4 is first expressed by most LMC motoneurons in limb-innervating regions, but later becomes restricted to LMCl regions. Further experiments should be conducted to determine whether EphA4 expression parallels the expression of Lim1 after the electroporation of Hoxd10 into T segments (see Figure 36).

Our findings also raise the possibility that HGF/c-met signaling mediates the long-range trajectories of Hoxd10 transfected T motoneurons. Although, Hoxd10 induces c-met expression in T segments, it unclear to what extent the c-met receptor operates to drive axon pathfinding. To verify whether the novel axonal projections of Hoxd10 transfected T motoneurons are primarily

mediated by HGF/c-met signaling, future studies might ectopically express c-met in the T spinal cord. If the HGF/c-met signaling mediates the novel trajectories of Hoxd10 transfected motoneurons we would expect to see comparable nerve patterns. In addition, recent studies showed that c-met signaling participates in the anterior recruitment of motoneurons to express Pea3 in limb-innervating regions of the spinal cord (Helmbacher et al., 2003). The proposed c-met misexpression studies would also test the hypothesis that c-met signaling induces an anterior expansion of Pea3+ cells.

Our data suggest that Hox gene expression in motoneurons has a prominent role in the navigation of motoneurons to their respective targets. Since Hox genes are expressed in both neural and non-neural tissue, we can not exclude the possibility that Hox gene expression in mesodermal tissue also contributes to motoneuron axon pathfinding. Future studies might seek to determine if Hoxd10 expression in the mesenchyme participates in the establishment of guidance cues for LS spinal motoneurons. During the early stages of hindlimb bud outgrowth, Hoxd10 is expressed uniformly throughout the mesoderm of the limb bud. Between stages 19-23, Hoxd10 expression becomes restricted to distinct domains within the limb bud mesoderm. By stage 23, Hoxd10 expression is restricted to two domains, the proximal- posterior and distal-posterior limb mesoderm (Nelson et al. 1996). The restriction of Hoxd10 expression to the posterior limb bud coincides with the entrance of posterior LS spinal axons into the limb. Misexpression studies combined with analyses of nerve patterns and the distribution of guidance molecules like members of the ephrin or Eph families might be used to determine if peripheral Hox expression contributes to axon pathfinding.

8.5 MOLECULES THAT ESTABLISH AND REGULATE HOXD10 EXPRESSION IN THE SPINAL CORD.

Our experiments did not address the question of what molecules establish and regulate the expression of Hoxd10 in the developing spinal cord. Previous studies demonstrated that the A-P identity of the spinal cord is sensitive to environmental signals from other tissues (Ensini et al., 1998). In the anterior spinal cord, studies suggest that a combination of signals from the paraxial mesoderm and Henson's node (tailbud) influence the expression of Hox genes in the

developing neural tube (Ensini et al., 1998). Recent transplantation experiments have shown that inductive signals from the tailbud are primarily responsible for establishing *Hoxd10* expression in the neural tube at early stages. These experiments raised the possibility that paraxial mesoderm from the cervical and thoracic levels provides repressive signals for posterior Hox genes (Omelchencko and Lance-Jones, 2003). The exact mechanisms by which extrinsic signals spatially and temporally regulate the expression of Hoxd10 are not entirely understood.

Recent studies have demonstrated that while signaling molecules are important in the induction of patterning genes, the sustained presence of signaling molecules is critical for normal cell differentiation. For example, in zebrafish the transcription factor Olig2 is required for neural tube cells to select a motoneuron cell fate. The overexpression of Olig2 in the presence of the Shh signaling molecule promotes the formation of excess motoneurons. However, in the absence of Shh, the overexpression of Olig2 is unable to promote motoneuron development. In addition to Shh's ability to induce Olig2 expression, the continued presence of Shh signaling appears to provide cells with the potential to become motoneurons (Park et al., 2002). This finding raises the possibility that the presence of extrinsic signaling molecules may enhance or repress the phenotype that we observed in Hoxd10 electroporated embryos.

Early FGF and RA signaling appear to integrate D-V and A-P patterning of developing neural tube. Several pieces of evidence suggest that FGFs from the tail bud and adjacent tissue are responsible for programming Hox expression at early neural tube stages (Liu et al., 2001, Bel-Vialar et al., 2002). The exposure of neural tube explants to FGFs and the misexpression of FGF8 in the developing neural tube induce the expression of posterior Hox genes. To determine if the presence of FGFs enhances the phenotype of Hoxd10 embryos, one might alter local levels of FGF (via a slow releasing FGF bead) adjacent to Hoxd10 transfected T segments, and look for changes in molecular identity and trajectories of developing motoneurons.

A number of studies have placed RA in several stages of motoneuron development. Retinoids are involved in 1) the selection of a neuronal cell fate, 2) the definition of generic spinal cord character, 3) the establishment of a rostral character within the spinal cord, and 4) the specification of motoneuron subtypes. Little is known about the roles of RA and Hox patterns during initial stages of axonal outgrowth. Forehand et al. (1998) manipulated local retinoid signals in the T spinal cord and demonstrated that retinoid signaling affects segment-specific nerve trajectories of thoracic preganglionic motoneurons. How local RA signals affect Hox gene

expression and the early development of axon outgrowth at limb levels is not known. Understanding how multiple extrinsic signaling molecules operate to regulate Hox genes and other determinants involved in establishing neuronal identity and the formation of local circuits are formidable challenges. By combining recent advances in genetic manipulations (*in ovo* electroporations and RNAi) with classical embryological techniques, future studies have the potential to identify unique and convergent roles for signaling molecules that regulate Hox gene expression and A-P identity in the spinal cord.

APPENDIX A

FIGURES

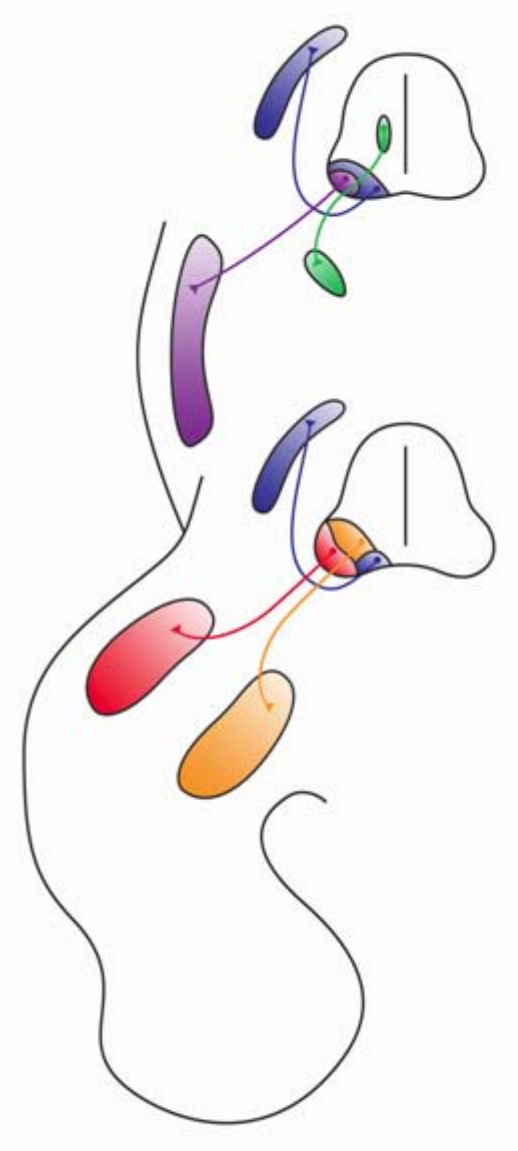

THORACIC

MMCm	axial musculature
MMCl	body wall musculature
CT	sympathetic ganglia

LUMBOSACRAL

MMCm	axial musculature
LMCL	dorsal limb musculature
LMCm	ventral limb musculature

Figure 1. Spinal motor columns and peripheral targets in thoracic and lumbosacral regions.

Figure 2. Milestones in motoneuron development in the chick posterior spinal cord from stages (st) 10-36 of Hamburger and Hamilton (1951) or 2-10 days *in ovo*.

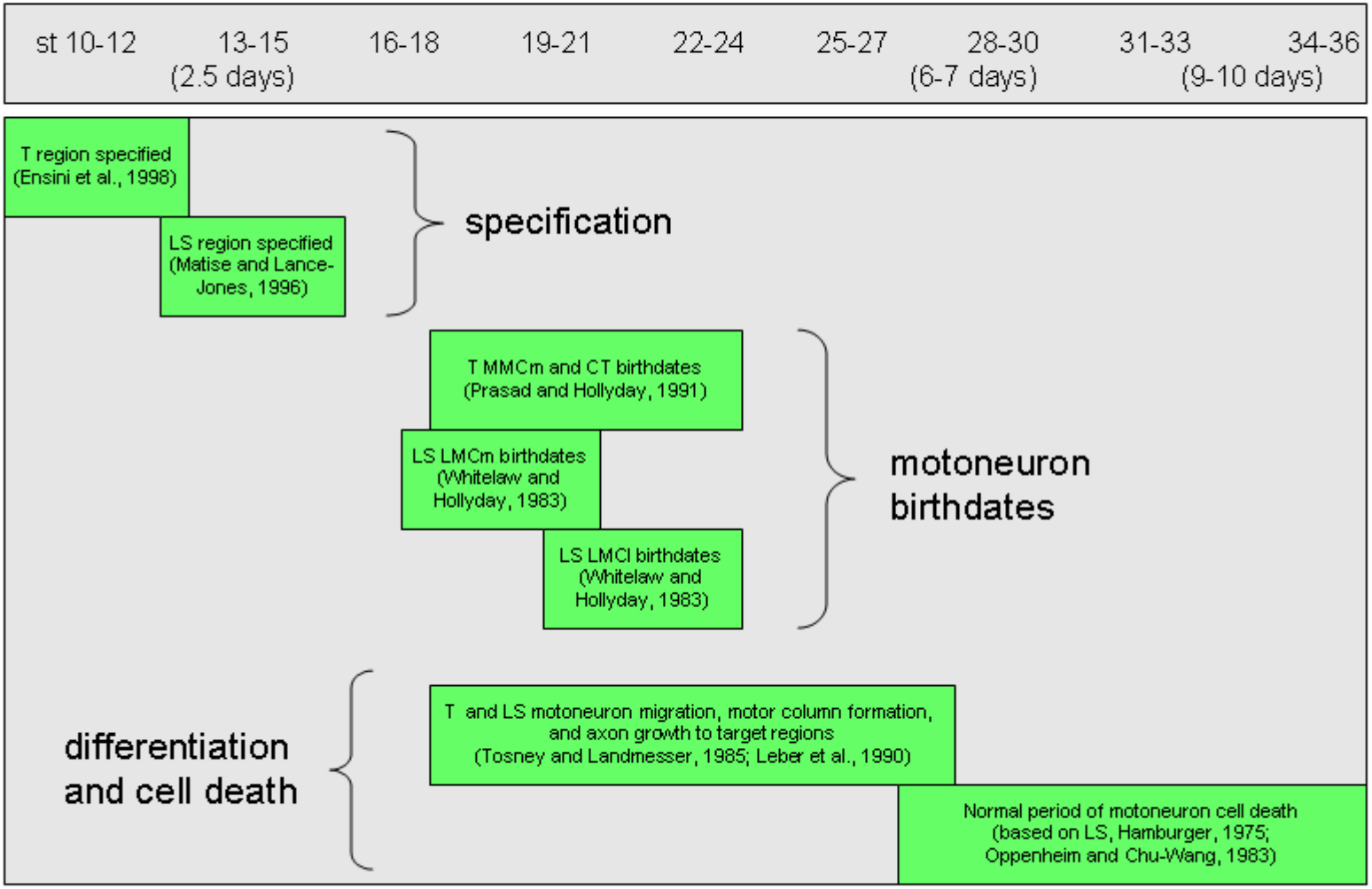

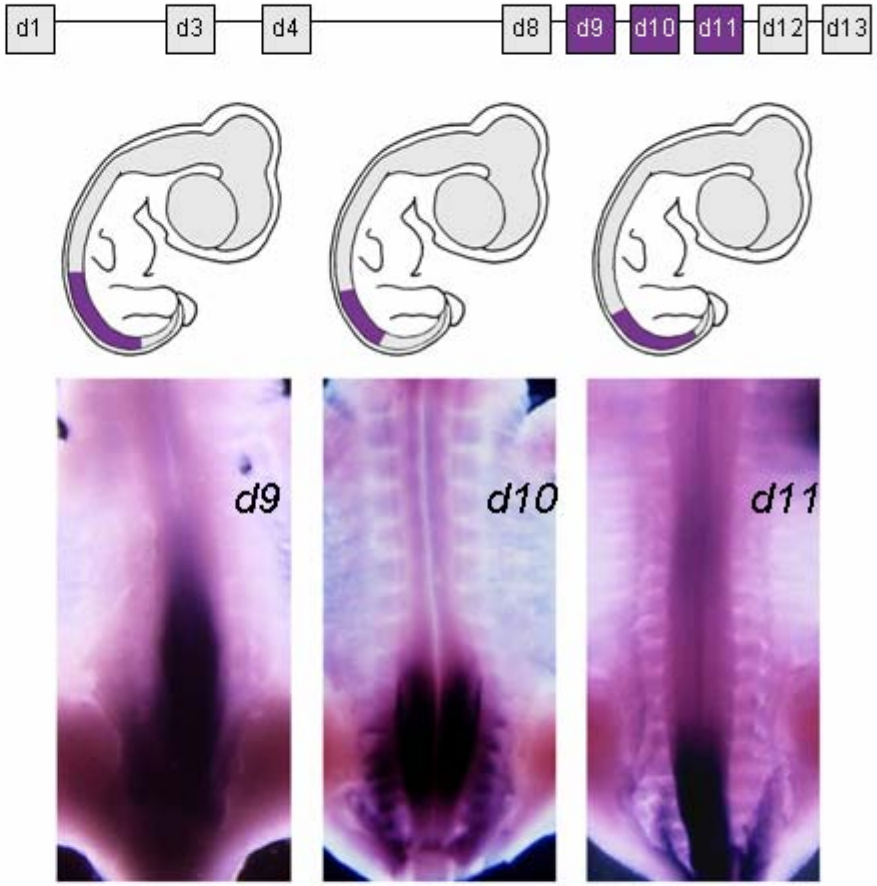

Figure 3. Hoxd gene arrangement and selected expression patterns in the stage 28-29 chick spinal cord. Top: Schematic of chromosomal arrangement after Krumlauf (1994). Middle: Drawings of the axial positions of neural *Hoxd9-11* expression. Bottom: Photos of the ventral surface of the posterior spinal cord after in situ hybridization with *Hoxd9-11* mRNA probes. *Hoxd9* expression begins at mid-T levels, *Hoxd10* at anterior LS levels, and *Hoxd11* at mid-LS levels. *Hoxd10* expression appears limited to the LS region. Preliminary observations suggest that *Hoxd9* and *Hoxd11* expression extends into the tail, however, the precise positions of posterior boundaries have not been defined. (Photo of *Hoxd11* expression courtesy of M. Misra.)

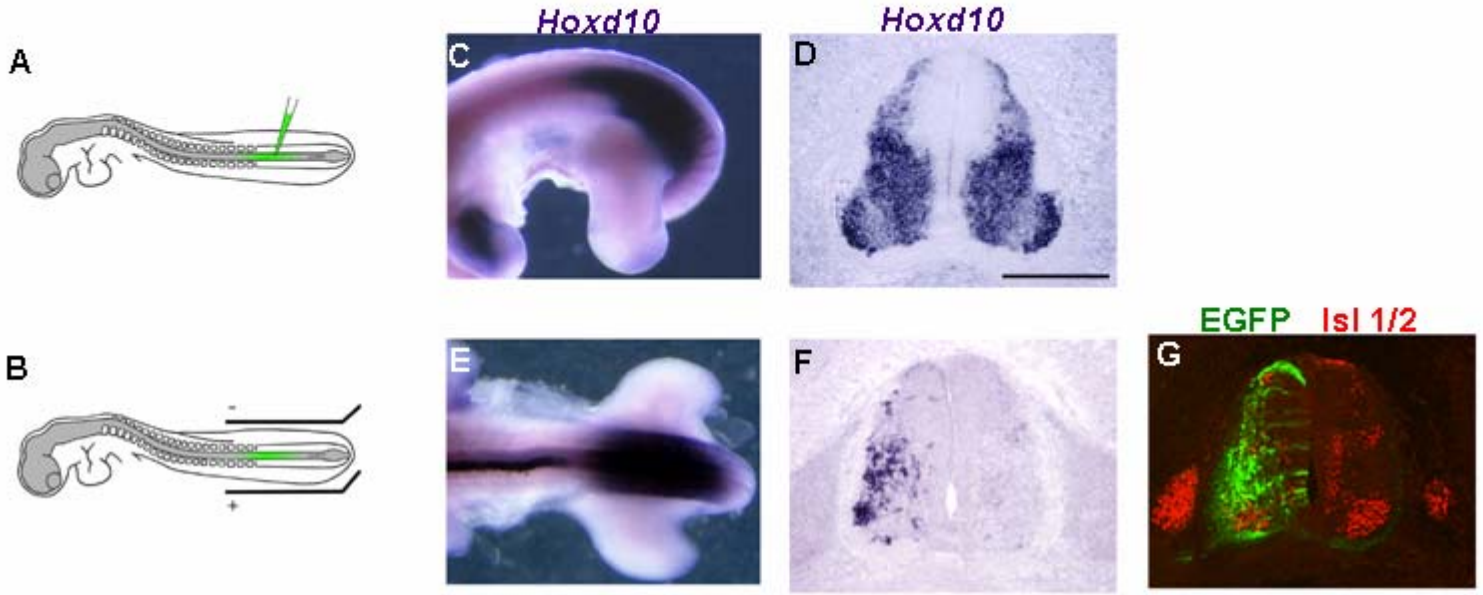

Figure 4. *Hoxd10* patterns in normal and and Hoxd10/EGFP-electroporated embryos. (A-B) Schematics depicting the microinjection of Hoxd10/EGFP or EGFP cDNA, and the placement of electrodes during *in ovo* electroporation of stage 13 chick embryos. (C-D) Normal *Hoxd10* expression in a stage 25 wholemount embryo, and in a transverse section of a normal stage 29 embryo. E. Electroporation of Hoxd10/EGFP results in high unilateral expression of *Hoxd10* in the T spinal cord as seen in a stage 24 wholemount embryo. F-G. Adjacent transverse sections from a stage 29 embryo probed for *Hoxd10* mRNA (F) and double-stained with antibodies to EGFP and Isl 1/2 (G). On the transfected side, the distribution of *Hoxd10*+ cells matches the distribution of EGFP+ cells. Scale bar in D= 200μm (applies to F and G as well).

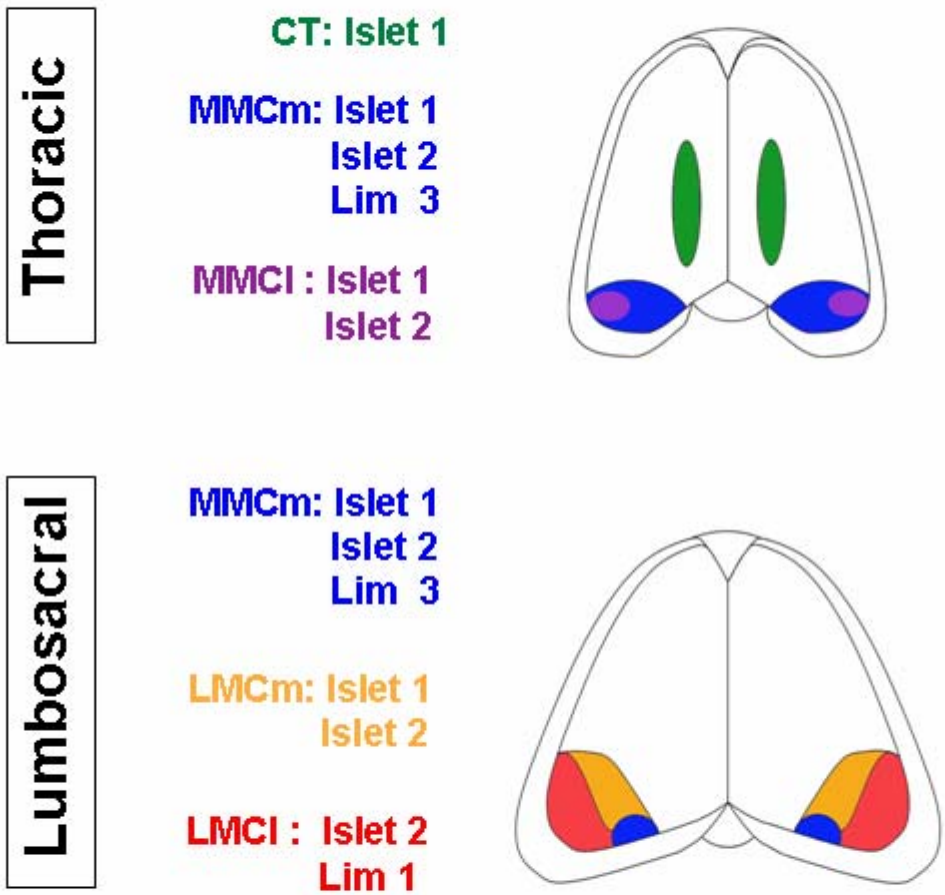

Figure 5. Schematics of normal LIM patterns in stage 28-29 T and LS segments. Adapted from Tsuchida et al., 1994.

Thoracic

Motor columns	Peripheral Targets	Isl1/2 antibody	Isl1 mRNA	Lim1/2 antibody	Lim 3 antibody
MMCm	Axial muscles	+	+	–	+
MMCl	Body wall muscles	+	+	–	–
CT	Visceral ganglia	+ Islet 1 only	+	–	–

Lumbosacral

Motor columns	Peripheral Targets	Isl1/2 antibody	Isl1 mRNA	Lim 1/2 antibody	Lim 3 antibody
MMCm	Axial muscles	+	+	–	+
LMCm	Ventral limb muscles	+	+	–	–
LMCl	Dorsal limb muscles	+ Islet 2 only	–	+ Lim1 only	–

Table 1. Staining characteristics for motoneuron subtypes.

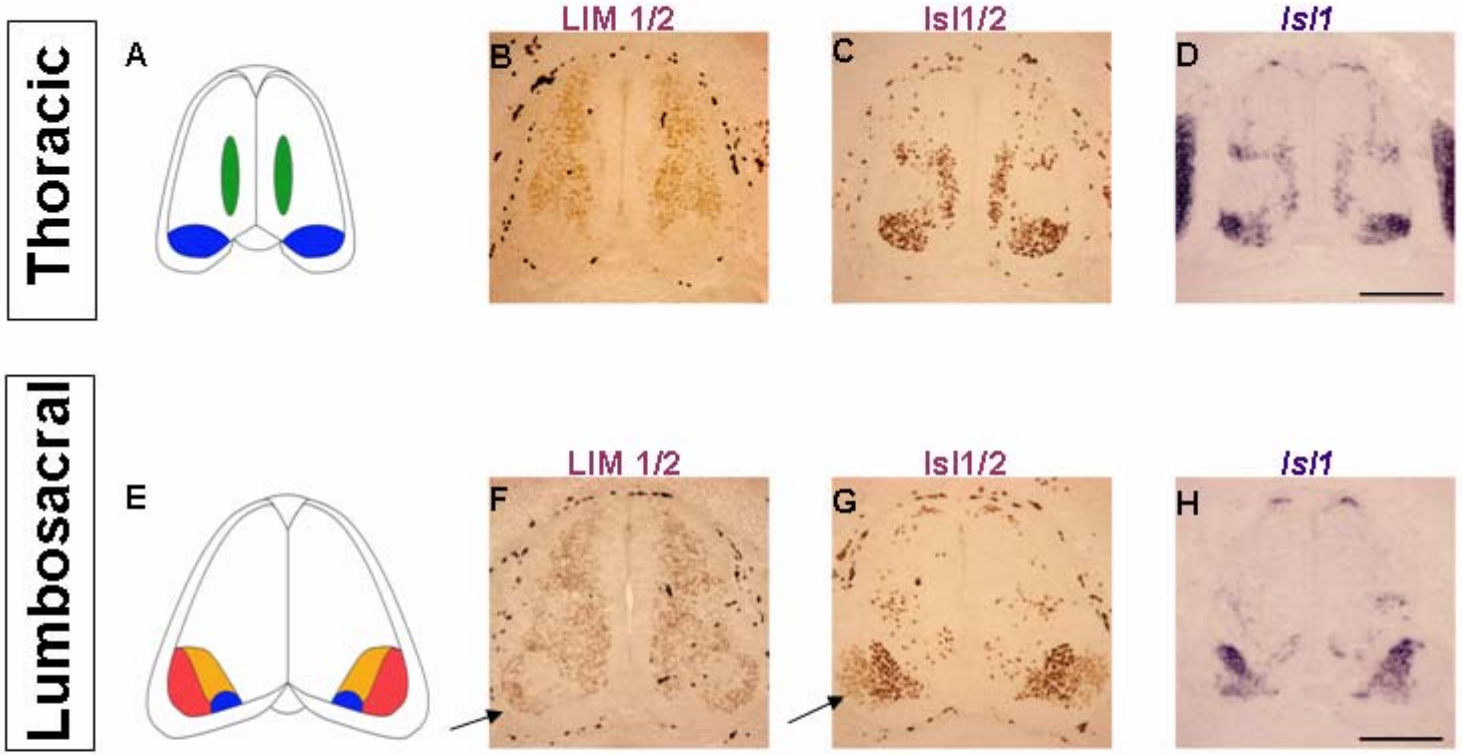

Figure 6. The identification of normal LIM patterns in T and LS spinal cord sections at stages 28-29. (A and E) Schematics showing normal motor column arrangements. Blue, MMC; green, CT; red, LMCl, orange, LMCm. (B-D) Adjacent transverse sections through a T6 segment stained with antibodies to Lim1/2 (B) , Isl 1/2 (C), and an mRNA probe for *Isl 1* (D). In the T cord, all motoneurons are either Isl1+ (CT) or Isl1/2+ (MMC) and can be identified by staining with the Isl1/2 antibody or the *Isl1* probe. No motoneurons are Lim1/2+. (F-H) Similarly-stained sections through an anterior LS segment. In the LS cord, LMCl motoneurons can be distinguished from all other motoneurons as they are Lim1/2+ (F, arrow). All LS motoneurons are Isl1/2+ but only LMCm and MMC are *Isl1* +. LMCl motoneurons express Isl2 but not Isl1 and appear more lightly stained with the Isl1/2 antibody (G, arrow). Scale Bar = 200 µm in D (applies to B-D and F-H).

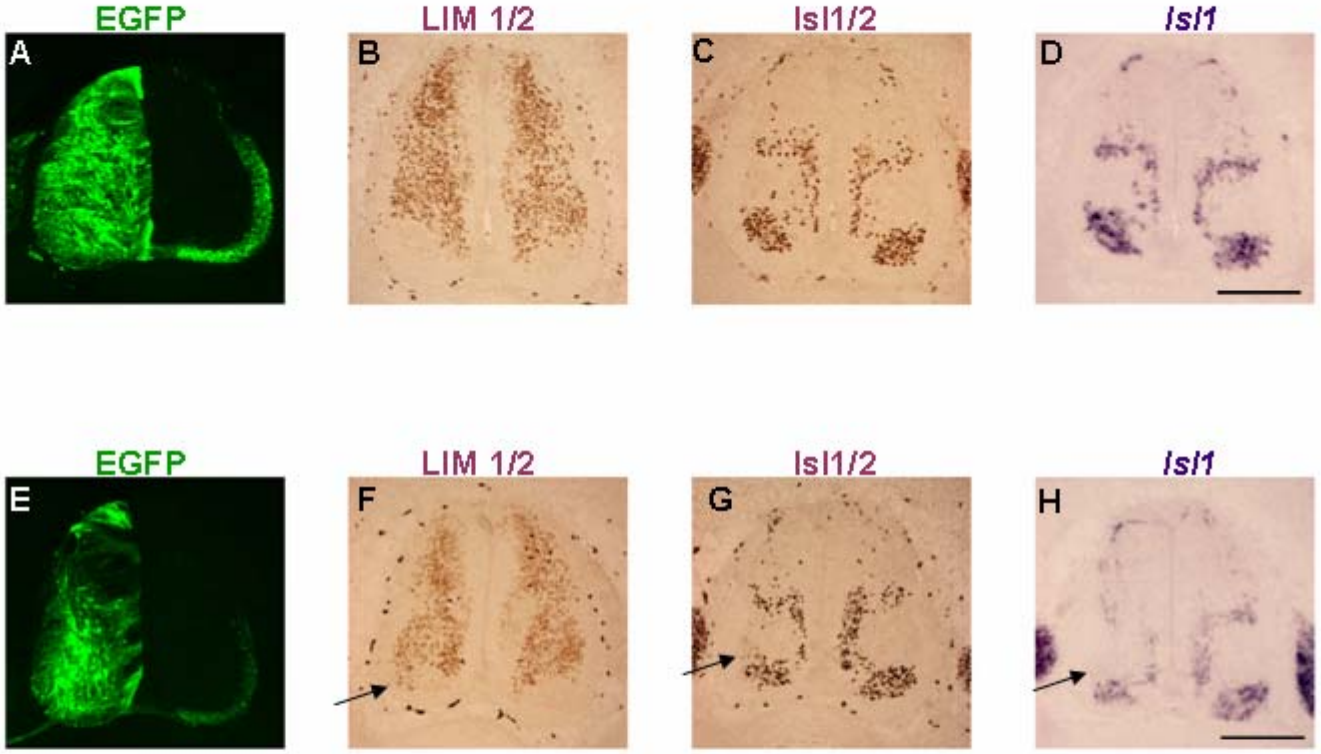

Figure 7. Ectopic expression of Hoxd10/EGFP but not EGFP in T segments induces changes in LIM profiles. (A-D) Transverse sections through T6 from a stage 29 embryo after electroporation with EGFP. Adjacent sections from the same embryo were stained with antibodies for (A) EGFP, (B) Lim1/2, (C) Isl 1/2, and (D) an mRNA probe for Isl 1. No change in LIM profiles are evident and the somatic motor region appears normal in size. (E-H) Similarly-stained sections through T6 from a stage 29 embryo after electroporation with Hoxd10/EGFP. On the transfected side, there is a ventral extension of Lim1/2+ cells into the somatic motor column (F, arrow). Arrows in G and H indicate cells in a similar position to those indicated by the arrow in F. This small ventrally-extending cluster of cells is lightly stained with the Isl1/2 antibody (G) and lacks *Isl1* expression (H). Note that a reduction in overall motoneuron numbers is evident on the transfected side of the Hoxd10/EGFP-electroporated embryo. Scale bars = 200 μm.

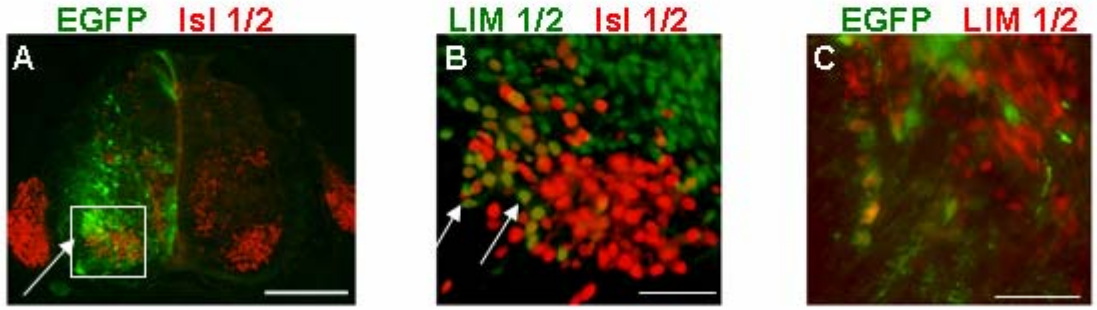

Figure 8. In Hoxd10-electroporated embryos, Lim 1/2+ cells in somatic regions are motoneurons. Transverse sections through posterior T segments from stage 29 Hoxd10/EGFP electroporated embryos double-labeled with EGFP, Lim 1/2 and/or Isl1/2 antibodies. (A) Transfected motoneurons (EGFP+/ Isl1/2+) occupy a dorsolateral position in the somatic motor region (white arrow). (B) Somatic motor region (boxed area in A) in an adjacent section from the same embryo. Double labeling with Lim1/2 and Isl1/2 antibodies indicates that Lim1/2+ cells are motoneurons (arrows). (C). Transverse section from a separate Hoxd10/EGFP electroporated embryo. Isolated clusters of EGFP+ cells are Lim1/2+, suggesting that Hoxd10 induces Lim1 expression in a cell autonomous manner. Scale bars= 200μm in A, 50μm in B and C.

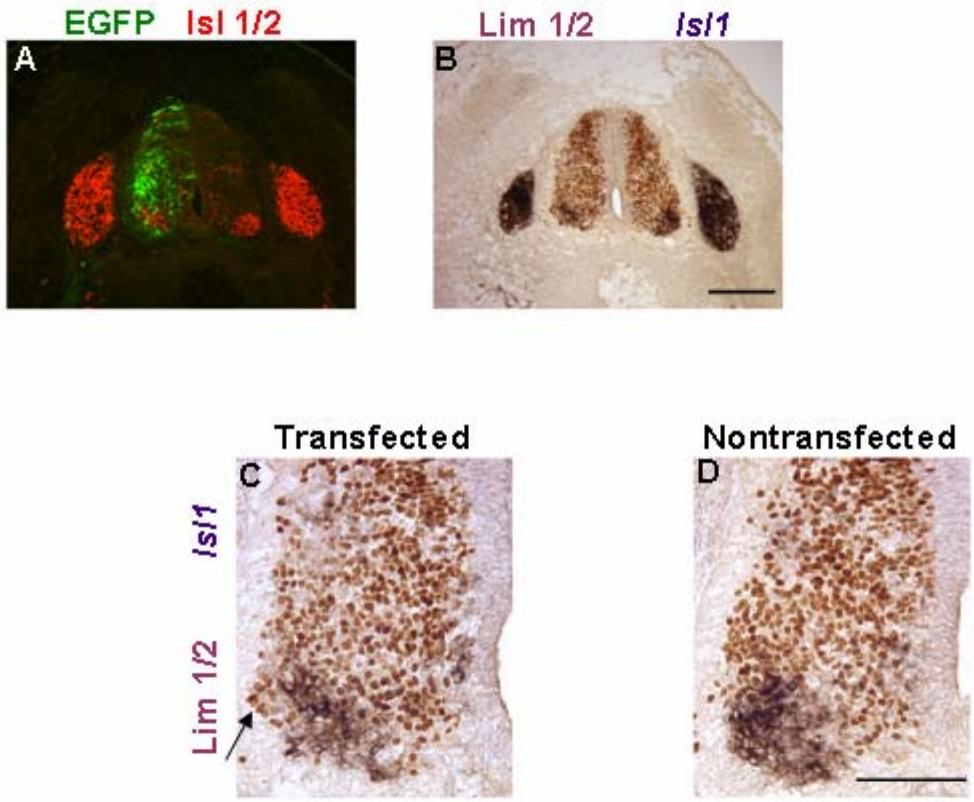

Figure 9. The ventral extension of Lim1/2+ cells does not express *Isl1* in Hoxd10/EGFP electroporated embryos. Transverse sections through a posterior T segment of a stage 29 embryo after electroporation with Hoxd10/EGFP. (A) Labeling with EGFP and Isl1/2 antibodies shows the dorsolateral position of transfected cells within motor regions (B) Adjacent section stained with the Lim1/2 antibody (brown stain) and the *Isl1* probe (purple stain). (C-D) Motor column regions on the transfected and nontransfected sides of the section shown in (B). On the transfected side, ventrally extending Lim1/2+ cells lack *Isl1* expression (C arrow). (D) No Lim1/2+, Isl 1- extensionof cells is evident on the nontransfected side. Scale bars= 400µm in B, 200µm in D.

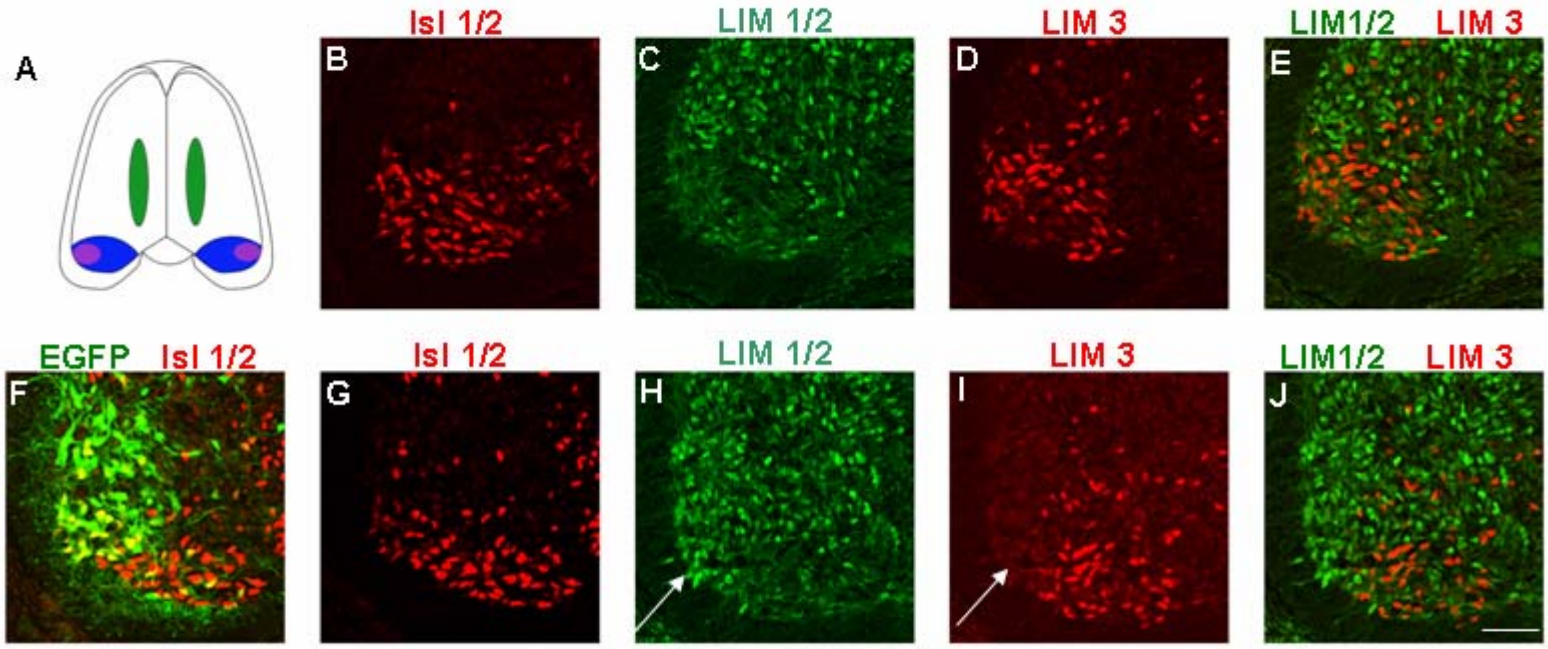

Figure 10. In Hoxd10/EGFP electroporated T segments, Lim1/2+ motoneurons are Lim 3-. (A) Schematic of the normal T spinal cord showing the positions of the MMCm (blue), MMCl (purple), and CT(green). (B-E) Sections through motor column regions in a normal stage 29 posterior T segment viewed with confocal microscopy. (B) Section stained with the Isl1/2 antibody. (C-E) Adjacent section stained with Lim1/2 +Lim3 antibodies. (C and D, single fluorochrome image; E, merged images). Lim1/2+ cells are absent from the somatic motor region. MMCm, but not MMCl motoneurons express Lim3. (F-J) Sections through motor column regions in a posterior T segment from a stage 29 embryo electroporated with Hoxd10/EGFP. (F-G) Section labeled with EGFP and Isl1/2 antibodies. (H-J) Adjacent section stained with Lim1/2 and Lim3 antibodies and photographed as in C-E. Lim1/2+ cells in somatic motor regions (H, white arrow) are Lim 3- (I, white arrow) . Scale bar = 50 μm.

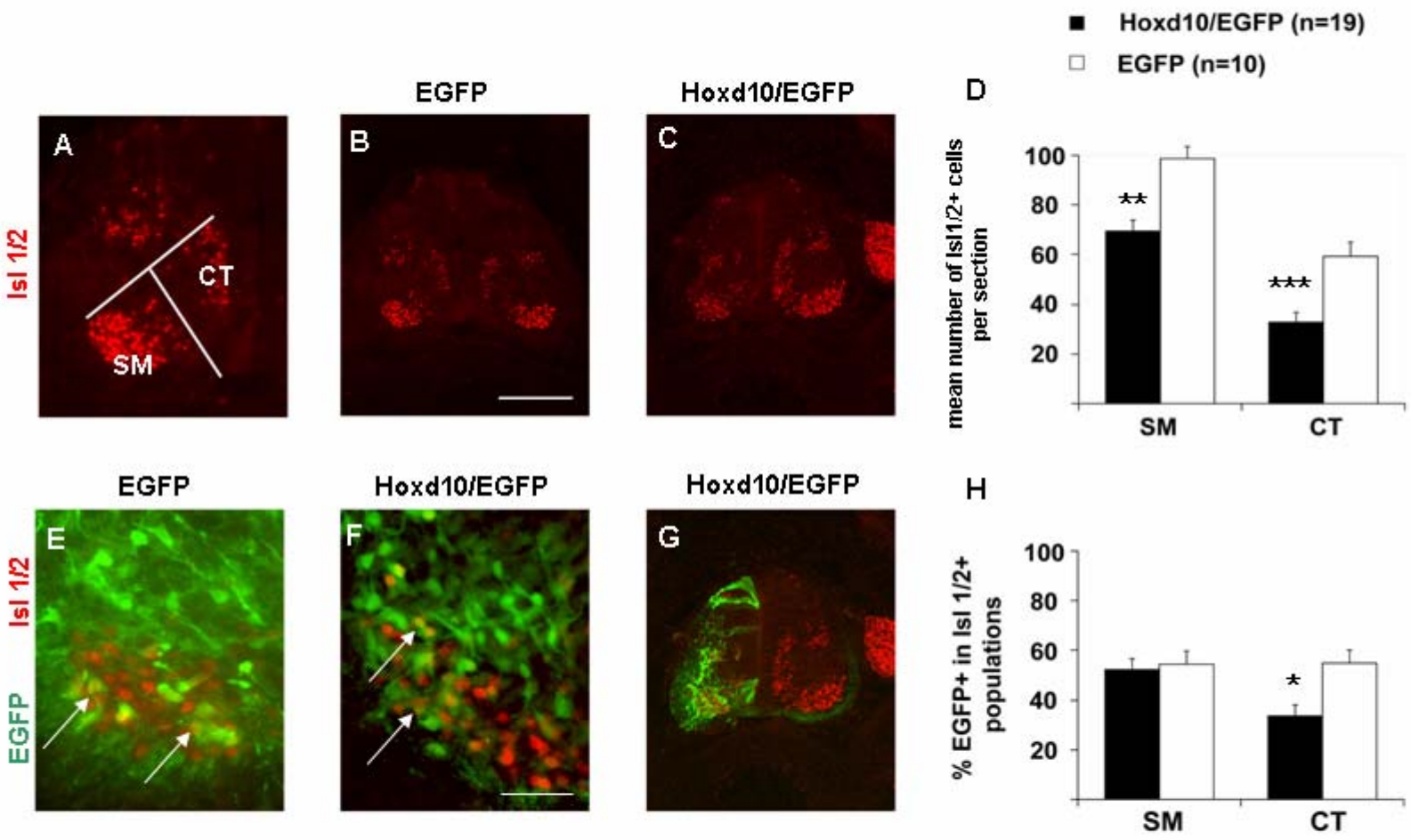

Figure 11. Hoxd10/EGFP electroporation of T segments leads to reductions in motoneuron numbers at stages 28-29.
See adjacent page for legend.

Figure 11. Hoxd10/EGFP electroporation of T segments leads to reductions in motoneuron numbers at stages 28-29. (A) Ventral quadrant of a T section stained with Isl1/2 antibodies. The white lines delineate boundaries used in counting cells in somatic motor (SM) and Column of Terni (CT) regions (see Methods). (B-C) Isl1/2 antibody-stained T6 sections from stage 29 embryos electroporated with EGFP (B) and HOXD10/EGFP (C). The number of motoneurons (Isl 1/2+ cells) in SM and CT regions are markedly reduced on the transfected side of the Hoxd10/EGFP embryo. (D) Histogram of mean motoneuron numbers per T6 section on the transfected sides of Hoxd10/EGFP and EGFP electroporated embryos. In SM and CT regions, the numbers in the Hoxd10/EGFP group are significantly lower than numbers in the EGFP group with a most pronounced reduction in the CT region. (E-F) Somatic motor regions from the transfected sides of EGFP (E) and Hoxd10/EGFP (F) electroporated embryos. These T6 sections were double labeled with Isl1/2 and EGFP antibodies. In EGFP electroporated embryos, transfected motoneurons (EGFP+/Isl 1/2+ cells) are found through the somatic motor region (arrow, E). In Hoxd10/EGFP electroporated embryos, the majority of the transfected motoneurons are found in dorsolateral portions of the somatic motor region (F, arrow). (H) Histogram of mean % EGFP+ cells among Isl1/2+cells per T6 section. The % transfection is significantly lower in the CT region of Hoxd10 transfected embryos than in other regions. Bars on histograms show standard error (n=19 Hoxd10/EGFP electroporated embryos, n=10 EGFP electroporated embryos). (Student T-Test, *=$p<0.1$, **=$p<0.001$). Scale bars= 200μm in B (applies also to C), 150μm in F (applies also to E).

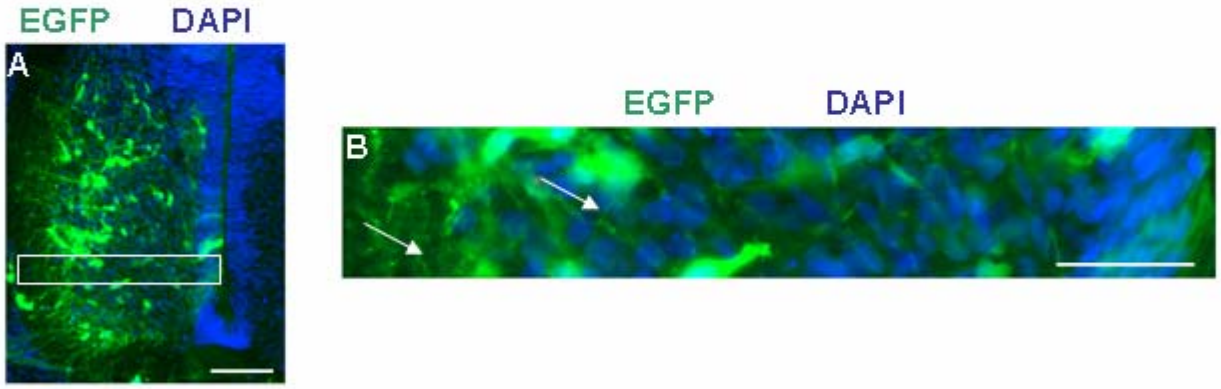

Figure 12. Sampling of cell numbers in ventral spinal regions after electroporation. (A) Ventral quadrant of T6 from a stage 29 electroporated embryo showing EGFP antibody and DAPI staining. (B) Boxed area shown in A. To obtain an estimate of the effect of electroporation on overall cell numbers, all DAPI+ cells were counted in a ventral strip on transfected sides of EGFP and Hoxd10/EGFP electroporated embryos. The strip was 50μm high and extended from the dorsolateral edge of the somatic motor region to the ventricular zone. The dorsolateral edge was defined by Isl1/2 antibody staining (not shown here). Scale bars= 200μm in B (applies to A), 100μm in C, and 50μm in D.

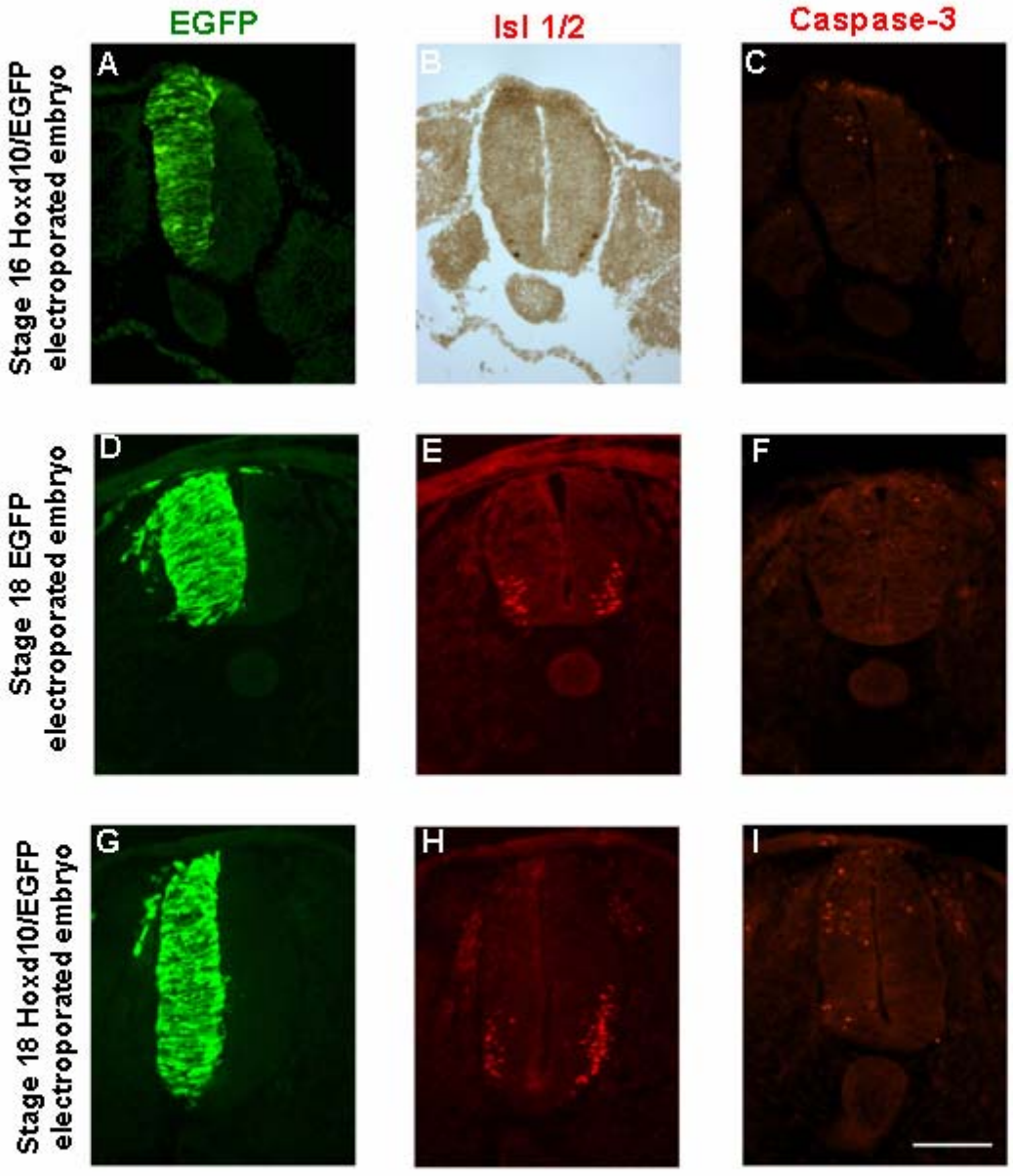

Figure 13. Hoxd10/EGFP electroporation alters motoneuron numbers and cell survival at early stages of motor column formation. See adjacent page for legend.

Figure 13. Hoxd10/EGFP electroporation alters motoneuron numbers and cell survival at early stages of motor column formation. (A-C) Transverse sections through a posterior T segment of a chick embryo electroporated with Hoxd10/EGFP at stage 13. The embryo was sacrificed at stage 16 before motoneurons are normally born. These adjacent or near-adjacent sections were stained with either (A) EGFP, (B) Isl1/2, or (C) activated caspase-3 antibodies. 2-4 Isl1/2+ cells are visible on each side of the cord, suggesting that Hoxd10 electroporation did not lead to an obvious premature onset of motor column formation. No clear difference in caspase staining is evident in transfected and non-transfected motor regions. (D-F) Transverse sections through a posterior T segment of a stage 18 embryo after electroporation with EGFP at stage 13. Adjacent sections stained as in A-C. Isl 1/2 + staining shows that the size of the somatic motor region is similar on the transfected and nontransfected side. Caspase staining shows no indication of motor cell death. (G-I) Transverse sections through a posterior T segment of a stage 18 embryo after electroporation with Hoxd10/EGFP at stage 13. Adjacent sections stained as described above. The numbers of Isl /2+ cells are reduced on the transfected side. A number of caspase+ cells are present in ventral spinal regions on the transfected side as well. These observations suggest that Hoxd10/EGFP electroporation leads to the death of some ventral spinal cells as early as stage 18. Scale bar= 200μm.

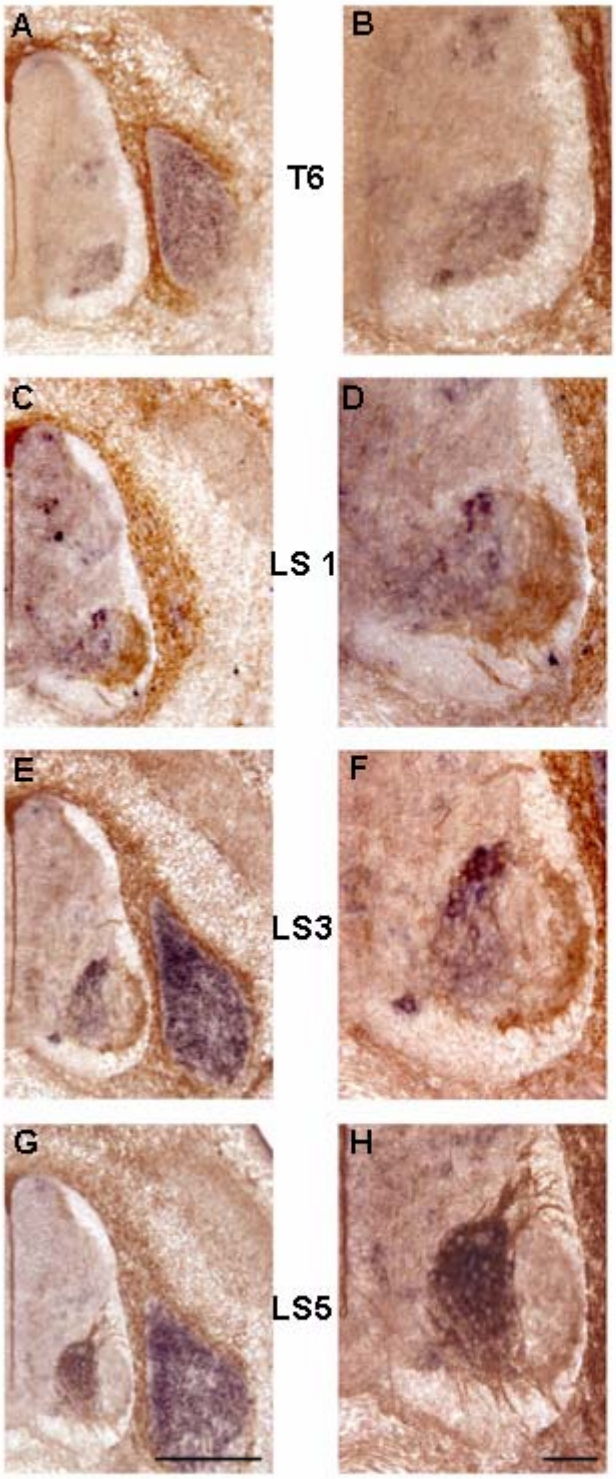

Figure 14. Normal expression patterns of RALDH2 in the T and LS spinal cord at stage 29. Sections double-labeled with an RALDH2 antibody (brown) and *Isl1* probe(purple). Photos at left show one half of the cord, while photos at right show the motor region of the same section.

(A,B) T6: No motoneurons (*Isl1*+ cells) express RALDH2. It is expressed in the roofplate and mesenchyme surrounding the cord at this and all other levels shown.

(C,D) LS1: RALDH2 is expressed by most LMCl cells but not by LMCm+MMC (*Isl1+) cells.*

(E,F) LS3: RALDH2 is expressed at the lateral edge of the LMCl and by a few cells in ventromedial motor regions.

(G,H) LS5: RALDH2 is expressed by LMCm+MMC (*Isl1*+) cells only.

Scale bars=200 μm in G, 50 μm in H.

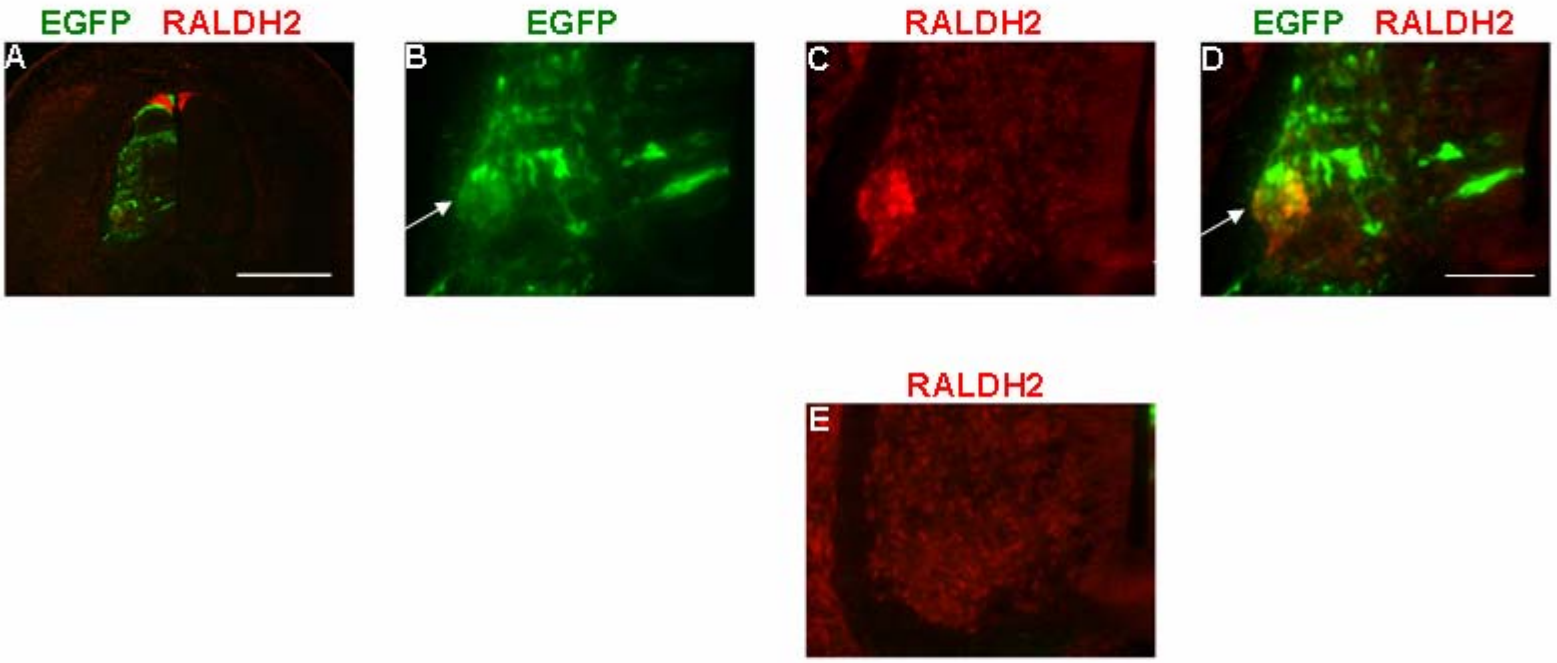

Figure 15. RALDH2 is expressed in somatic motor regions after Hoxd10/EGFP electroporation. (A-E) Photos from a single stage 29 posterior T section after electroporation with Hoxd10/EGFP. The section was double-labeled with EGFP and RALDH2 antibodies. (A) Photo of the whole cord shows EGFP staining that is predominantly lateral. (B-D) Photos of the transfected motor region. D is a fused image of B and C. EGFP+ cells in dorsolateral somatic motor regions express RALDH2 (white arrow in D). (E) Photo of the non-transfected motor region shows no RALDH2 expression. Scale bars= 200μm in A, 50 μm= D.

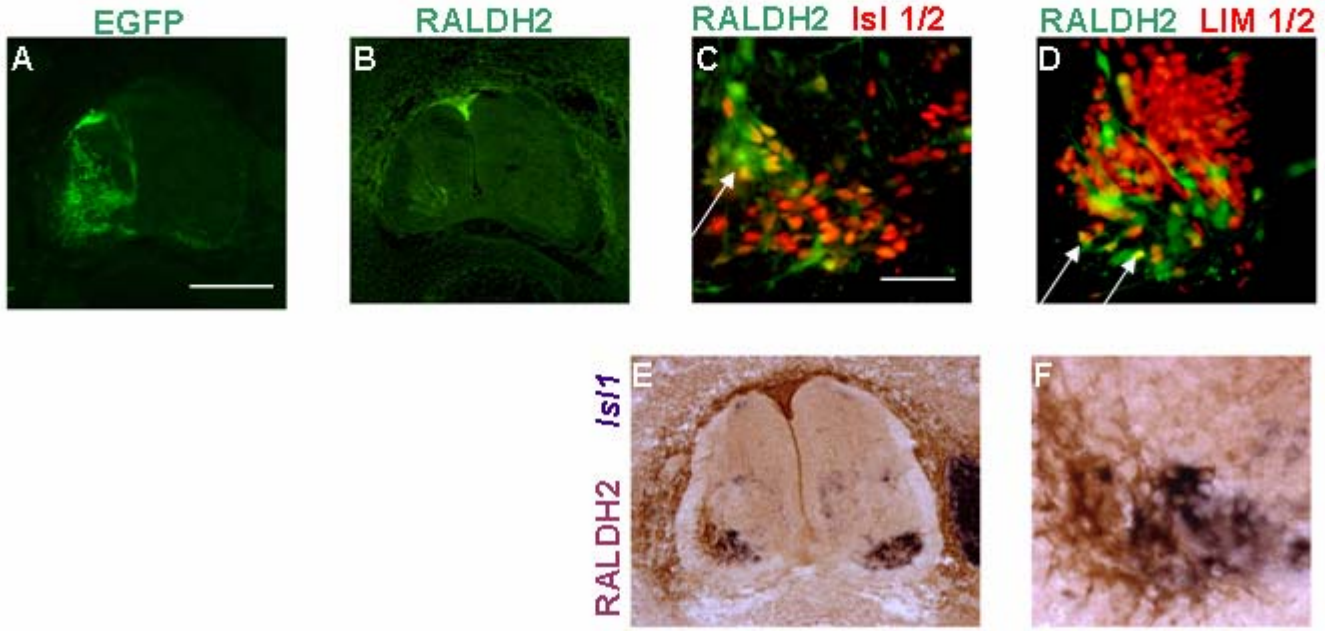

Figure 16. RALDH2 is expressed predominantly by cells with an LMCl profile in Hoxd10/EGFP electroporated T segments. (A-B). Full sections through the cord of a stage 29 experimental embryo after electroporation. Double-labeling with EGFP and RALDH2 antibodies indicates induction of RALDH2 expression in transfected motor regions (see also Figure 15.) . RALDH2 is expressed in the somatic motor region on the HOXD10/EGFP transfected side but not in the corresponding region on the non-transfected side. (C-D) Somatic motor regions from adjacent sections double labeled with RALDH2 antibodies and either Isl1/2 or Lim1/2 antibodies. RALDH2+ cells are laterally positioned Isl1/2+ motoneurons (arrow, C). Many RALDH2+ cells also appear to be Lim1/2+, suggesting that they are like LMCl cells normally found in anterior LS segments (see Figure 14.). (E-F) Sections showing the full cord (E) and the transfected motor region (F) from a second stage 29 embryo electroporated with Hoxd10/EGFP. Double-labeling with the RALDH2 antibody and the *Isl1* probe indicates a lack of overlap between RALDH2+ cells and *Isl1*+ LMCm+MMC motoneurons. Scale bars=200μm in A (also applies to B and F), 50μm in C (also applies to D and G).

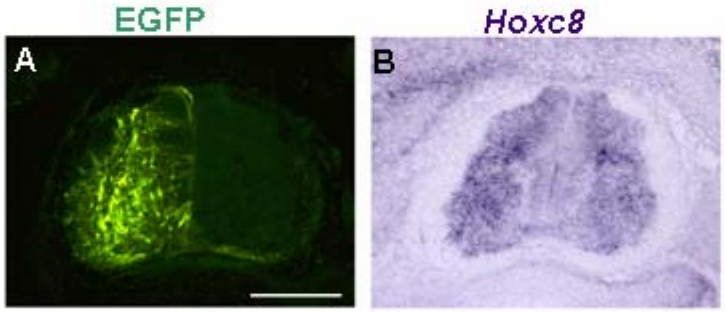

Figure 17. Hoxd10/EGFP transfected T segments show normal *Hoxc8* expression. Transverse section through a posterior T segment from a stage 29 embryo electroporated with Hoxd10/EGFP. (A) Section stained with the EGFP antibody. (B) Adjacent section stained for *Hoxc8* mRNA. Hoxc8 expression appears similar on transfected and non-transfected sides. Scale bar = 200 μm..

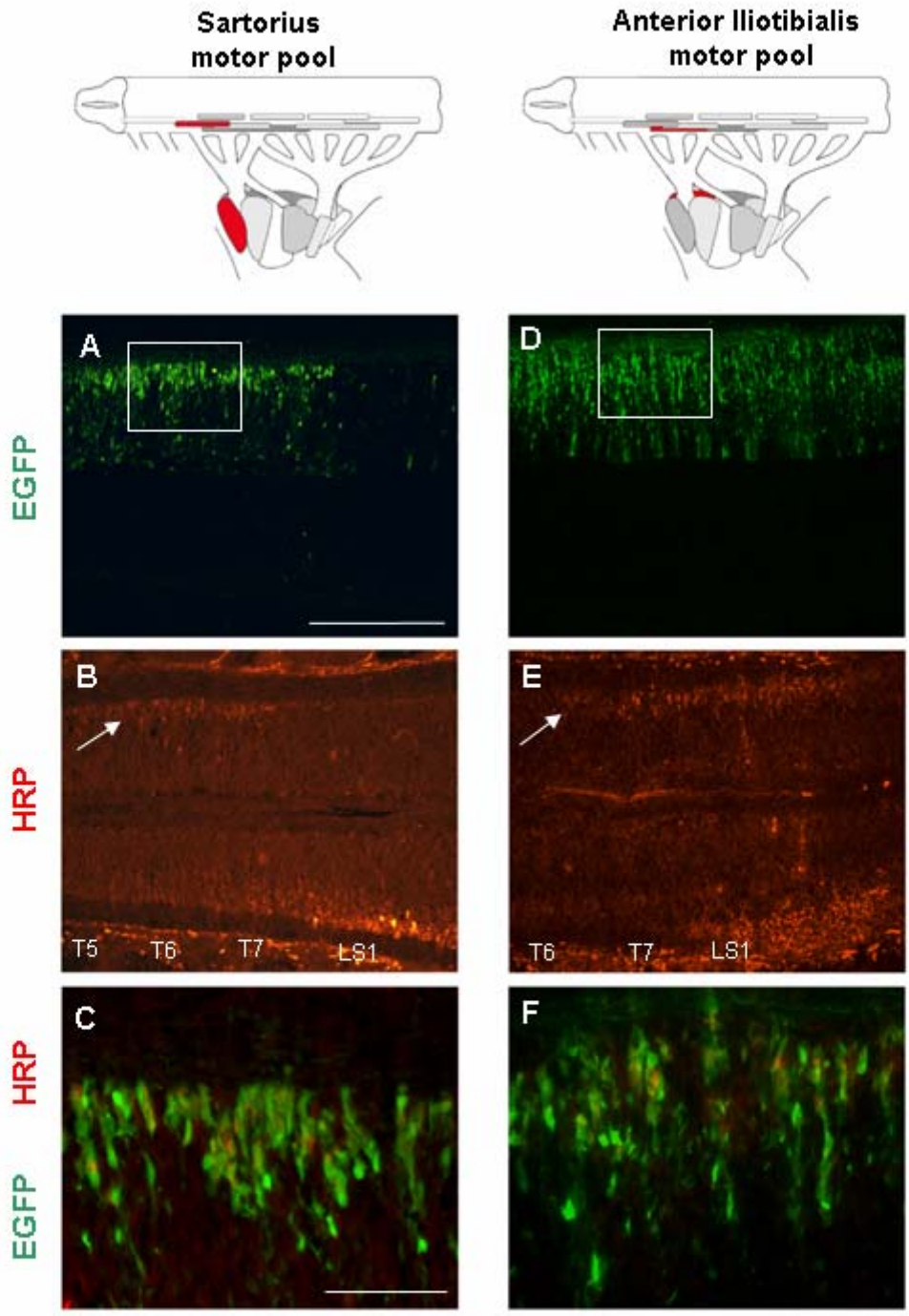

Figure 18. The AP position of motor pools to hindlimb muscles in stage 29 embryos with ectopic Hoxd10/EGFP expression. See adjacent page for legend.

Figure 18. The AP position of motor pools to hindlimb muscles in stage 29 embryos with ectopic Hoxd10/EGFP expression. (Top) Schematics of sartorius and anterior iliotibialis motor pool and target position in the anterior thigh. (A-D) Horizontal sections through the posterior T and anterior LS spinal cord. Anterior is at left. (A , D) EGFP expression. (B, E). HRP staining in the same sections. (C, F) Merged higher magnification images. (A-C) Sartorius motor pools in an embryo with high EGFP expression in posterior T segments (A). HRP + cells are present as far anteriorly as T5 on the transfected side of the cord (arrow in B). On the non-transfected side, the sartorius pool begins at T7. HRP+ cells are also visible in LS segments on the non-transfected side. They are not visible in LS segments on the transfected side in this section, but were present in adjacent sections. (C) A higher magnification merged image from a section adjacent to that shown in A-B. White box in (A) shows the approximate position of the region shown in C. (D-F). Anterior iliotibialis motor pools in an embryo with high EGFP expression in T (and LS) segments. (D) HRP + cells are present as far anteriorly as T6 on the transfected side (arrow in E). F. A high magnification merged view of the same section shown in D and E (see box in D). Scale bars=200μm in A, 50μm in C.

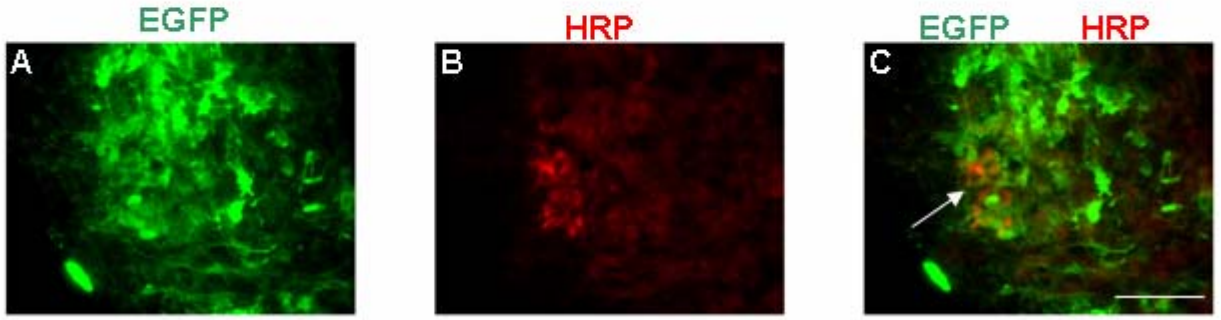

Figure 19. The position of a motor pool n the transverse plane in a stage 29 embryo electroporated with Hoxd10/EFP. Somatic motor column regions of a single T6 section stained with EGFP(A) and anti-HRP (B) antibodies (C=merged image). This section was taken from a Hoxd10/EGFP electroporated embryo after T6 after HRP injection of the sartorius muscle. (A) Most EGFP +/ HRP+ cells are found in a dorsolateral position (arrow, C) a position corresponding to that of the normal LMCl and the sartorius pool (Landmesser, 1978). Scale bars= 50μm.

.

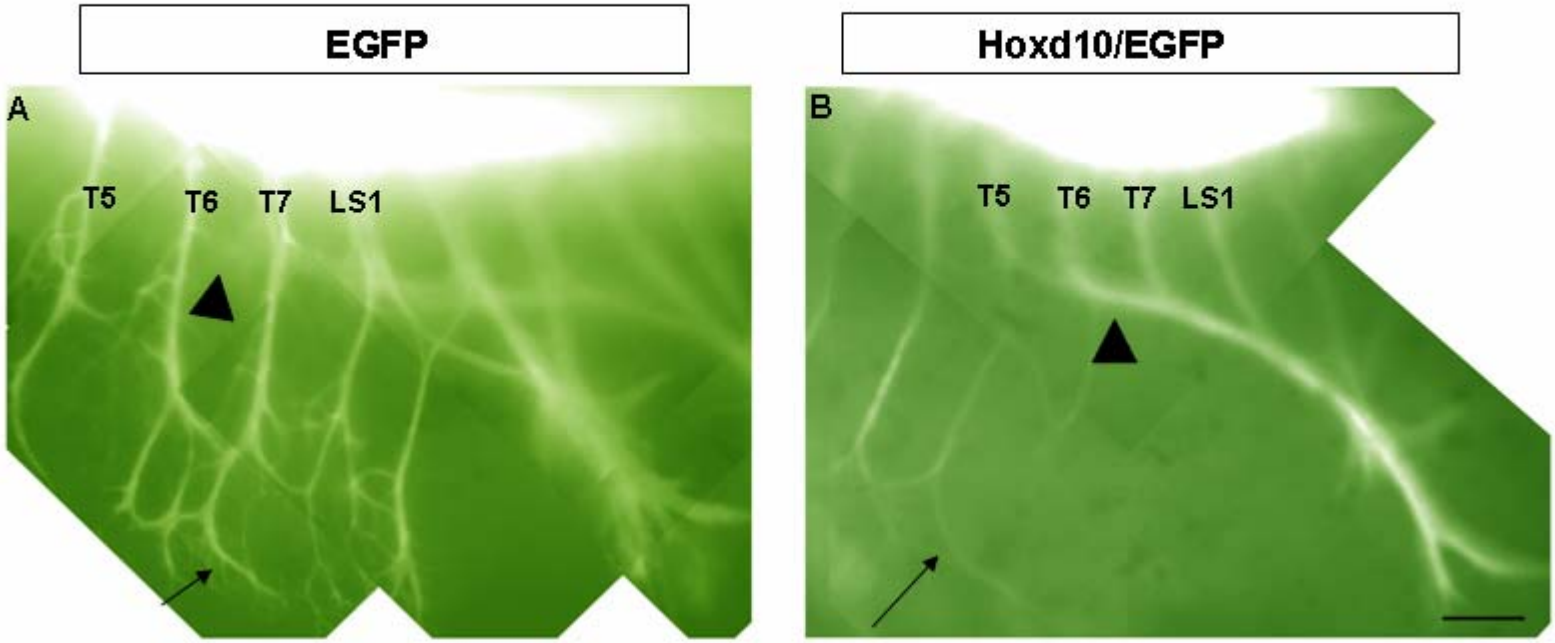

Figure 20. EGFP+ peripheral nerve patterns in electroporated embryos. (A) Nerve pattern visible in a stage 28 embryo electroporated with EGFP. T nerves have fine proximal connectives (arrowhead) and an extensive network of nerves in the body wall (small arrow) . (B) Nerve pattern visible in a stage 28 embryo electroporated with Hoxd10/EGFP. Posterior T nerve connectives are larger than those in EGFP electroporated embryos and distal nerves in the body wall appear depleted. Scale bar= 500 μm.

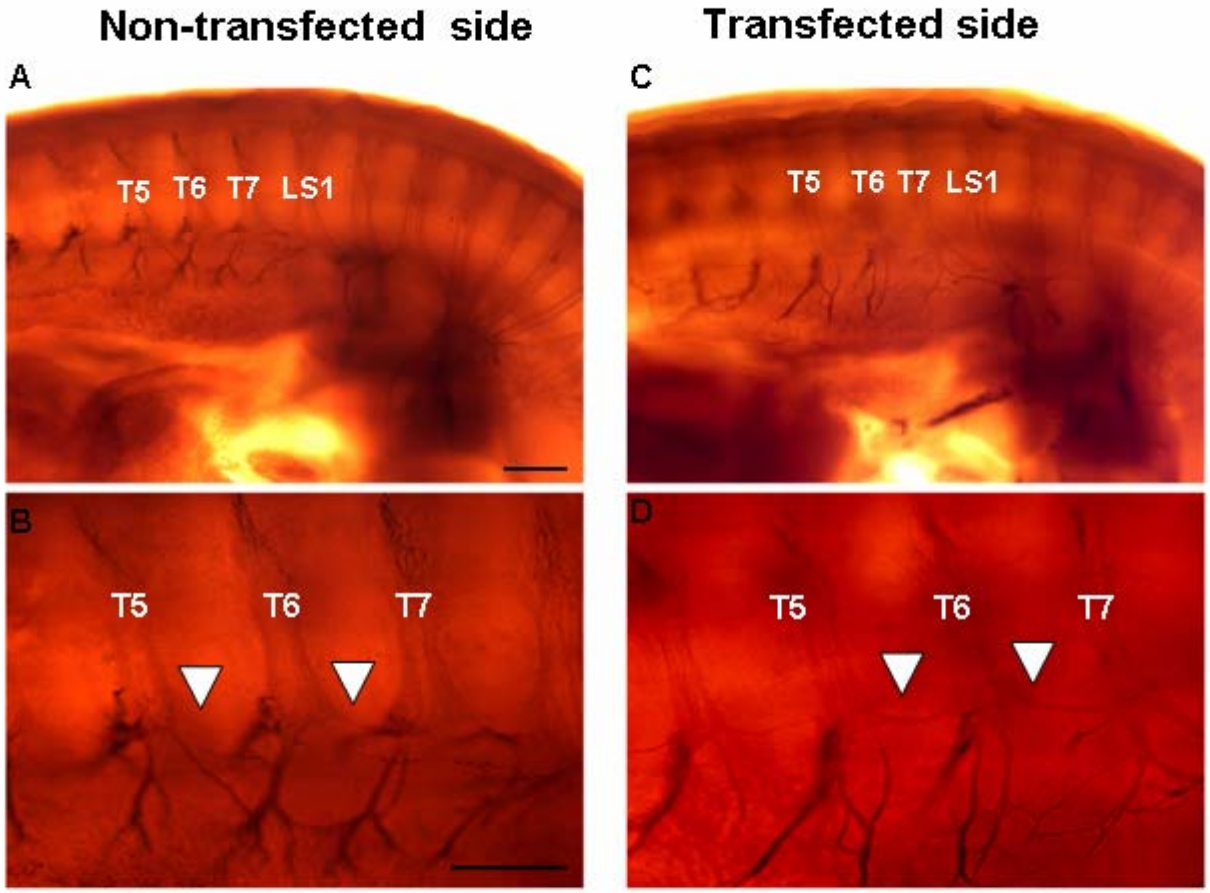

Figure 21. Gross nerve patterns in electroporated embryos identified via neurofilament staining. (A, B) Low and high magnification views showing fine proximal connectives between spinal nerves on the non-transfected side of an experimental embryo. (C,D) Similar views of the nerves on the Hoxd10/EGFP transfected side of the same embryo. Proximal connectives between T5-T7 appear slightly larger(arrowheads) than on the non transfected side. Scale bars= 500 μm.

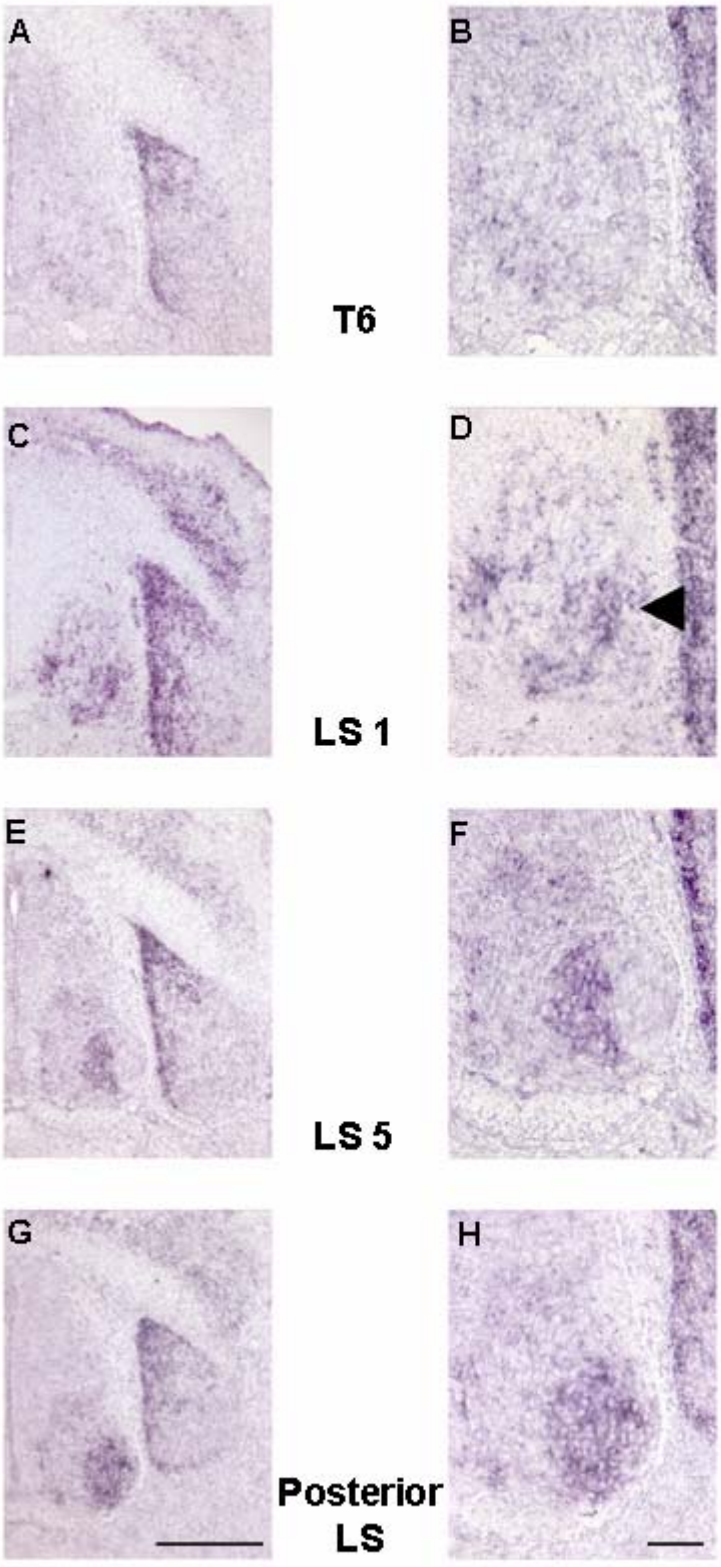

Figure 22 . Normal expression patterns of *c-met* in the T and LS spinal cord at stage 29. *In situ* hybridization with a *c-met* probe was carried out on sections through posterior T and LS regions. Photos at left show one half of the cord and dorsal root ganglia, Photos at right show motor regions of the same section.

(A,B) T6: Very low levels of c-met expression are present in the T cord.

(C-D) LS1: *C-met* + cells are present ventromedially and along the lateral edge of the LMCl region (arrowhead) in the position of LMC1.

(E-F) LS5: *C-met* + cells are present in the LMCm.

(G-H) posterior LS: *C-met* expression is more widespread in motor regions than it is in middle LS (LS5) segments.

Scale bars= 200 μm in G, 50 μm in H.

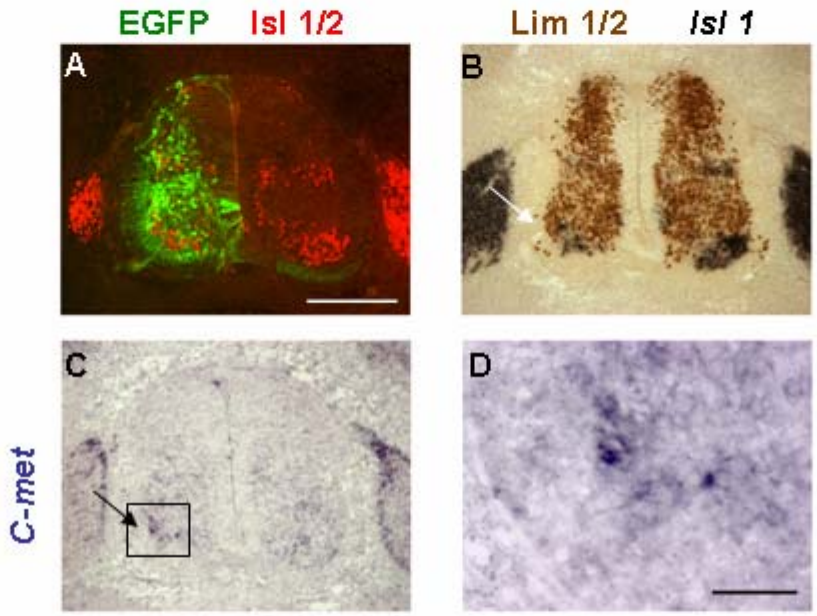

Figure 23. Ectopic expression of Hoxd10/EGFP in T segments leads to the induction of the c-met receptor. Adjacent sections through a posterior T segment from a stage 29 embryo after electroporation with Hoxd10/EGFP. (A) Section double-labeled with an EGFP and Isl 1/2 antibody, show that many EGFP+ cells occupy a dorsolateral position in the somatic motor region. (B). Section double-labeled with an *Isl1* probe (black stain) and a Lim1/2 antibody (brown stain). On the transfected side, there is an extension of Lim1/2+ cells (white arrow). (C, D) Low and high magnification views of *c-met* expression. Boxed area in C corresponds to the region shown in D. Small clusters of *c-met*+ cells (arrow) occupy the same position in the motor regions as the Lim1/2 cells marked in B. Scale bars= 200μm in A (applies also to B and C), 50μm in D.

Figure 24. Ectopic expression of Hoxd10/EGFP in T segments leads to the induction of the ETS protein, pea3. Adjacent sections through a posterior T segment from a stage 29 embryo after electroporation with Hoxd10/EGFP. (A) Section double-labeled with an EGFP and Isl 1/2 antibody, show the lateral position of EGFP+ cells (B, C) Low and high magnification views of a section stained with a pea3 antibody. Boxed area in C corresponds to the region shown in D. Pea3+ cells are located laterally in the somatic motor region,. Scale bars= 200μm in A (applies also to B), 50μm in C.

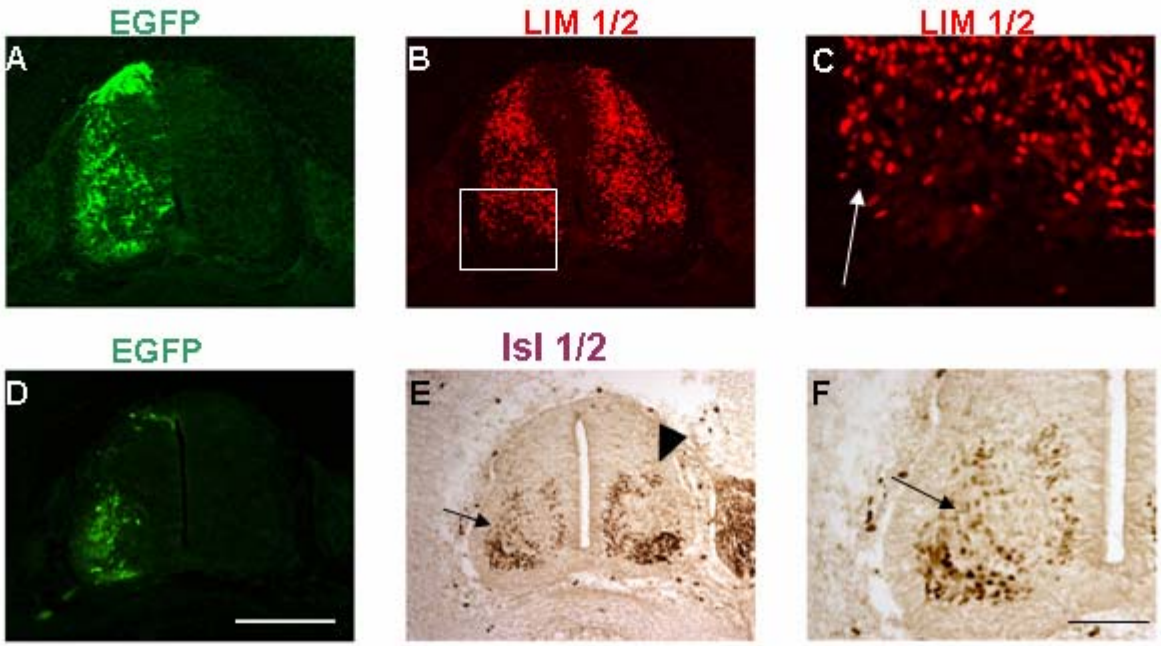

Figure 25. Electroporation of Hoxd10/EGFP at early stages of motoneuron differentiation (stages 17-18) induces an LMC1 LIM profile and ectopically-positioned Isl 1/2 + cells. (A-C) Sections through a posterior T segment from a stage 29 embryo electroporated with Hoxd10/EGFP at stage 17. (A) Position of transfected (EGFP+) cells. (B-C). Low and high magnification views showing the distribution of Lim1/2+ cells. On the transfected side, there is a ventral extension of Lim1/2+ cells (arrow). (D) Sections through a posterior T segment from a second stage 29 embryo electroporated with Hoxd10/EGFP at stage 17. (D) Position of transfected (EGFP+) cells. (E-F) Low and high magnification views of a near adjacent Isl1/2-stained section. On the transfected side, lightly-stained Isl1/2 + cells (black arrows) extend dorsally, well beyond the normal somatic motor region. These Isl1/2+ cells could correspond to interneurons that are normally found in a small cluster lateral to the top of the CT (see arrowhead in E). Scale bars= 200μm in D (applies to A,B, and E), 50μm in C, 100 μm in F.

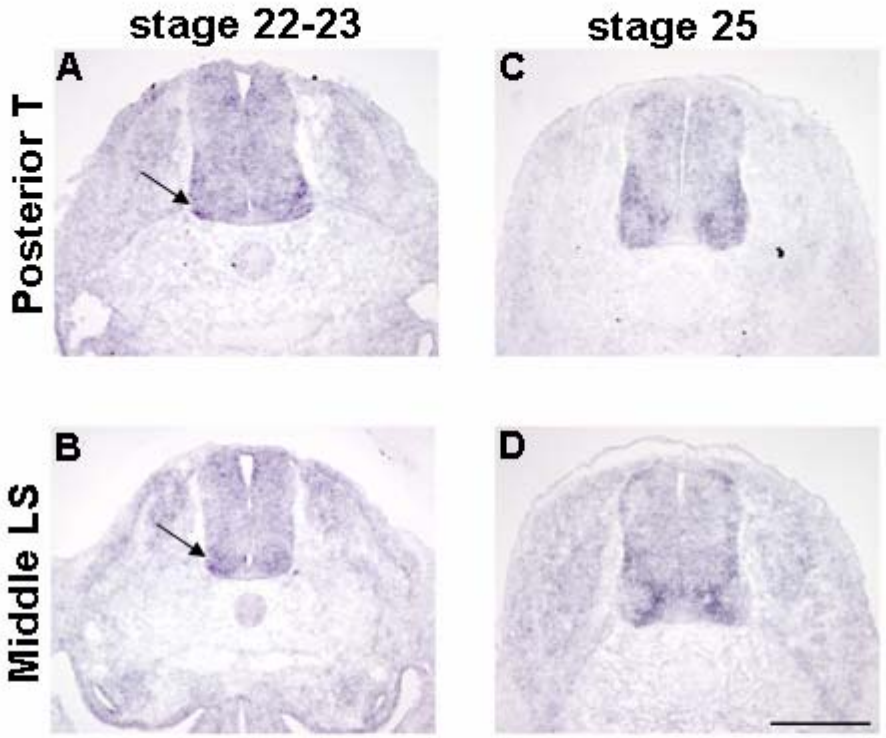

Figure 26. Early expression of *Hoxd9* in the developing T and LS spinal cord. *In situ* hybridization with a *Hoxd9* probe was performed on sections through T and LS regions. (A-B) Stages 22-23: *Hoxd9* is expressed by postmitotic cells in the ventral spinal cord in both T and LS segments. (C-D) Stage 25: In posterior T segments, *Hoxd9* is expressed by both medial and lateral cells in future somatic motor regions (arrows) . Cells in the central core of the motor region express low levels of *Hoxd9*. In middle LS segments, *Hoxd9* is mainly expressed in medial motor regions.
Scale bar= 200μm.

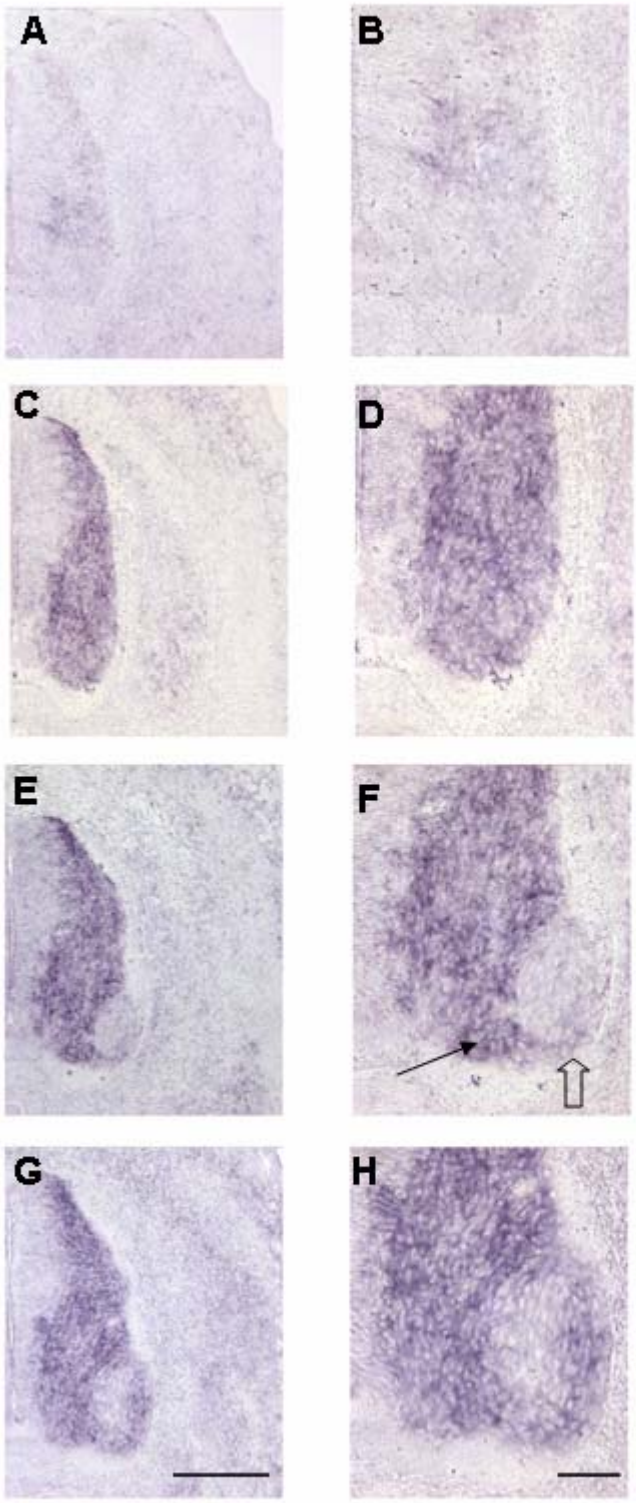

Figure 27. Normal expression patterns of *Hoxd9* in the T and LS spinal cord at stage 29. *In situ* hybridization with a *Hoxd9* probe was carried out on sections through posterior T and LS regions. Photos at left show one half of the cord. Photos at right show motor regions of the same section.

(A,B) Anterior T (T2-3): Few if any cells in ventral motor regions express *Hoxd9*.

(C-D) Posterior T (T6) : Almost all post-mitotic cells express *Hoxd9*, including cells in MMC and CT regions.

(E-F) Anterior LS (LS1-2): *Hoxd9* is expressed in the MMC(arrow) and a small crescent-shaped cluster of cells that extends ventrolaterally along the edge of the motor column (open arrow).

(G-H) Middle LS (LS4-5): *Hoxd9* is expressed in the MMC and LMC1 region

Scale bars= 200 μm in G, 50 μm in H.

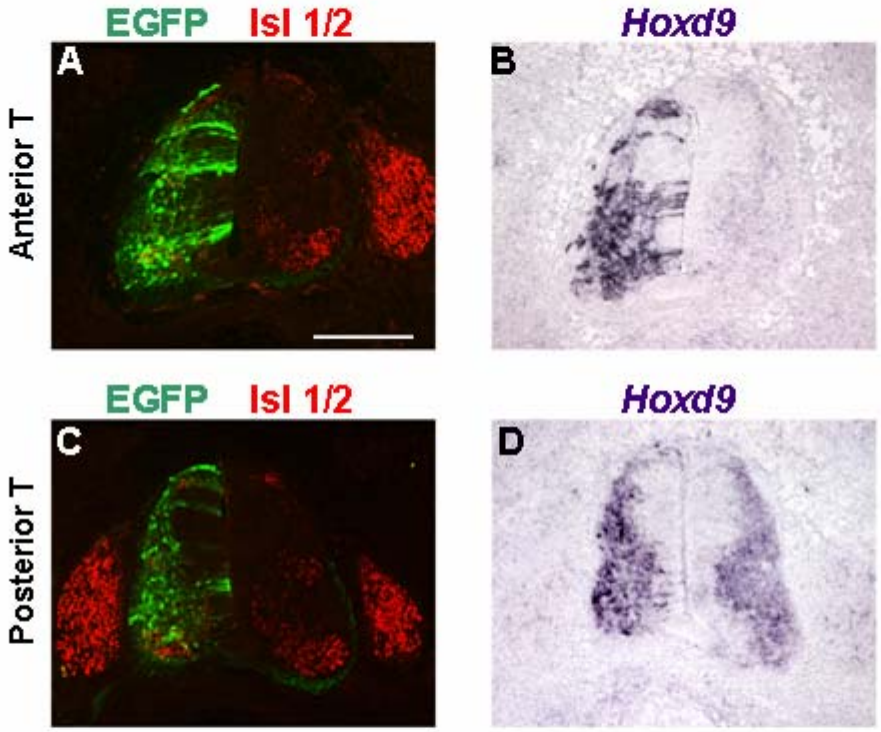

Figure 28. Hoxd9/EGFP electroporation of anterior and posterior T spinal segments. (A and C) T sections stained with EGFP + Isl1/2 antibodies show transfected motor regions at stage 29. (B and D) Adjacent T sections probed for *Hoxd9* mRNA. (B) At anterior T levels, ectopic expression of *Hoxd9* is initiated. (D) At posterior T levels, Hoxd9 is overexpressed. Scale bar= 200μm in A.

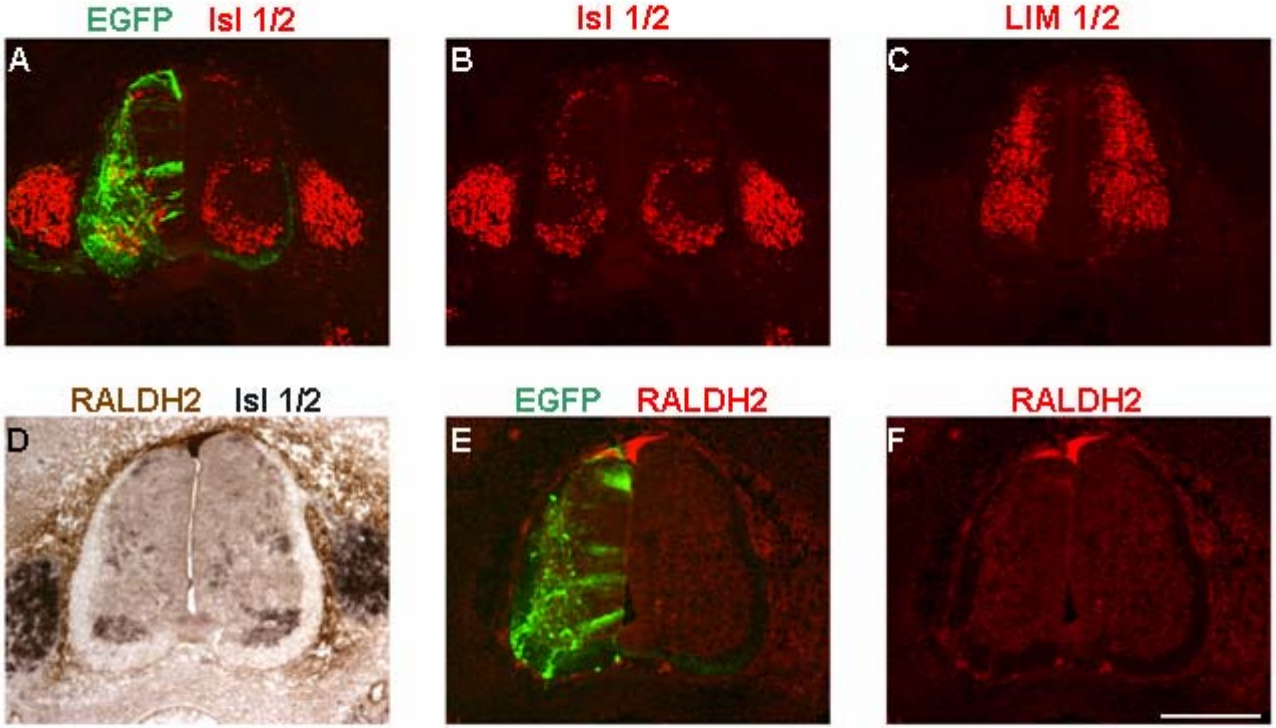

Figure 29. Misexpression of Hoxd9/EGFP does not induce motoneurons with an LS LMC molecular profile. (A-C) Posterior T sections from a single stage 29 Hoxd9 electroporated embryo. (A) EGFP+ cells are distributed throughout the somatic motor region. Isl1/2 staining (A and B) shows that the motor columns are slightly reduced in size on the transfected side (see also D). (C) Lim 1/2 staining shows no evidence of Lim1/2 expression in somatic motor regions. (D) Section stained with the RALDH2 antibody and probed for *Isl1* mRNA shows no indication that *Isl1*+ cells express RALDH2. (E-F) Adjacent section stained with EGFP and RALDH2 antibodies shows that Hoxd9/EGFP transfection does not lead to an induction of RALDH2 expression. Scale bar=200μm.

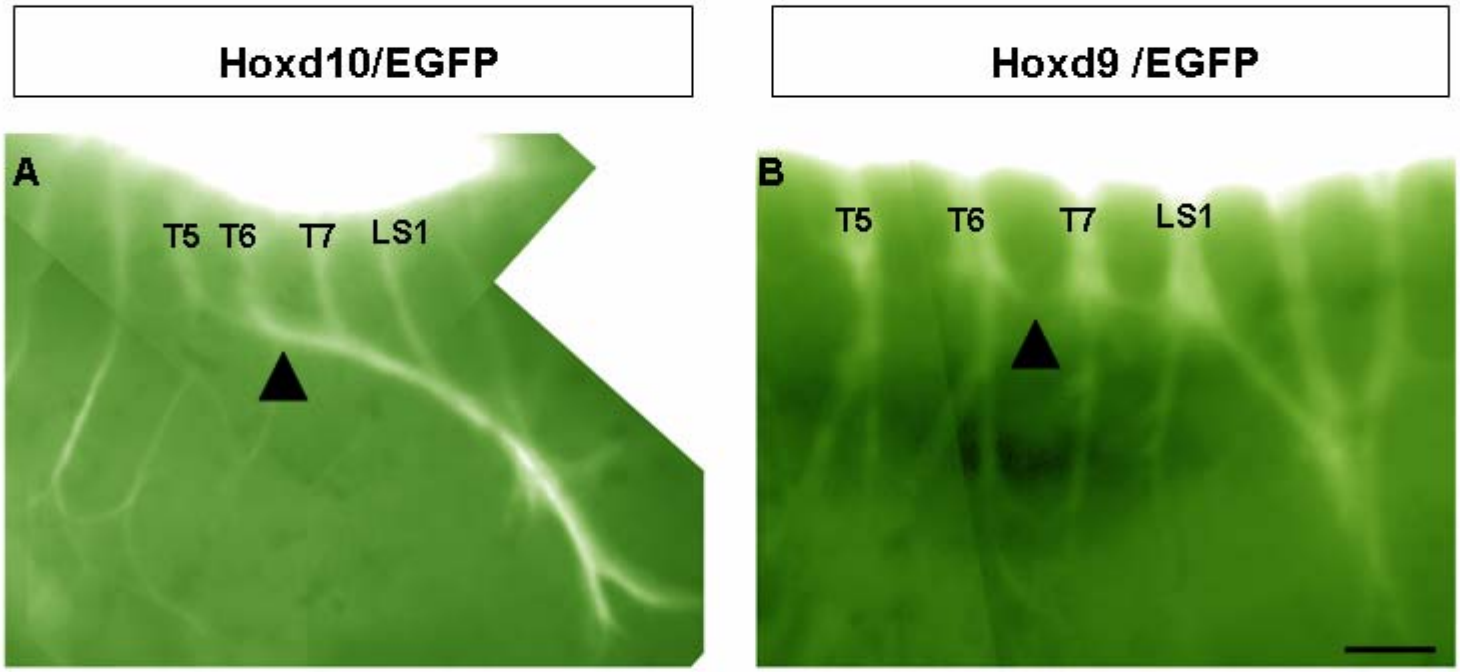

Figure 30. EGFP+ nerve patterns in Hoxd9/EGFP and Hoxd10/EGFP electroporated embryos. A stage 29 Hoxd9/EGFP embryo (B) does not show the large proximal connectives (arrowheads) found in a Hoxd10/EGFP embryo (A). Scale bar= 500 μm

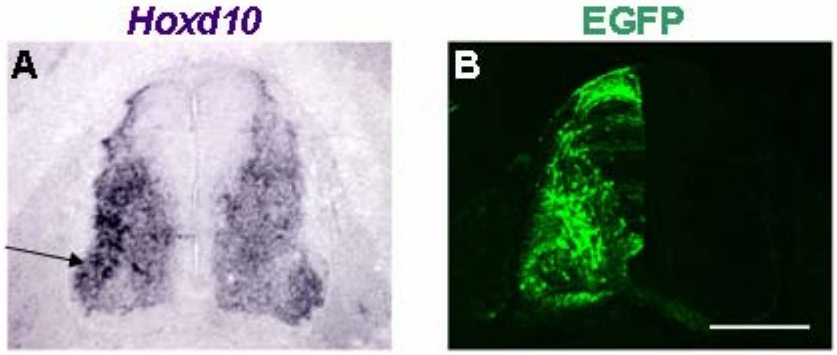

Figure 31. Overexpression of Hoxd10/EGFP in the LS spinal cord. Adjacent sections through an anterior LS segment in a stage 29 embryo after electroporation with Hoxd10/EGFP. (A) Electroporation of Hoxd10/EGFP construct results in higher unilateral expression of *Hoxd10* on the transfected side of the LS spinal cord than on the non-transfected side. (B) Most transfected (EGFP+) cells occupy a lateral position like the cells that show high levels of *Hoxd10* expression (arrow in A). Scale bar= 200μm.

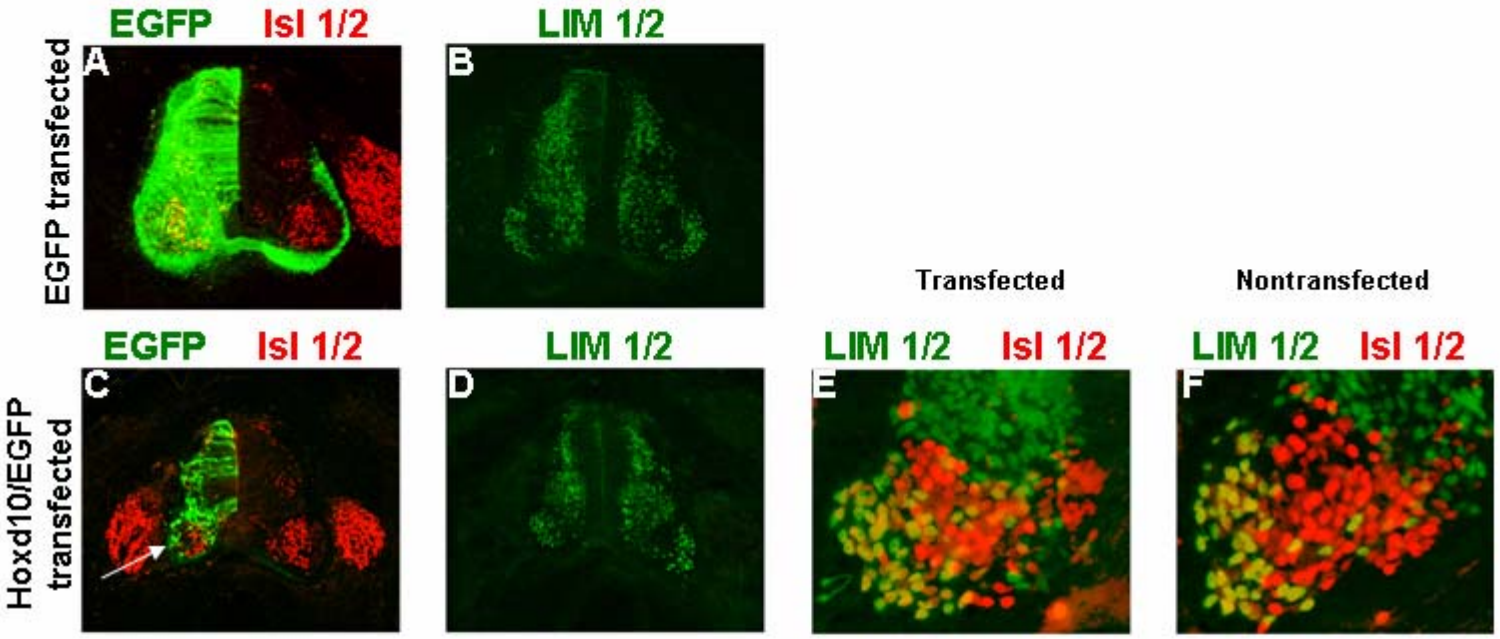

Figure 32. Overexpression of Hoxd10EGFP in LS segments leads to a proportionate increase in LMC1 motoneurons. (A-B) Anterior LS sections from a stage 29 embryo after electroporation with EGFP alone. EGFP+ cells (A) are broadly distributed in the somatic motor regions and Lim1/2 staining patterns (B) appear similar on transfected and non-transfected sides. ((C-D) Equivalently-stained LS sections from a stage 29 embryo after electroporation with Hoxd10/EGFP. EGFP+ cells are largely lateral and the motor columns are reduced in size on the transfected side. (E-F) High magnification views of transfected and non-transfected motor columns from a Hoxd10/EGFP electroporated LS2. (The non-transfected motor column has been reversed for ease of comparison.) Section stained with Lim1/2 and Isl1/2 antibodies. The total numbers of Isl1/2+ cells on the transfected side appear less than on the nontransfected side but, the proportion of Lim1/2+ motoneurons (LMC1 cells, yellow) appears higher.

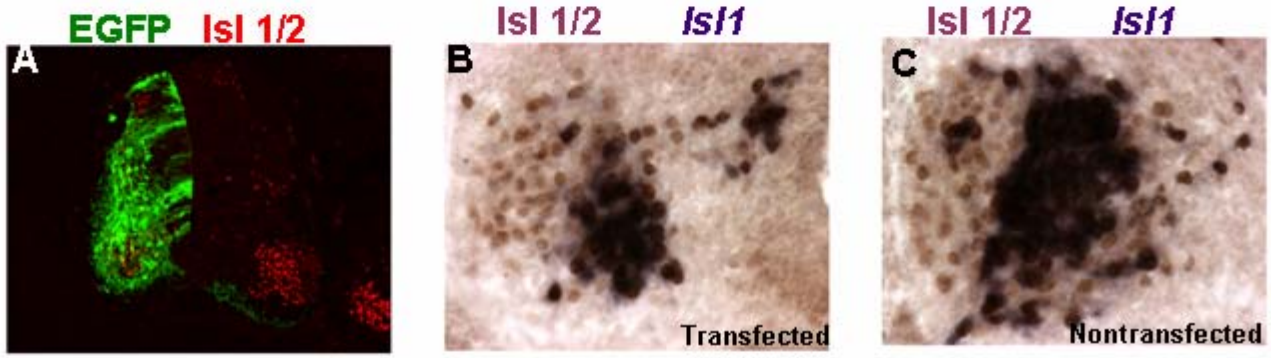

Figure 33. Overexpression of Hoxd10EGFP in LS segments leads to a decrease in the size of the LMCm+MMC. (A-C) Anterior LS sections from a stage 29 embryo after electroporation with Hoxd10/EGFP. (A) Low magnification view shows laterally-positioned EGFP+ cells in the motor region. (B and C) Higher magnification views of motor regions on transfected and non-transfected sides of an adjacent section. Section stained with the Isl1/2 antibody and an *Isl1* probe. The cluster of *Isl1* + cells that makes up the LMCm+MMC is markedly reduced on the transfected side.

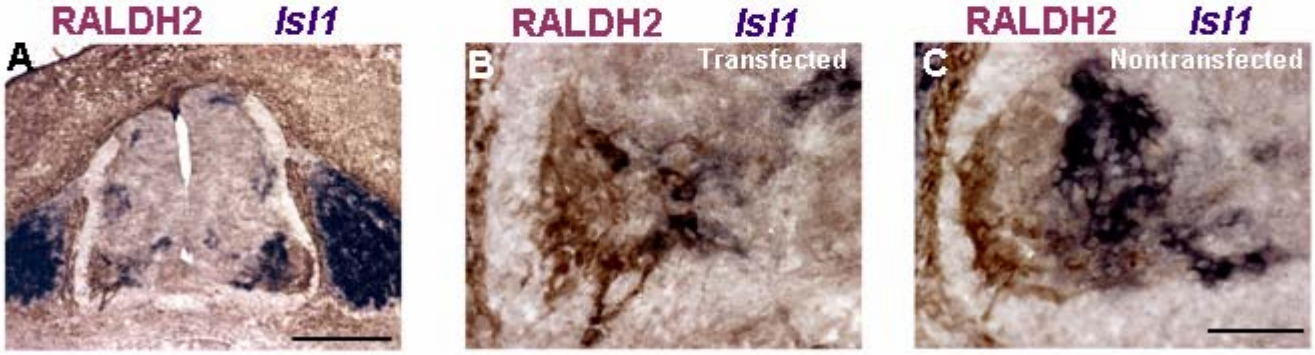

Figure 34. Overexpression of Hoxd10/EGFP in LS segments can lead to an increase in RALDH2+ cells. (A-C) Low and high magnification views of an LS2 section from an embryo electroporated with Hoxd10/EGFP. Section stained with the RALDH2 antibody and probed for *Isl1*. While the transfected somatic motor column is reduced in size on the transfected side, the RALDH2+ population is large and overlaps with few if any *Isl1*+ cells. Scale bars=200 μm in A , 50μm in C.

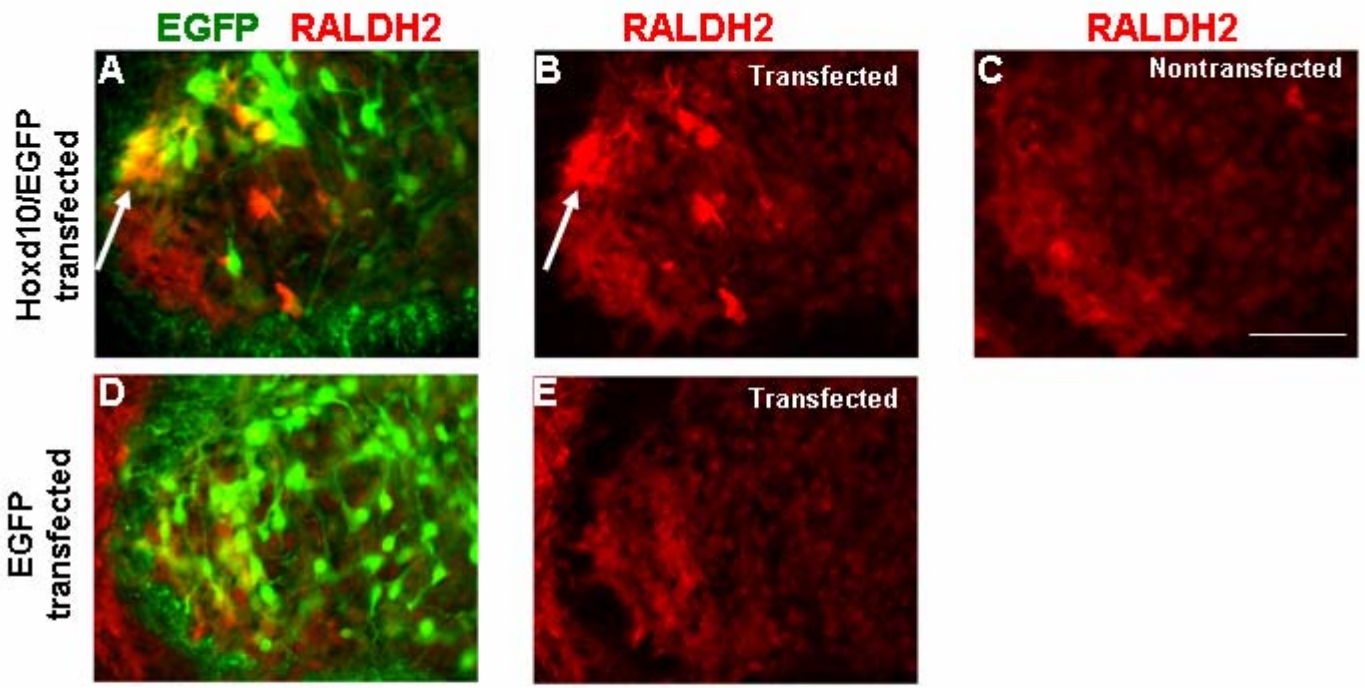

Figure 35. Hoxd10/EGFP transfected LS motoneurons show an increase in RALDH2 staining intensity. (A-C) Anterior LS motor regions from a stage 29 embryo after electroporation with Hoxd10/EGFP. Photos from a single section double-labeled with EGFP and RALDH2 antibodies. (A) Fused image of transfected motor region. (B and C) RALDH2 expression alone. The transfected motor region (B) contains more intensely-stained RALDH2+ cells than the non-transfected region (C). Most intensely stained cells are located in the LMC1 region and are EGFP+. (D-E) Equivalently-stained motor region from an EGFP electroporated embryo. No increase in RALDH2 expression is evident. Scale bar= 50μm.

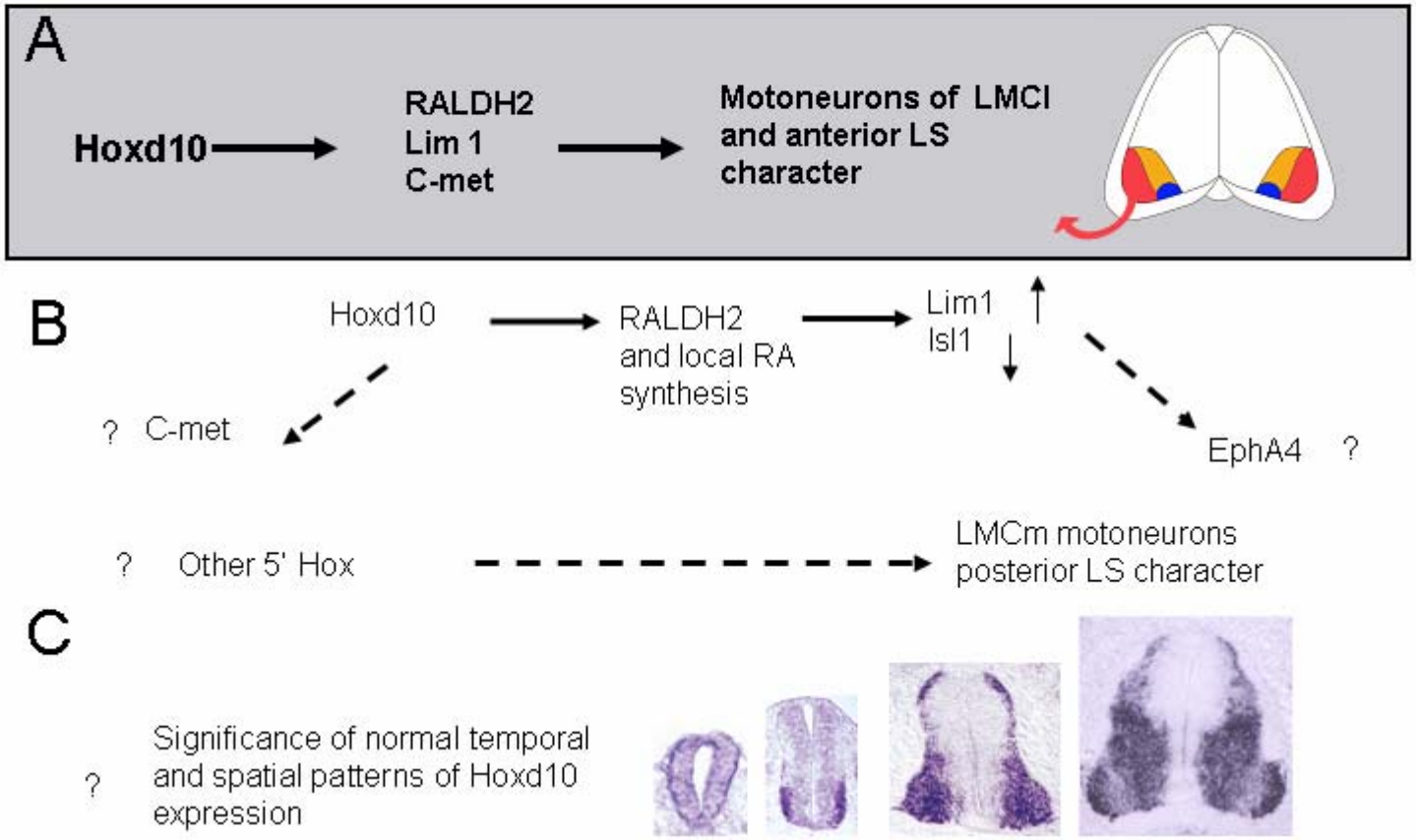

Figure 36. Conclusions and new questions. A. Our data indicate that Hoxd10 promotes the development and/or survival of motoneurons with an anterior LS LMCl molecular profile and axon projections to limb muscles. B. A proposed sequence of events in the induction of this phenotype (based on prior data from Sockanathan and Jessell, 1998; Eberhart et al., 2002; Vermot et al., 2005). Dashed arrows indicate events that might be substantiated by further experiments. C. Two major questions are raised by our studies. What is the role of other 5' Hox genes in LS motoneuron development? What is the significance of the changing pattern of Hoxd10 expression during motor column development? (Photos of *Hoxd10* expression in the LS spinal cord during motor column formation from Lance-Jones et al., 2001 and this thesis).

APPENDIX B

CELL COUNTS FROM ELECTROPORATED EMBRYOS AT STAGE 29

Appendix B1. Cell Counts on Hoxd10/EGFP Embryos at stage 29

Hoxd10/EGFP electroporated embryos							Somatic Motor column (SM)				Column of Terni (CT)				SM +CT= Total Isl 1/2 +
Embryo #	No. of somites at surgery	DNA con (µg/µl)	Sacrifice Stage (HH)	Total DAPI(+) cells in strip	Percentage of EGFP+ DAPI+		Total Isl 1/2 (+) cells	EGFP(+) Isl1/2 (+) cells	Percentage of EGFP(+) Isl1/2 (+) cells		Total Isl1/2 (+) cells	EGFP(+) Isl1/2 (+) cells	Percentage of EGFP(+) Isl1/2 (+) cells		Total Isl 1/2 (+) cells
V250	26	2.5	29	118.7	29.7		79	27.3	35.1		33.3	7	23		112.7
V149	27	2.5	29	104.3	62.3		81.3	70	87		33.3	23.3	69.7		114.6
V228	24	2.5	29	-	-		66.3	23.3	35.1		25	4.6	18.4		91.3
V157	26	1.25	29	137.7	31		102	31.3	31.6		86	20	23.1		188
V251	27	2.5	29	160.7	47		28	21	73.4		24	12.6	53.1		52
V151	24	2.5	29	-	-		55.3	25	45.2		32.6	7.6	23.3		87.9
V253	21	2.5	29	114.7	39.6		33.7	16.3	47.2		33	7.6	23.9		66.7
V155	21	2.5	29	83.3	63.6		71.3	63.7	90.4		16.3	9	574		87.6
V189	20	2.5	29	111.7	30.6		87.3	57.3	52.5		25.3	10	38.5		112.6
V143	21	1.25	29	90.7	68.5		74	41.7	56.2		25	15	59.9		99
V133	19	2.5	29	124.7	43.1		59	46.3	80.8		26	15.3	60.5		85
V256	19	2.5	29	111	27.6		57.3	37	55.8		40.3	10.3	26		97.6
V622	25	0.625	29	-	-		69.3	24.3	35.1		20.3	5.3	26.3		89.6
V623	25	0.625	29	-	-		97.3	34	34.9		48.6	14.7	30.2		15.9
V626	26	0.625	29	-	-		59	18.3	33.3		14.7	5.3	36.4		73.7
V480	28	0.625	29	-	-		51.7	23.3	45.2		14.7	1.7	11.3		66.4
V842	21	0.625	29	-	-		86	43	50		44.3	4.3	9.7		130.3
V843	19	0.625	29	-	-		79.3	43	52.9		49	14.7	33.3		128.3
V844	19	0.625	29	-	-		80	43	53.8		35.7	8.3	23.4		115.7

Appendix B2. Cell Counts on EGFP Embryos at stage 29

		EGFP electroporated embryos					Somatic Motor column (SM)				Column of Terni (CT)				SM +CT= Total Isl 1/2 +
Embryo Numbers	No. of somites at surgery	DNA con (µg/µl)	Sacrifice Stage (HH)	Total DAPI(+) cells in strip	Percentage of EGFP+ DAPI+		Total Isl 1/2 (+) cells	EGFP(+) Isl1/2 (+) cells	Percentage of EGFP(+) Isl1/2 (+) cells		Total Isl 1/2 (+) cells	EGFP(+) Isl1/2 (+) cells	Percentage of EGFP(+) Isl1/2 (+) cells		Total Isl 1/2 (+) cells
V160	24	2.5	29	138	52.1		95	61.3	62.1		41	26.6	66		136
V167	25	2.5	29	133	57.7		99	73	72.3		65.7	44	67.3		164.7
V114	26	2.5	29	109.7	36.4		127.3	52.3	41.2		31.3	12.3	40.4		158
V511	22	0.625	29	-	-		92	47	51		94.6	51.3	54,2		186
V208	17	2.5	29	158.3	66.2		96	83.3	85.9		54.3	46	83.8		150.3
V220	18	2.5	29	-	59		86.3	38.3	44.4		56.7	27.3	48.2		142
V209	20	2.5	29	160	40.9		85.3	34.7	40.7		52.6	18.6	34.9		137.9
V222	20	2.5	29	133.7	40.5		90	46.3	50.2		46.3	27.3	57.6		136.3
V514	20	0.625	29	-	-		124.7	77.7	62.3		82.3	53.3	64.8		203
V517	20	0.625	29	-	-		90.3	32.7	36.2		67.3	36	33.3		157.6

Appendix B3: Comparison of Overall Isl 1/2 + cells on the Transfected side vs. Nontransfected side of EGFP embryos.

Paired t-test
Hypothesized Difference = 0

	Mean Diff.	DF	t-Value	P-Value
Column 1, Column 2	-6.325	3	-.671	.5500

Transfected	Non-transfected
152.500	176.300
139.700	156.000
88.300	92.800
98.900	79.600

Legend :Paired t-test, <u>p-value = .5500</u>, No difference in the number of Isl 1/2 + motoneurons between the transfected and nontransfected side of EGFP embryos. Counts for Isl 1/2 + on the transfected and nontransfected side of EGFP embryos were conducted on DAB immunostained sections. Cell counts were carried on 3 non-adjacent sections in a posterior T segment (T6), and the numbers below reflect the mean of those counts.

Embryo #		**Transfected side**	**Nontransfected side**
V115	23	176.3	152.5
V116	24	156	139.7
V222	20	92.8	88.3
V209	20	79.6	98.9
		126.2	**119.85**

Appendix B4: Quantification of Total number of Motoneurons (Isl 1/2 +cells) in the Somatic motor region (SM) on the transfected side of EGFP and Hoxd10/EGFP embryos.

Unpaired t-test for Column 2
Grouping Variable: Column 1
Hypothesized Difference = 0

	Mean Diff.	DF	t-Value	P-Value
1.000, 2.000	-29.269	27	-4.145	.0003

Group Info for Column 2
Grouping Variable: Column 1

	Count	Mean	Variance	Std. Dev.	Std. Err
1.000	19	69.321	376.602	19.406	4.452
2.000	10	98.590	226.597	15.053	4.760

Group 1= Hoxd10 embryos

Group 2= EGFP embryos

1.000 69.300

1.000 97.300

1.000 59.000

1.000 51.700

1.000 86.000

1.000 79.300

1.000 80.000

1.000 79.000

1.000 81.300

1.000 66.300

1.000 102.000

1.000 28.000

1.000 55.300

1.000 33.700

1.000 71.300

1.000 87.300

1.000 74.000

1.000 59.000

1.000 57.300

2.000 95.000

2.000 99.000

2.000 127.300

2.000 92.000

2.000 96.000

2.000 86.300

2.000 85.300

2.000 90.000

2.000 124.700

2.000 90.300

Legend : Un-paired t-test, p-value = .0003 . There is a significant difference in the total number of motoneurons (Isl 1/2 +cells) in the somatic motor region (SM) when comparing the transfected side of EGFP and Hoxd10/EGFP embryos. A 30.0% reduction is observed in the total number of motoneurons in the somatic motor region of Hoxd10/EGFP embryos.

Appendix B5: Quantification of the Percentage of transfected motoneurons in the SM region (Isl 1/2+ GFP+ / total Isl1/2/+) on the transfected side of EGFP and Hoxd10/EGFP embryos

Unpaired t-test for Column 2
Grouping Variable: Column 1
Hypothesized Difference = 0

	Mean Diff.	DF	t-Value	P-Value
1.000, 2.000	2.561	27	.372	.7131

Group Info for Column 2
Grouping Variable: Column 1

	Count	Mean	Variance	Std. Dev.	Std. Err
1.000	10	54.640	250.280	15.820	5.003
2.000	19	52.079	341.746	18.486	4.241

1.000 62.100
1.000 72.300
1.000 41.200
1.000 51.000
1.000 85.900
1.000 44.400
1.000 40.700
1.000 50.200
1.000 62.300
1.000 36.300
2.000 35.100
2.000 87.000
2.000 35.100
2.000 31.600
2.000 73.400
2.000 45.200
2.000 41.200
2.000 90.400
2.000 52.500

Group 1= EGFP embryos
Group 2= Hoxd10 embryos

2.000 56.200
2.000 80.800
2.000 55.800
2.000 35.100
2.000 34.900
2.000 33.300
2.000 45.200
2.000 50.000
2.000 52.900
2.000 53.800

Legend : Un-paired t-test, <u>p-value = 0.713</u> No significant difference in the percentage of transfected motoneurons in the SM region (Isl 1/2+ GFP+ / total Isl1/2/+) when comparing the transfected side of EGFP and Hoxd10/EGFP embryos.

Appendix B6: Quantification of Total number of Motoneurons (Isl 1/2 +cells) in the Colunn of Terni region (CT) on the transfected side of EGFP and Hoxd10/EGFP embryos

Unpaired t-test for Column 2
Grouping Variable: Column 1
Hypothesized Difference = 0

	Mean Diff.	DF	t-Value	P-Value
1.000, 2.000	-26.189	27	-3.854	.0007

Group Info for Column 2
Grouping Variable: Column 1

	Count	Mean	Variance	Std. Dev.	Std. Err
1.000	19	33.021	273.567	16.540	3.795
2.000	10	59.210	360.501	18.987	6.004

1.000 20.300
1.000 48.600
1.000 14.700
1.000 14.700
1.000 44.300
1.000 49.000
1.000 35.700
1.000 33.300
1.000 33.300
1.000 25.000
1.000 86.000
1.000 24.000
1.000 32.600
1.000 33.000
1.000 16.300
1.000 25.300
1.000 25.000
1.000 26.000

Group 1= EGFP embryos

Group 2= Hoxd10 embryos

1.000 40.300

2.000 41.000

2.000 65.700

2.000 31.300

2.000 94.600

2.000 54.300

2.000 56.700

2.000 52.600

2.000 46.300

2.000 82.300

2.000 67.300

Legend : Un-paired t-test, p-value = .0007 . There is a significant difference in the total number of motoneurons (Isl 1/2 +cells) in the CT region when comparing the transfected side of EGFP and Hoxd10/EGFP embryos. A 44.0 % reduction is observed in the total number of motoneurons in the CT region of Hoxd10/EGFP embryos.

Appendix B7: Quantification of the Percentage of transfected motoneurons in the CT region (Isl 1/2+ GFP+ / total Isl1/2/+) on the transfected side of EGFP and Hoxd10/EGFP embryos.

Unpaired t-test for Column 2
Grouping Variable: Column 1
Hypothesized Difference = 0

	Mean Diff.	DF	t-Value	P-Value
1.000, 2.000	20.966	27	3.121	.0043

Group Info for Column 2
Grouping Variable: Column 1

	Count	Mean	Variance	Std. Dev.	Std. Err
1.000	10	55.040	260.265	16.133	5.102
2.000	19	34.074	313.436	17.704	4.062

Group 1= EGFP embryos

Group 2= Hoxd10 embryos

1.000	66.000
1.000	67.300
1.000	40.300
1.000	54.200
1.000	83.800
1.000	48.200
1.000	34.900
1.000	57.600
1.000	64.800
1.000	33.300
2.000	23.000
2.000	69.700
2.000	18.400
2.000	23.100
2.000	53.100
2.000	23.300
2.000	23.900
2.000	57.400

2.000	38.500
2.000	59.900
2.000	60.500
2.000	26.000
2.000	26.300
2.000	30.200
2.000	36.400
2.000	11.300
2.000	9.700
2.000	33.300
2.000	23.400

Legend : Un-paired t-test, p-value = 0.0043 There is a significant difference in percentage of transfected motoneurons in the CT region (Isl 1/2+ GFP+ / total Isl1/2/+) when comparing the transfected side of EGFP and Hoxd10/EGFP embryos. A 38.0 % reduction in the percentage of transfected motoneurons in the CT region of Hoxd10/EGFP embryos.

Appendix B8: Comparison of total number of motoneurons (Isl 1/2 +cells) in the SM region on the transfected side of experimental embryos electroporated at stage 13 vs stage 15

Unpaired t-test for Column 2
Grouping Variable: Column 1
Hypothesized Difference = 0

	Mean Diff.	DF	t-Value	P-Value
1.000, 2.000	-.847	17	-.092	.9275

Group Info for Column 2
Grouping Variable: Column 1

	Count	Mean	Variance	Std. Dev.	Std. Err
1.000	10	68.920	490.720	22.152	7.005
2.000	9	69.767	294.870	17.172	5.724

1= Stage 15

2= Stage 13

1.000 79.000
1.000 81.300
1.000 66.300
1.000 102.000
1.000 28.000
1.000 69.300
1.000 97.300
1.000 59.000
1.000 51.700
1.000 55.300
2.000 33.700
2.000 71.300
2.000 87.300
2.000 74.000
2.000 59.000

2.000 57.300

2.000 86.000

2.000 79.300

2.000 80.000

Legend : Un-paired t-test, <u>p-value = 0.9275</u> No significant difference in total number of motoneurons (Isl 1/2 +cells) in the SM region when comparing the transfected side of experimental embryos electroporated at stage 13 or stage 15**.**

Appendix B9: Comparison of the Percentage of transfected motoneurons in the SM region on the transfected side of experimental embryos electroporated at stage 13 vs stage 15

Unpaired t-test for Column 2
Grouping Variable: Column 1
Hypothesized Difference = 0

	Mean Diff.	DF	t-Value	P-Value
1.000, 2.000	-14.366	17	-1.809	.0882

Group Info for Column 2
Grouping Variable: Column 1

	Count	Mean	Variance	Std. Dev.	Std. Err
1.000	10	45.590	364.405	19.089	6.037
2.000	9	59.956	224.725	14.991	4.997

1= Stage 15

2= Stage 13

1.000 35.100
1.000 87.000
1.000 31.600
1.000 35.100
1.000 34.900
1.000 33.300
1.000 45.200
1.000 35.100
1.000 73.400
1.000 45.200
2.000 47.200
2.000 90.400
2.000 52.500
2.000 56.200
2.000 80.800

2.000 55.800

2.000 50.000

2.000 52.900

2.000 53.800

Legend : Un-paired t-test, p-value = 0..0882 No significant difference in total number of motoneurons (Isl 1/2 +cells) in the SM region when comparing the transfected side of experimental embryos electroporated at stage 13 or stage 15..

Appendix B10: Comparison of total number of motoneurons (Isl 1/2 +cells) in the SM region on the transfected side of experimental embryos electroporated with either 0.625 (µg/µl) or 2.5 (µg/µl) Hoxd10/EGFP cDNA .

Unpaired t-test for Column 2
Grouping Variable: Column 1
Hypothesized Difference = 0

	Mean Diff.	DF	t-Value	P-Value
1.000, 2.000	13.237	15	1.473	.1614

Group Info for Column 2
Grouping Variable: Column 1

	Count	Mean	Variance	Std. Dev.	Std. Err
1.000	7	74.657	248.723	15.771	5.961
2.000	10	61.420	388.331	19.706	6.232

Group 1= 0.625 (µg/µl) electroporated embryos

Group 2 = 2.5 (µg/µl) electroporated embryos

1.000 69.300
1.000 97.300
1.000 59.000
1.000 51.700
1.000 86.000
1.000 79.300
1.000 80.000
2.000 79.000
2.000 81.300
2.000 66.300
2.000 59.000
2.000 28.000
2.000 55.300

2.000 33.700

2.000 71.300

2.000 87.300

2.000 53.000

Legend : Un-paired t-test, <u>p-value = 0.1614</u> No significant difference in total number of motoneurons (Isl 1/2 +cells) in the SM region when comparing the transfected side of experimental embryos electroporated with either 0.625 (µg/µl) or 2.5 (µg/µl) Hoxd10/EGFP cDNA

Appendix B11: Quantification of Transfection efficiency (DAPI+ GFP+ / total DAPI+) in the ventral strip on the transfected side of EGFP and Hoxd10/EGFP embryos.

Unpaired t-test for Column 2
Grouping Variable: Column 1
Hypothesized Difference = 0

	Mean Diff.	DF	t-Value	P-Value
1.000, 2.000	-6.100	15	-.885	.3901

Group Info for Column 2
Grouping Variable: Column 1

	Count	Mean	Variance	Std. Dev.	Std. Err
1.000	10	44.300	241.064	15.526	4.910
2.000	7	50.400	127.340	11.285	4.265

Group 1= Hoxd10 embryos

Group 2= EGFP embryos

1.000 29.700
1.000 62.300
1.000 31.000
1.000 47.000
1.000 39.600
1.000 63.600
1.000 30.600
1.000 68.500
1.000 43.100
1.000 27.600
2.000 52.100
2.000 57.700
2.000 36.400
2.000 66.200
2.000 59.000
2.000 40.900

2.000 40.500

Legend : Un-paired t-test, p-value = .3901. No difference in the percentage of Transfection (DAPI+ GFP+ / total DAPI+) in ventral strip when comparing the transfected side of EGFP and Hoxd10/EGFP embryos. Counts for Isl 1/2 + on the transfected and nontransfected side of EGFP embryos were conducted on DAB immunostained sections. Cell counts were carried on 3 non-adjacent sections in posterior T spinal cord (T6), and the numbers below reflect the mean of those counts

Appendix B12: Quantification of Total number of cells (DAPI+cells) in the ventral strip on the transfected side of EGFP and Hoxd10/EGFP embryos.

Unpaired t-test for Column 2
Grouping Variable: Column 1
Hypothesized Difference = 0

	Mean Diff.	DF	t-Value	P-Value
1.000, 2.000	-22.207	15	-2.215	.0427

Group Info for Column 2
Grouping Variable: Column 1

	Count	Mean	Variance	Std. Dev.	Std. Err
1.000	10	115.750	493.643	22.218	7.026
2.000	7	137.957	294.243	17.154	6.483

Group 1= Hoxd10 embryos

Group 2= EGFP embryos

1.000 118.700
1.000 104.300
1.000 137.700
1.000 160.700
1.000 114.700
1.000 83.300
1.000 111.700
1.000 90.700
1.000 124.700
1.000 111.000
2.000 138.000
2.000 133.000
2.000 109.700
2.000 158.300
2.000 133.000
2.000 160.000
2.000 133.700

Legend : Un-paired t-test, p-value = 0.0427 . There is a significant difference in the number of total DAPI+ cells in the ventral strip when comparing the transfected side of EGFP and Hoxd10/EGFP embryos. A 16.1 % reduction is observed in the total number of cells in the Hoxd10/EGFP ventral strip.

APPENDIX C

CELL COUNTS FROM ELECTROPORATED EMBRYOS AT STAGE 18

C1. Cell counts from stage 18 Hoxd10/EGPF Electroporated Embryos						
Embryo Numbers	**DNA con(µg/µl)**	**No. of somites at electropration**	**Sacrifice Stage (HH)**	**Sections**	**Isl 1/2 + cells on transfected side**	**Isl 1/2 + cells on nontransfected side**
V1046	2.5	22	18	A	4	9
				B	7	16
				C	11	15
				Total Avg	**7.3**	**13.3**
V1047	2.5	26	18	A	10	30
				B	9	28
				C	15	31
				Total Avg	**11.3**	**29.7**
V1050	2.5	23	18	A	12	25
				B	9	24
				C	23	30
				Total Avg	**14.7**	**26.3**
V835	2.5	19	18	A	6	25
				B	15	28
				C	10	26
				Total Avg	**10.3**	**26.3**

C2. Cell counts from stage 18 EGPF Electroporated Embryos

Embryo Numbers	DNA con(µg/µl)	No. of somites at electropration	Sacrifice Stage (HH)	Sections	Isl 1/2 + cells on transfected side	Isl 1/2 + cells on nontransfected side
V1095	2.5	23	18	A	26	28
				B	26	30
				C	40	42
				Total Avg	**31.3**	**33.3**
V930	2.5	23	18	A	18	22
				B	28	27
				C	11	13
				Total Avg	**19**	**20.7**
V925	2.5	24	18	A	10	7
				B	10	12
				C	16	22
				Total Avg	**12**	**13.7**

Appendix C3. Unpaired t-test analysis of Isl 1/2 (+) cells counts on the TRANSFECTED and NONTRANSFECTED side of EGFP–electroporated embryos sacrificed at Stage 18

Unpaired t-test for Isl 1/2
Grouping Variable: Groups
Hypothesized Difference = 0

	Mean Diff.	DF	t-Value	P-Value
1.000, 2.000	-1.800	4	-.224	.8339

Group Info for Isl 1/2
Grouping Variable: Groups

	Count	Mean	Variance	Std. Dev.	Std. Err
1.000	3	20.767	95.463	9.771	5.641
2.000	3	22.567	98.653	9.932	5.734

1= transfected

2= nontransfected

1.000 31.300
1.000 19.000
1.000 12.000
2.000 33.300
2.000 20.700
2.000 13.700

Legend: Un-paired t-test was not used for analysis due high variation in cell numbers in embryos sacrificed at stage 18.

Appendix C4. Paired t-test analysis of Isl 1/2 (+) cells counts on the TRANSFECTED and NONTRANSFECTED side of EGFP–electroporated embryos sacrificed at Stage 18

Paired t-test
Hypothesized Difference = 0

	Mean Diff.	DF	t-Value	P-Value
TRANSFECTED, NONTRANSFECTED	-1.800	2	-18.000	.0031

Transfected	Nonelectroporated
31.300	33.300
19.000	20.700
12.000	13.700

Legend : Un-paired t-test, p-value = .0031 . There is a small (-1.8) but significant difference in the total number of motoneurons (Isl 1/2 +cells) in the EGFP–electroporated embryos sacrificed at Stage 18.

Appendix C5. Unpaired t-test analysis of Isl 1/2 (+) cells counts on the TRANSFECTED and NONTRANSFECTED side of Hoxd10/EGFP–electroporated embryos sacrificed at Stage 18

Unpaired t-test for Isl 1/2
Grouping Variable: Groups
Hypothesized Difference = 0

	Mean Diff.	DF	t-Value	P-Value
1.000, 2.000	-13.000	6	-3.307	.0163

Group Info for Isl 1/2
Grouping Variable: Groups

	Count	Mean	Variance	Std. Dev.	Std. Err
1.000	4	10.900	9.307	3.051	1.525
2.000	4	23.900	52.507	7.246	3.623

1= transfected

2= nontransfected

1.000 7.300
1.000 11.300
1.000 14.700
1.000 10.300
2.000 13.300
2.000 29.700
2.000 26.300
2.000 26.300

Legend : Un-paired t-test was not used for analysis due high variation in Isl 1/2+ numbers in embryos sacrificed at stage 18.

Appendix C6. Paired t-test analysis of Isl 1/2 (+) cells counts on the TRANSFECTED and NONTRANSFECTED side of Hoxd10/EGFP–electroporated embryos sacrificed at Stage 18.

Paired t-test
Hypothesized Difference = 0

	Mean Diff.	DF	t-Value	P-Value
TRANSFECTED, NONTRANSFECTED	-13.000	3	-4.770	.0175

TRANSFECTED	NONTRANSFECTED
7.300	13.300
11.300	29.700
14.700	26.300
10.300	26.300

Legend : Un-paired t-test, p-value = .0175 . There significant difference in the total number of motoneurons (Isl 1/2 +cells) in the Hoxd10/EGFP–electroporated embryos sacrificed at Stage 18.

Appendix C7. Unpaired t-test analysis of the Total Isl 1/2 (+) cells (SM+CM) counts on the TRANSFECTED side of EGFP and Hoxd10/EGFP–electroporated embryos sacrificed at Stage 29.

Unpaired t-test for TRANSFECTED
Grouping Variable: groups
Hypothesized Difference = 0

	Mean Diff.	DF	t-Value	P-Value
1.000, 2.000	55.037	27	4.856	<.0001

Group Info for TRANSFECTED
Grouping Variable: groups

	Count	Mean	Variance	Std. Dev.	Std. Err
1.000	10	157.400	503.107	22.430	7.093
2.000	19	102.363	1010.706	31.792	7.293

1.000 136.000
1.000 164.700
1.000 158.600
1.000 186.600
1.000 150.300
1.000 143.000
1.000 137.900
1.000 136.300
1.000 203.000
1.000 157.600
2.000 112.700
2.000 114.600
2.000 91.300
2.000 188.000
2.000 52.000
2.000 87.900
2.000 66.700
2.000 87.600

2.000 112.600
2.000 99.000
2.000 85.000
2.000 97.600
2.000 89.600
2.000 145.900
2.000 73.700
2.000 66.400
2.000 130.300
2.000 128.300
2.000 115.700

Legend : Un-paired t-test, p-value = <.0001 . There is a significant difference in the total number of motoneurons (Isl 1/2 +cells) when comparing the transfected side of EGFP and Hoxd10/EGFP– electroporated embryos at stage 29. There is a 34.9% reduction in total

APPENDIX D

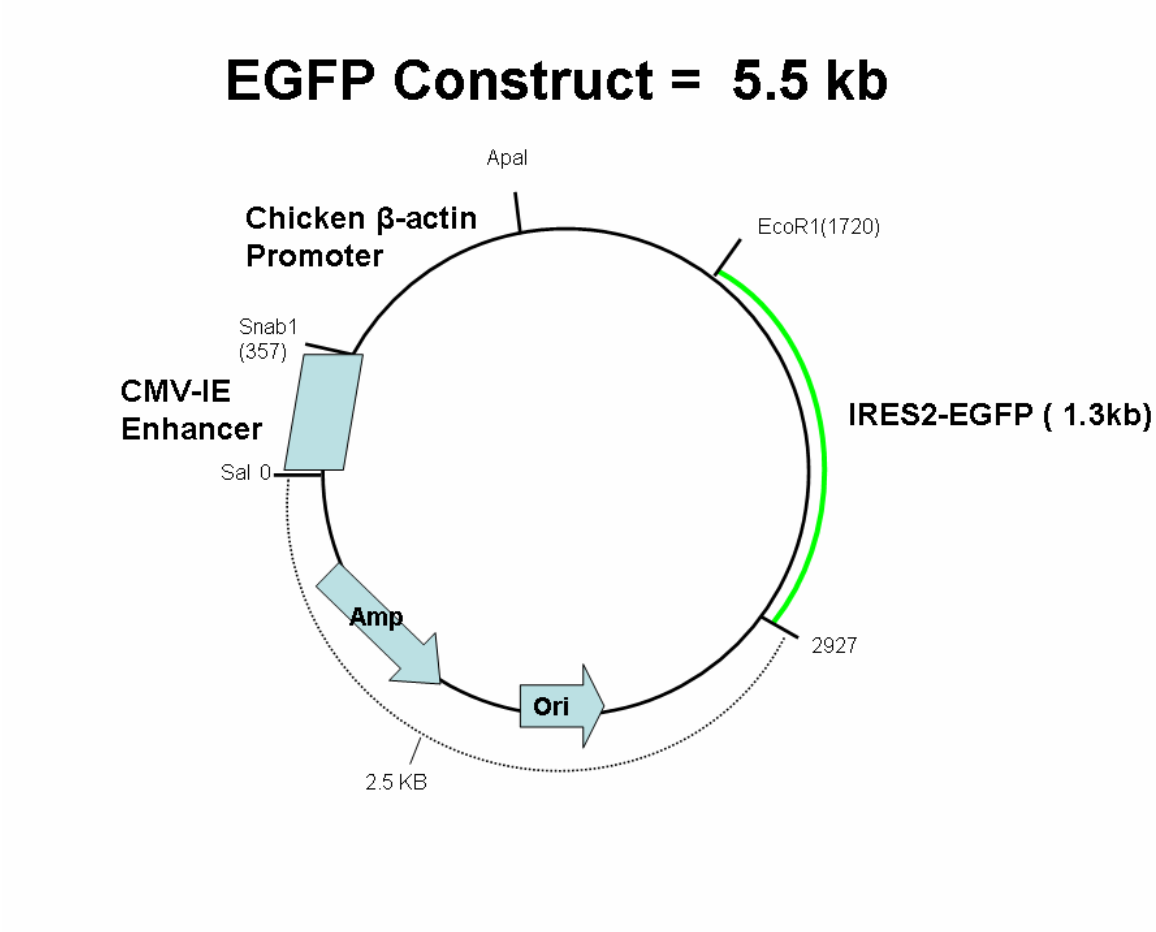
EGFP Construct = 5.5 kb
ApaI
Chicken β-actin Promoter
EcoR1(1720)
Snab1 (357)
CMV-IE Enhancer
IRES2-EGFP (1.3kb)
Sal 0
Amp
2927
Ori
2.5 KB

Hoxd10/EGFP Construct = 7.3 kb

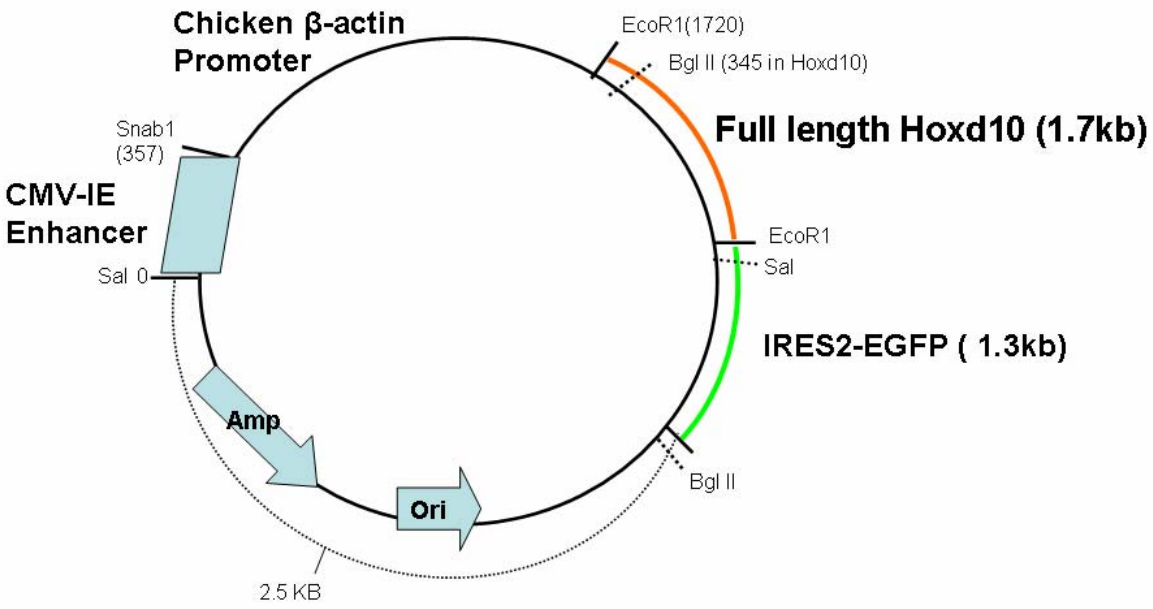

Hoxd9/EGFP Construct = 6.76 kb

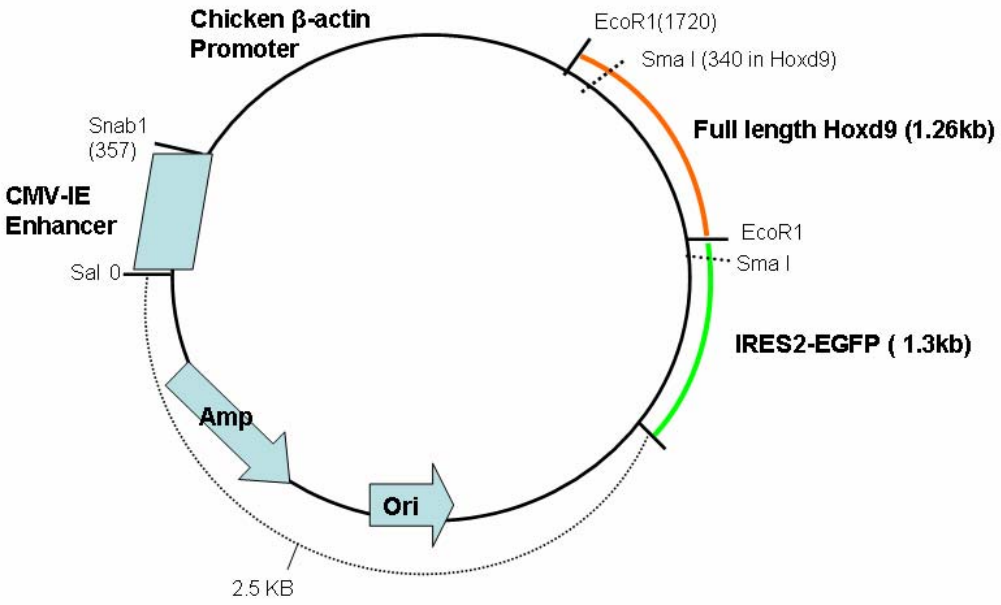

BIBLIOGRAPHY

Abzhanov, A., E. Tzahor, et al. (2003). "Dissimilar regulation of cell differentiation in mesencephalic (cranial) and sacral (trunk) neural crest cells in vitro." Development **130**(19): 4567-79.

Akam, M. (1989). "Hox and HOM: homologous gene clusters in insects and vertebrates." Cell **57**(3): 347-9.

Appel, B., V. Korzh, et al. (1995). "Motoneuron fate specification revealed by patterned LIM homeobox gene expression in embryonic zebrafish." Development **121**(12): 4117-25.

Bel-Vialar, S., N. Itasaki, et al. (2002). "Initiating Hox gene expression: in the early chick neural tube differential sensitivity to FGF and RA signaling subdivides the HoxB genes in two distinct groups." Development **129**(22): 5103-15.

Bell, E., R. J. Wingate, et al. (1999). "Homeotic transformation of rhombomere identity after localized Hoxb1 misexpression." Science **284**(5423): 2168-71.

Bello, B. C., F. Hirth, et al. (2003). "A pulse of the Drosophila Hox protein Abdominal-A schedules the end of neural proliferation via neuroblast apoptosis." Neuron **37**(2): 209-19.

Berggren, K., P. McCaffery, et al. (1999). "Differential distribution of retinoic acid synthesis in the chicken embryo as determined by immunolocalization of the retinoic acid synthetic enzyme, RALDH-2." Dev Biol **210**(2): 288-304.

Bertrand, N., F. Medevielle, et al. (2000). "FGF signalling controls the timing of Pax6 activation in the neural tube." Development **127**(22): 4837-43.

Bjornsson, J. M., E. Andersson, et al. (2001). "Proliferation of primitive myeloid progenitors can be reversibly induced by HOXA10." Blood **98**(12): 3301-8.

Boulet, A. M. and M. R. Capecchi (2004). "Multiple roles of Hoxa11 and Hoxd11 in the formation of the mammalian forelimb zeugopod." Development **131**(2): 299-309.

Briscoe, J., L. Sussel, et al. (1999). "Homeobox gene Nkx2.2 and specification of neuronal identity by graded Sonic hedgehog signalling." Nature **398**(6728): 622-7.

Brose, K., K. S. Bland, et al. (1999). "Slit proteins bind Robo receptors and have an evolutionarily conserved role in repulsive axon guidance." Cell **96**(6): 795-806.

Burke, A. C., C. E. Nelson, et al. (1995). "Hox genes and the evolution of vertebrate axial morphology." Development **121**(2): 333-46.

Burke, A. C. and C. J. Tabin (1996). "Virally mediated misexpression of Hoxc-6 in the cervical mesoderm results in spinal nerve truncations." Dev Biol **178**(1): 192-7.

Cacalano, G., I. Farinas, et al. (1998). "GFRalpha1 is an essential receptor component for GDNF in the developing nervous system and kidney." Neuron **21**(1): 53-62.

Capdevila, J., T. Tsukui, et al. (1999). "Control of vertebrate limb outgrowth by the proximal factor Meis2 and distal antagonism of BMPs by Gremlin." Mol Cell **4**(5): 839-49.

Carlon, N., J. Pizant, et al. (1983). "Mesonephric origin of the gonadal primitive medulla in chick embryos." Anat Embryol (Berl) **166**(3): 399-414.

Caronia, G., F. R. Goodman, et al. (2003). "An I47L substitution in the HOXD13 homeodomain causes a novel human limb malformation by producing a selective loss of function." Development **130**(8): 1701-12.

Carpenter, E. M. (2002). "Hox genes and spinal cord development." Dev Neurosci **24**(1): 24-34.

Carpenter, E. M., J. M. Goddard, et al. (1993). "Loss of Hox-A1 (Hox-1.6) function results in the reorganization of the murine hindbrain." Development **118**(4): 1063-75.

Carpenter, E. M., J. M. Goddard, et al. (1997). "Targeted disruption of Hoxd-10 affects mouse hindlimb development." Development **124**(22): 4505-14.

Carpenter, E. M. and M. Hollyday (1992). "The distribution of neural crest-derived Schwann cells from subsets of brachial spinal segments into the peripheral nerves innervating the chick forelimb." Dev Biol **150**(1): 160-70.

Carpenter, E. M. and M. Hollyday (1992). "The location and distribution of neural crest-derived Schwann cells in developing peripheral nerves in the chick forelimb." Dev Biol **150**(1): 144-59.

Chen, F. and M. R. Capecchi (1997). "Targeted mutations in hoxa-9 and hoxb-9 reveal synergistic interactions." Dev Biol **181**(2): 186-96.

Chen, F. and M. R. Capecchi (1999). "Paralogous mouse Hox genes, Hoxa9, Hoxb9, and Hoxd9, function together to control development of the mammary gland in response to pregnancy." Proc Natl Acad Sci U S A **96**(2): 541-6.

Colbert, M. C., W. W. Rubin, et al. (1995). "Retinoid signaling and the generation of regional and cellular diversity in the embryonic mouse spinal cord." Dev Dyn **204**(1): 1-12.

Conlon, R. A. and J. Rossant (1992). "Exogenous retinoic acid rapidly induces anterior ectopic expression of murine Hox-2 genes in vivo." Development **116**(2): 357-68.

Crossley, P. H. and G. R. Martin (1995). "The mouse Fgf8 gene encodes a family of polypeptides and is expressed in regions that direct outgrowth and patterning in the developing embryo." Development **121**(2): 439-51.

Dasen, J. S., J. P. Liu, et al. (2003). "Motor neuron columnar fate imposed by sequential phases of Hox-c activity." Nature **425**(6961): 926-33.

Dasen, J. S., B. C. Tice, et al. (2005). "A hox regulatory network establishes motor neuron pool identity and target-muscle connectivity." Cell **123**(3): 477-91.

Davenne, M., M. K. Maconochie, et al. (1999). "Hoxa2 and Hoxb2 control dorsoventral patterns of neuronal development in the rostral hindbrain." Neuron **22**(4): 677-91.

Dawid, I. B., J. J. Breen, et al. (1998). "LIM domains: multiple roles as adapters and functional modifiers in protein interactions." Trends Genet **14**(4): 156-62.

de la Cruz, C. C., A. Der-Avakian, et al. (1999). "Targeted disruption of Hoxd9 and Hoxd10 alters locomotor behavior, vertebral identity, and peripheral nervous system development." Dev Biol **216**(2): 595-610.

de Santa Barbara, P. and D. J. Roberts (2002). "Tail gut endoderm and gut/genitourinary/tail development: a new tissue-specific role for Hoxa13." Development **129**(3): 551-61.

Debby-Brafman, A., T. Burstyn-Cohen, et al. (1999). "F-Spondin, expressed in somite regions avoided by neural crest cells, mediates inhibition of distinct somite domains to neural crest migration." Neuron **22**(3): 475-88.

Diez del Corral, R. and K. G. Storey (2004). "Opposing FGF and retinoid pathways: a signalling switch that controls differentiation and patterning onset in the extending vertebrate body axis." Bioessays **26**(8): 857-69.

Duboule, D. and P. Dolle (1989). "The structural and functional organization of the murine HOX gene family resembles that of Drosophila homeotic genes." Embo J **8**(5): 1497-505.

Durston, A. J., J. P. Timmermans, et al. (1989). "Retinoic acid causes an anteroposterior transformation in the developing central nervous system." Nature **340**(6229): 140-4.

Ebens, A., K. Brose, et al. (1996). "Hepatocyte growth factor/scatter factor is an axonal chemoattractant and a neurotrophic factor for spinal motor neurons." Neuron **17**(6): 1157-72.

Eberhart, J., J. Barr, et al. (2004). "Ephrin-A5 exerts positive or inhibitory effects on distinct subsets of EphA4-positive motor neurons." J Neurosci **24**(5): 1070-8.

Eberhart, J., M. E. Swartz, et al. (2002). "EphA4 constitutes a population-specific guidance cue for motor neurons." Dev Biol **247**(1): 89-101.

Economides, K. D., L. Zeltser, et al. (2003). "Hoxb13 mutations cause overgrowth of caudal spinal cord and tail vertebrae." Dev Biol **256**(2): 317-30.

Ensini, M., T. N. Tsuchida, et al. (1998). "The control of rostrocaudal pattern in the developing spinal cord: specification of motor neuron subtype identity is initiated by signals from paraxial mesoderm." Development **125**(6): 969-82.

Ericson, J., J. Briscoe, et al. (1997). "Graded sonic hedgehog signaling and the specification of cell fate in the ventral neural tube." Cold Spring Harb Symp Quant Biol **62**: 451-66.

Ericson, J., S. Morton, et al. (1996). "Two critical periods of Sonic Hedgehog signaling required for the specification of motor neuron identity." Cell **87**(4): 661-73.

Ericson, J., P. Rashbass, et al. (1997). "Pax6 controls progenitor cell identity and neuronal fate in response to graded Shh signaling." Cell **90**(1): 169-80.

Ericson, J., S. Thor, et al. (1992). "Early stages of motor neuron differentiation revealed by expression of homeobox gene Islet-1." Science **256**(5063): 1555-60.

Fan, J. and J. A. Raper (1995). "Localized collapsing cues can steer growth cones without inducing their full collapse." Neuron **14**(2): 263-74.

Feng, G., M. B. Laskowski, et al. (2000). "Roles for ephrins in positionally selective synaptogenesis between motor neurons and muscle fibers." Neuron **25**(2): 295-306.

Ferguson, B. A. (1983). "Development of motor innervation of the chick following dorsal-ventral limb bud rotations." J Neurosci **3**(9): 1760-72.

Forehand, C. J., E. B. Ezerman, et al. (1998). "Segment-specific pattern of sympathetic preganglionic projections in the chicken embryo spinal cord is altered by retinoids." Proc Natl Acad Sci U S A **95**(18): 10878-83.

Forehand, C. J., E. B. Ezerman, et al. (1994). "Segmental patterning of rat and chicken sympathetic preganglionic neurons: correlation between soma position and axon projection pathway." J Neurosci **14**(1): 231-41.

Fredette, B. J., J. Miller, et al. (1996). "Inhibition of motor axon growth by T-cadherin substrata." Development **122**(10): 3163-71.

Fromental-Ramain, C., X. Warot, et al. (1996). "Specific and redundant functions of the paralogous Hoxa-9 and Hoxd-9 genes in forelimb and axial skeleton patterning." Development **122**(2): 461-72.

Gabellini, D., I. N. Colaluca, et al. (2003). "Early mitotic degradation of the homeoprotein HOXC10 is potentially linked to cell cycle progression." Embo J **22**(14): 3715-24.

Garces, A., G. Haase, et al. (2000). "GFRalpha 1 is required for development of distinct subpopulations of motoneuron." J Neurosci **20**(13): 4992-5000.

Gaunt, S. J., R. Krumlauf, et al. (1989). "Mouse homeo-genes within a subfamily, Hox-1.4, -2.6 and -5.1, display similar anteroposterior domains of expression in the embryo, but show stage- and tissue-dependent differences in their regulation." Development **107**(1): 131-41.

Gavalas, A., M. Davenne, et al. (1997). "Role of Hoxa-2 in axon pathfinding and rostral hindbrain patterning." Development **124**(19): 3693-702.

Gavalas, A., C. Ruhrberg, et al. (2003). "Neuronal defects in the hindbrain of Hoxa1, Hoxb1 and Hoxb2 mutants reflect regulatory interactions among these Hox genes." Development **130**(23): 5663-79.

Gavalas, A., M. Studer, et al. (1998). "Hoxa1 and Hoxb1 synergize in patterning the hindbrain, cranial nerves and second pharyngeal arch." Development **125**(6): 1123-36.

Gehring, W. J. (1993). "Exploring the homeobox." Gene **135**(1-2): 215-21.

Giger, R. J., J. F. Cloutier, et al. (2000). "Neuropilin-2 is required in vivo for selective axon guidance responses to secreted semaphorins." Neuron **25**(1): 29-41.

Goddard, J. M., M. Rossel, et al. (1996). "Mice with targeted disruption of Hoxb-1 fail to form the motor nucleus of the VIIth nerve." Development **122**(10): 3217-28.

Goncalves, M. B., J. Boyle, et al. (2005). "Timing of the retinoid-signalling pathway determines the expression of neuronal markers in neural progenitor cells." Dev Biol **278**(1): 60-70.

Gonzalez-Reyes, A. and G. Morata (1990). "The developmental effect of overexpressing a Ubx product in Drosophila embryos is dependent on its interactions with other homeotic products." Cell **61**(3): 515-22.

Gould, A., A. Morrison, et al. (1997). "Positive cross-regulation and enhancer sharing: two mechanisms for specifying overlapping Hox expression patterns." Genes Dev **11**(7): 900-13.

Guidato, S., F. Prin, et al. (2003). "Somatic motoneurone specification in the hindbrain: the influence of somite-derived signals, retinoic acid and Hoxa3." Development **130**(13): 2981-96.

Gundersen, R. W. and J. N. Barrett (1979). "Neuronal chemotaxis: chick dorsal-root axons turn toward high concentrations of nerve growth factor." Science **206**(4422): 1079-80.

Guthrie, S. and A. Pini (1995). "Chemorepulsion of developing motor axons by the floor plate." Neuron **14**(6): 1117-30.

Gutman, C. R., M. K. Ajmera, et al. (1993). "Organization of motor pools supplying axial muscles in the chicken." Brain Res **609**(1-2): 129-36.

Haase, G., E. Dessaud, et al. (2002). "GDNF acts through PEA3 to regulate cell body positioning and muscle innervation of specific motor neuron pools." Neuron **35**(5): 893-905.

Helmbacher, F., E. Dessaud, et al. (2003). "Met signaling is required for recruitment of motor neurons to PEA3-positive motor pools." Neuron **39**(5): 767-77.

Helmbacher, F., S. Schneider-Maunoury, et al. (2000). "Targeting of the EphA4 tyrosine kinase receptor affects dorsal/ventral pathfinding of limb motor axons." Development **127**(15): 3313-24.

Hollyday, M. (1980). "Organization of motor pools in the chick lumbar lateral motor column." J Comp Neurol **194**(1): 143-70.

Hollyday, M. and V. Hamburger (1976). "Reduction of the naturally occurring motor neuron loss by enlargement of the periphery." J Comp Neurol **170**(3): 311-20.

Hollyday, M. and V. Hamburger (1977). "An autoradiographic study of the formation of the lateral motor column in the chick embryo." Brain Res **132**(2): 197-208.

Inoue, T., O. Chisaka, et al. (1997). "Cadherin-6 expression transiently delineates specific rhombomeres, other neural tube subdivisions, and neural crest subpopulations in mouse embryos." Dev Biol **183**(2): 183-94.

Izpisua-Belmonte, J. C., H. Falkenstein, et al. (1991). "Murine genes related to the Drosophila AbdB homeotic genes are sequentially expressed during development of the posterior part of the body." Embo J **10**(8): 2279-89.

Jessell, T. M. (2000). "Neuronal specification in the spinal cord: inductive signals and transcriptional codes." Nat Rev Genet **1**(1): 20-9.

Jungbluth, S., E. Bell, et al. (1999). "Specification of distinct motor neuron identities by the singular activities of individual Hox genes." Development **126**(12): 2751-8.

Kania, A. and T. M. Jessell (2003). "Topographic motor projections in the limb imposed by LIM homeodomain protein regulation of ephrin-A:EphA interactions." Neuron **38**(4): 581-96.

Kania, A., R. L. Johnson, et al. (2000). "Coordinate roles for LIM homeobox genes in directing the dorsoventral trajectory of motor axons in the vertebrate limb." Cell **102**(2): 161-73.

Kapfhammer, J. P. and J. A. Raper (1987). "Collapse of growth cone structure on contact with specific neurites in culture." J Neurosci **7**(1): 201-12.

Karlsson, O., S. Thor, et al. (1990). "Insulin gene enhancer binding protein Isl-1 is a member of a novel class of proteins containing both a homeo- and a Cys-His domain." Nature **344**(6269): 879-82.

Katahira, T. and H. Nakamura (2003). "Gene silencing in chick embryos with a vector-based small interfering RNA system." Dev Growth Differ **45**(4): 361-7.

Kessel, M. and P. Gruss (1991). "Homeotic transformations of murine vertebrae and concomitant alteration of Hox codes induced by retinoic acid." Cell **67**(1): 89-104.

Keynes, R. J. and C. D. Stern (1984). "Segmentation in the vertebrate nervous system." Nature **310**(5980): 786-9.

Kilpatrick, T. J., A. Brown, et al. (1996). "Expression of the Tyro4/Mek4/Cek4 gene specifically marks a subset of embryonic motor neurons and their muscle targets." Mol Cell Neurosci **7**(1): 62-74.

Kitsukawa, T., M. Shimizu, et al. (1997). "Neuropilin-semaphorin III/D-mediated chemorepulsive signals play a crucial role in peripheral nerve projection in mice." Neuron **19**(5): 995-1005.

Kobayashi, A. and R. R. Behringer (2003). "Developmental genetics of the female reproductive tract in mammals." Nat Rev Genet **4**(12): 969-80.

Komuves, L. G., E. Michael, et al. (2002). "HOXB4 homeodomain protein is expressed in developing epidermis and skin disorders and modulates keratinocyte proliferation." Dev Dyn **224**(1): 58-68.

Kraut, R. and K. Zinn (2004). "Roundabout 2 regulates migration of sensory neurons by signaling in trans." Curr Biol **14**(15): 1319-29.

Krull, C. E. (2004). "A primer on using in ovo electroporation to analyze gene function." Dev Dyn **229**(3): 433-9.

Krull, C. E. and S. A. Koblar (2000). "Motor axon pathfinding in the peripheral nervous system." Brain Res Bull **53**(5): 479-87.

Krumlauf, R. (1994). "Hox genes in vertebrate development." Cell **78**(2): 191-201.

Kury, P., N. Gale, et al. (2000). "Eph receptors and ephrin expression in cranial motor neurons and the branchial arches of the chick embryo." Mol Cell Neurosci **15**(2): 123-40.

Lance-Jones, C. and L. Landmesser (1980). "Motoneurone projection patterns in the chick hind limb following early partial reversals of the spinal cord." J Physiol **302**: 581-602.

Lance-Jones, C. and L. Landmesser (1981). "Pathway selection by chick lumbosacral motoneurons during normal development." Proc R Soc Lond B Biol Sci **214**(1194): 1-18.

Lance-Jones, C., N. Omelchenko, et al. (2001). "Hoxd10 induction and regionalization in the developing lumbosacral spinal cord." Development **128**(12): 2255-68.

Landmesser, L. (1978). "The development of motor projection patterns in the chick hind limb." J Physiol **284**: 391-414.

Landmesser, L. (1978). "The distribution of motoneurones supplying chick hind limb muscles." J Physiol **284**: 371-89.

Langman, J. and C. C. Haden (1970). "Formation and migration of neuroblasts in the spinal cord of the chick embryo." J Comp Neurol **138**(4): 419-25.

Laskowski, M. B. and J. R. Sanes (1987). "Topographic mapping of motor pools onto skeletal muscles." J Neurosci **7**(1): 252-60.

Le Douarin, N. M., S. Creuzet, et al. (2004). "Neural crest cell plasticity and its limits." Development **131**(19): 4637-50.

Leber, S. M. and J. R. Sanes (1991). "Lineage analysis with a recombinant retrovirus: application to chick spinal motor neurons." Adv Neurol **56**: 27-36.

Leber, S. M. and J. R. Sanes (1995). "Migratory paths of neurons and glia in the embryonic chick spinal cord." J Neurosci **15**(2): 1236-48.

Lee, S. K. and S. L. Pfaff (2003). "Synchronization of neurogenesis and motor neuron specification by direct coupling of bHLH and homeodomain transcription factors." Neuron **38**(5): 731-45.

Lewis, K. E. and J. S. Eisen (2004). "Paraxial mesoderm specifies zebrafish primary motoneuron subtype identity." Development **131**(4): 891-902.

Liem, K. F., Jr., T. M. Jessell, et al. (2000). "Regulation of the neural patterning activity of sonic hedgehog by secreted BMP inhibitors expressed by notochord and somites." Development **127**(22): 4855-66.

Liem, K. F., Jr., G. Tremml, et al. (1997). "A role for the roof plate and its resident TGFbeta-related proteins in neuronal patterning in the dorsal spinal cord." Cell **91**(1): 127-38.

Lin, A. W. and E. M. Carpenter (2003). "Hoxa10 and Hoxd10 coordinately regulate lumbar motor neuron patterning." J Neurobiol **56**(4): 328-37.

Lin, J. H., T. Saito, et al. (1998). "Functionally related motor neuron pool and muscle sensory afferent subtypes defined by coordinate ETS gene expression." Cell **95**(3): 393-407.

Liu, J. P., E. Laufer, et al. (2001). "Assigning the positional identity of spinal motor neurons: rostrocaudal patterning of Hox-c expression by FGFs, Gdf11, and retinoids." Neuron **32**(6): 997-1012.

Livet, J., M. Sigrist, et al. (2002). "ETS gene Pea3 controls the central position and terminal arborization of specific motor neuron pools." Neuron **35**(5): 877-92.

Logan, M., H. G. Simon, et al. (1998). "Differential regulation of T-box and homeobox transcription factors suggests roles in controlling chick limb-type identity." Development **125**(15): 2825-35.

Lufkin, T., A. Dierich, et al. (1991). "Disruption of the Hox-1.6 homeobox gene results in defects in a region corresponding to its rostral domain of expression." Cell **66**(6): 1105-19.

Lumsden, A. and R. Krumlauf (1996). "Patterning the vertebrate neuraxis." Science **274**(5290): 1109-15.

Maden, M., P. Hunt, et al. (1991). "Retinoic acid-binding protein, rhombomeres and the neural crest." Development **111**(1): 35-43.

Maden, M., E. Sonneveld, et al. (1998). "The distribution of endogenous retinoic acid in the chick embryo: implications for developmental mechanisms." Development **125**(21): 4133-44.

Marshall, H., S. Nonchev, et al. (1992). "Retinoic acid alters hindbrain Hox code and induces transformation of rhombomeres 2/3 into a 4/5 identity." Nature **360**(6406): 737-41.

Martini, R. and M. Schachner (1991). "Complex expression pattern of tenascin during innervation of the posterior limb buds of the developing chicken." J Neurosci Res **28**(2): 261-79.

Matise, M. P. and C. Lance-Jones (1996). "A critical period for the specification of motor pools in the chick lumbosacral spinal cord." Development **122**(2): 659-69.

Mercader, N., E. Leonardo, et al. (2000). "Opposing RA and FGF signals control proximodistal vertebrate limb development through regulation of Meis genes." Development **127**(18): 3961-70.

Muhr, J., E. Graziano, et al. (1999). "Convergent inductive signals specify midbrain, hindbrain, and spinal cord identity in gastrula stage chick embryos." Neuron **23**(4): 689-702.

Muhr, J., T. M. Jessell, et al. (1997). "Assignment of early caudal identity to neural plate cells by a signal from caudal paraxial mesoderm." Neuron **19**(3): 487-502.

Muramatsu, T., Y. Mizutani, et al. (1997). "Comparison of three nonviral transfection methods for foreign gene expression in early chicken embryos in ovo." Biochem Biophys Res Commun **230**(2): 376-80.

Nakano, T., M. Windrem, et al. (2005). "Identification of a conserved 125 base-pair Hb9 enhancer that specifies gene expression to spinal motor neurons." Dev Biol **283**(2): 474-85.

Nelson, C. E., B. A. Morgan, et al. (1996). "Analysis of Hox gene expression in the chick limb bud." Development **122**(5): 1449-66.

Niederreither, K., V. Subbarayan, et al. (1999). "Embryonic retinoic acid synthesis is essential for early mouse post-implantation development." Nat Genet **21**(4): 444-8.

Niswander, L. and G. R. Martin (1992). "Fgf-4 expression during gastrulation, myogenesis, limb and tooth development in the mouse." Development **114**(3): 755-68.

Noakes, P. G. and M. R. Bennett (1987). "Growth of axons into developing muscles of the chick forelimb is preceded by cells that stain with Schwann cell antibodies." J Comp Neurol **259**(3): 330-47.

Novak, K. D., D. Prevette, et al. (2000). "Hepatocyte growth factor/scatter factor is a neurotrophic survival factor for lumbar but not for other somatic motoneurons in the chick embryo." J Neurosci **20**(1): 326-37.

Novitch, B. G., A. I. Chen, et al. (2001). "Coordinate regulation of motor neuron subtype identity and pan-neuronal properties by the bHLH repressor Olig2." Neuron **31**(5): 773-89.

Novitch, B. G., H. Wichterle, et al. (2003). "A requirement for retinoic acid-mediated transcriptional activation in ventral neural patterning and motor neuron specification." Neuron **40**(1): 81-95.

Nowicki, J. L. and A. C. Burke (2000). "Hox genes and morphological identity: axial versus lateral patterning in the vertebrate mesoderm." Development **127**(19): 4265-75.

O'Brien, M. K., L. Landmesser, et al. (1990). "Development and survival of thoracic motoneurons and hindlimb musculature following transplantation of the thoracic neural tube to the lumbar region in the chick embryo: functional aspects." J Neurobiol **21**(2): 341-55.

Oakley, R. A. and K. W. Tosney (1993). "Contact-mediated mechanisms of motor axon segmentation." J Neurosci **13**(9): 3773-92.

Ohta, K., H. Iwamasa, et al. (1997). "The inhibitory effect on neurite outgrowth of motoneurons exerted by the ligands ELF-1 and RAGS." Mech Dev **64**(1-2): 127-35.

Omelchenko, N. and C. Lance-Jones (2003). "Programming neural Hoxd10: in vivo evidence that early node-associated signals predominate over paraxial mesoderm signals at posterior spinal levels." Dev Biol **261**(1): 99-115.

Oppenheim, R. W., T. Cole, et al. (1989). "Early regional variations in motoneuron numbers arise by differential proliferation in the chick embryo spinal cord." Dev Biol **133**(2): 468-74.

Pachnis, V., B. Mankoo, et al. (1993). "Expression of the c-ret proto-oncogene during mouse embryogenesis." Development **119**(4): 1005-17.

Park, H. C., A. Mehta, et al. (2002). "olig2 is required for zebrafish primary motor neuron and oligodendrocyte development." Dev Biol **248**(2): 356-68.

Pekarik, V., D. Bourikas, et al. (2003). "Screening for gene function in chicken embryo using RNAi and electroporation." Nat Biotechnol **21**(1): 93-6.

Pfaff, S. L., M. Mendelsohn, et al. (1996). "Requirement for LIM homeobox gene Isl1 in motor neuron generation reveals a motor neuron-dependent step in interneuron differentiation." Cell **84**(2): 309-20.

Pike, S. H. and J. S. Eisen (1990). "Identified primary motoneurons in embryonic zebrafish select appropriate pathways in the absence of other primary motoneurons." J Neurosci **10**(1): 44-9.

Prasad, A. and M. Hollyday (1991). "Development and migration of avian sympathetic preganglionic neurons." J Comp Neurol **307**(2): 237-58.

Price, S. R., N. V. De Marco Garcia, et al. (2002). "Regulation of motor neuron pool sorting by differential expression of type II cadherins." Cell **109**(2): 205-16.

Rijli, F. M., R. Matyas, et al. (1995). "Cryptorchidism and homeotic transformations of spinal nerves and vertebrae in Hoxa-10 mutant mice." Proc Natl Acad Sci U S A **92**(18): 8185-9.

Roberts, D. J., R. L. Johnson, et al. (1995). "Sonic hedgehog is an endodermal signal inducing Bmp-4 and Hox genes during induction and regionalization of the chick hindgut." Development **121**(10): 3163-74.

Rossant, J., R. Zirngibl, et al. (1991). "Expression of a retinoic acid response element-hsplacZ transgene defines specific domains of transcriptional activity during mouse embryogenesis." Genes Dev **5**(8): 1333-44.

Rossel, M. and M. R. Capecchi (1999). "Mice mutant for both Hoxa1 and Hoxb1 show extensive remodeling of the hindbrain and defects in craniofacial development." Development **126**(22): 5027-40.

Schaeren-Wiemers, N. and A. Gerfin-Moser (1993). "A single protocol to detect transcripts of various types and expression levels in neural tissue and cultured cells: in situ hybridization using digoxigenin-labelled cRNA probes." Histochemistry **100**(6): 431-40.

Segawa, H., T. Miyashita, et al. (2001). "Functional repression of Islet-2 by disruption of complex with Ldb impairs peripheral axonal outgrowth in embryonic zebrafish." Neuron **30**(2): 423-36.

Serpente, P., S. Tumpel, et al. (2005). "Direct crossregulation between retinoic acid receptor {beta} and Hox genes during hindbrain segmentation." Development **132**(3): 503-13.

Shah, V., E. Drill, et al. (2004). "Ectopic expression of Hoxd10 in thoracic spinal segments induces motoneurons with a lumbosacral molecular profile and axon projections to the limb." Dev Dyn **231**(1): 43-56.

Sharma, K., H. Z. Sheng, et al. (1998). "LIM homeodomain factors Lhx3 and Lhx4 assign subtype identities for motor neurons." Cell **95**(6): 817-28.

Shirasaki, R. and S. L. Pfaff (2002). "Transcriptional codes and the control of neuronal identity." Annu Rev Neurosci **25**: 251-81.

Shrimpton, A. E., E. M. Levinsohn, et al. (2004). "A HOX gene mutation in a family with isolated congenital vertical talus and Charcot-Marie-Tooth disease." Am J Hum Genet **75**(1): 92-6.

Sieber-Blum, M. and A. M. Cohen (1980). "Clonal analysis of quail neural crest cells: they are pluripotent and differentiate in vitro in the absence of noncrest cells." Dev Biol **80**(1): 96-106.

Simeone, A., D. Acampora, et al. (1991). "Differential regulation by retinoic acid of the homeobox genes of the four HOX loci in human embryonal carcinoma cells." Mech Dev **33**(3): 215-27.

Smith, C. L. and M. Hollyday (1983). "The development and postnatal organization of motor nuclei in the rat thoracic spinal cord." J Comp Neurol **220**(1): 16-28.

Sockanathan, S. and T. M. Jessell (1998). "Motor neuron-derived retinoid signaling specifies the subtype identity of spinal motor neurons." Cell **94**(4): 503-14.

Sonnenberg, E., D. Meyer, et al. (1993). "Scatter factor/hepatocyte growth factor and its receptor, the c-met tyrosine kinase, can mediate a signal exchange between mesenchyme and epithelia during mouse development." J Cell Biol **123**(1): 223-35.

Stadler, H. S., K. M. Higgins, et al. (2001). "Loss of Eph-receptor expression correlates with loss of cell adhesion and chondrogenic capacity in Hoxa13 mutant limbs." Development **128**(21): 4177-88.

Studer, M., A. Gavalas, et al. (1998). "Genetic interactions between Hoxa1 and Hoxb1 reveal new roles in regulation of early hindbrain patterning." Development **125**(6): 1025-36.

Summerbell, D. and R. V. Stirling (1981). "The innervation of dorsoventrally reversed chick wings: evidence that motor axons do not actively seek out their appropriate targets." J Embryol Exp Morphol **61**: 233-47.

Swindell, E. C., C. Thaller, et al. (1999). "Complementary domains of retinoic acid production and degradation in the early chick embryo." Dev Biol **216**(1): 282-96.

Tanabe, Y. and T. M. Jessell (1996). "Diversity and pattern in the developing spinal cord." Science **274**(5290): 1115-23.

Tanabe, Y., H. Roelink, et al. (1995). "Induction of motor neurons by Sonic hedgehog is independent of floor plate differentiation." Curr Biol **5**(6): 651-8.

Tanabe, Y., C. William, et al. (1998). "Specification of motor neuron identity by the MNR2 homeodomain protein." Cell **95**(1): 67-80.

Tang, J., U. Rutishauser, et al. (1994). "Polysialic acid regulates growth cone behavior during sorting of motor axons in the plexus region." Neuron **13**(2): 405-14.

Taniguchi, M., S. Yuasa, et al. (1997). "Disruption of semaphorin III/D gene causes severe abnormality in peripheral nerve projection." Neuron **19**(3): 519-30.

Tannahill, D., G. M. Cook, et al. (1997). "Axon guidance and somites." Cell Tissue Res **290**(2): 275-83.

Tessier-Lavigne, M. and C. S. Goodman (1996). "The molecular biology of axon guidance." Science **274**(5290): 1123-33.

Thaler, J. P., S. J. Koo, et al. (2004). "A postmitotic role for Isl-class LIM homeodomain proteins in the assignment of visceral spinal motor neuron identity." Neuron **41**(3): 337-50.

Thaler, J. P., S. K. Lee, et al. (2002). "LIM factor Lhx3 contributes to the specification of motor neuron and interneuron identity through cell-type-specific protein-protein interactions." Cell **110**(2): 237-49.

Thor, S., J. Ericson, et al. (1991). "The homeodomain LIM protein Isl-1 is expressed in subsets of neurons and endocrine cells in the adult rat." Neuron **7**(6): 881-9.

Thor, S. and J. B. Thomas (1997). "The Drosophila islet gene governs axon pathfinding and neurotransmitter identity." Neuron **18**(3): 397-409.

Tiret, L., H. Le Mouellic, et al. (1998). "Increased apoptosis of motoneurons and altered somatotopic maps in the brachial spinal cord of Hoxc-8-deficient mice." Development **125**(2): 279-91.

Tokumoto, M., Z. Gong, et al. (1995). "Molecular heterogeneity among primary motoneurons and within myotomes revealed by the differential mRNA expression of novel islet-1 homologs in embryonic zebrafish." Dev Biol **171**(2): 578-89.

Tosney, K. W. and L. T. Landmesser (1984). "Pattern and specificity of axonal outgrowth following varying degrees of chick limb bud ablation." J Neurosci **4**(10): 2518-27.

Tosney, K. W. and L. T. Landmesser (1985). "Development of the major pathways for neurite outgrowth in the chick hindlimb." Dev Biol **109**(1): 193-214.

Tosney, K. W. and L. T. Landmesser (1985). "Growth cone morphology and trajectory in the lumbosacral region of the chick embryo." J Neurosci **5**(9): 2345-58.

Tsuchida, T., M. Ensini, et al. (1994). "Topographic organization of embryonic motor neurons defined by expression of LIM homeobox genes." Cell **79**(6): 957-70.

Vallstedt, A., J. Muhr, et al. (2001). "Different levels of repressor activity assign redundant and specific roles to Nkx6 genes in motor neuron and interneuron specification." Neuron **31**(5): 743-55.

Varela-Echavarria, A., A. Tucker, et al. (1997). "Motor axon subpopulations respond differentially to the chemorepellents netrin-1 and semaphorin D." Neuron **18**(2): 193-207.

Vermeren, M. M., G. M. Cook, et al. (2000). "Spinal nerve segmentation in the chick embryo: analysis of distinct axon-repulsive systems." Dev Biol **225**(1): 241-52.

Vermot, J., B. Schuhbaur, et al. (2005). "Retinaldehyde dehydrogenase 2 and Hoxc8 are required in the murine brachial spinal cord for the specification of Lim1+ motoneurons and the correct distribution of Islet1+ motoneurons." Development **132**(7): 1611-21.

Wahba, G. M., S. L. Hostikka, et al. (2001). "The paralogous Hox genes Hoxa10 and Hoxd10 interact to pattern the mouse hindlimb peripheral nervous system and skeleton." Dev Biol **231**(1): 87-102.

Wang, H. U. and D. J. Anderson (1997). "Eph family transmembrane ligands can mediate repulsive guidance of trunk neural crest migration and motor axon outgrowth." Neuron **18**(3): 383-96.

Whitelaw, V. and M. Hollyday (1983). "Neural pathway constraints in the motor innervation of the chick hindlimb following dorsoventral rotations of distal limb segments." J Neurosci **3**(6): 1226-33.

Whitelaw, V. and M. Hollyday (1983). "Thigh and calf discrimination in the motor innervation of the chick hindlimb following deletions of limb segments." J Neurosci **3**(6): 1199-1215.

Wohl, C. A. and S. Weiss (1998). "Retinoic acid enhances neuronal proliferation and astroglial differentiation in cultures of CNS stem cell-derived precursors." J Neurobiol **37**(2): 281-90.

Yamamoto, Y., J. Livet, et al. (1997). "Hepatocyte growth factor (HGF/SF) is a muscle-derived survival factor for a subpopulation of embryonic motoneurons." Development **124**(15): 2903-13.

Yip, J. W., Y. P. Yip, et al. (1995). "The expression, origin and function of tenascin during peripheral nerve formation in the chick." Brain Res Dev Brain Res **86**(1-2): 297-310.